Appendix A. Details of Events of Pilot Study

Table A-1. Summary of Pilot Study Field Measurements

12/12/00		
		Equipment transport, unpack and testing. Set up MPL lidar and camera.
12/13/00		
	14:50	First time running lidar. 5 mins vertical test
	15:05	Start horizontal scan ± 10 degrees, 1 degree / sec
	15:08:05	**Test 1** Start generating sieved indigenous soil .540 kg in 5 sec
	16:31:00	**Test 2** Start generating indigenous soil 5.5 kg in 50 sec
	17:35	5 mins vertical test, then stop running lidar
12/14/00		
	9:55	start MPL lidar
	10:55:00	**Test 3** Start generating indigenous soil 5kg in 70seconds
	11:40:00	**Test 4** Start generating indigenous soil 5kg in 50 seconds
	12:11:00	**Test 5** Start generating indigenous soil 22kg steady release
	14:34:00	**Test 6** Start generating indigenous soil 22kg steady release
	15:15:30	**Test 7** Start generating white powder 5.04 kg in 2 mins 45 seconds
	15:45:00	**Test 8** Start generating white powder 4.66 kg in 3 mins 15 seconds
	16:11:00	**Test 9** Start generating indigenous soil 5 kg in 70 seconds
	16:31:00	**Test 10** Start generating indigenous soil 5 kg in 90 seconds
	16:55:00	**Test 11** Start generating indigenous soil 5 kg in 90 seconds
	17:21:00	**Test 12** Start generating indigenous soil 5 kg in 90 seconds
	17:45:00	**Test 13** Start generating indigenous soil 5 kg in 90 seconds
	18:18:20	start vertical test
	18:34	point the laser to reference point (white board)
	18:42:00	lidar stop running
12/15/00		
	09:50	lidar on
	10:01:00	start vertical test
	11:48:00	**Test 14** Start generating indigenous soil 1.5 kg in 90 seconds
	12:02:00	**Test 15** Start generating white powder 1.45 kg in 60 seconds
	12:14:00	**Test 16** Start generating dust using vehicle upwind of tower
	14:18:00	**Test 17** Start generating dust using vehicle, 50m line source
	14:31:00	**Test 18** Start generating dust using vehicle, 50 m line source
	15:14:00	**Test 19** Start generating dust using vehicle, 150m line source
	16:48:00	start vertical test
	17:32:00	point the laser to reference point (white board)
12/16/00		
	04:50	lidar on (windy morning)
	05:10	start vertical test
	05:42	point the laser to reference point (white board) for 15 mins
	12:15:00	**Test 20** Start generating dust using vehicle
	18:17:50	start vertical test
12/18/00		
	09:55	lidar on (very windy morning – Santa Ana in progress). 10 mins vertical profile and 10 min horizontal profile was taken
	11:00	dissemble equipment, start packing

Table A-2. Summary of the data runs conducted during the Pilot Study

Filename	Start Time	End Time	Description
00121121.36G(R)	12/11/00 21:36:04	21:36:53	
00121121.38G(R)	12/11/00 21:38:33	21:42:14	
00121121.42G(R)	12/11/00 21:42:59	21:47:24	
00121121.47G(R)	12/11/00 21:47:48	21:47:55	
00121121.48G(R)	12/11/00 21:48:02	21:54:49	
00121213.27G(R)	12/12/00 13:27:04	14:00:00	scan +-20 degrees at 1 deg/sec.
00121214.00G(R)	12/12/00 14:00:00	14:15:51	
00121314.53G(R)			NO Data
00121314.54G(R)	12/13/00 14:54:17	14:58:06	
00121314.59G(R)	12/13/00 14:59:56	15:00:01	
00121315.00G(R)	12/13/00 15:00:03	15:00:29	
00121315.03G(R)	12/13/00 15:03:11	15:00:19	
00121315.04G(R)	12/13/00 15:04:08	16:00:00	
00121316.00G(R)	12/13/00 16:00:03	16:26:14	
00121316.28G(R)	12/13/00 16:28:50	16:33:26	
00121316.33G(R)	12/13/00 16:33:53	17:00:01	
00121317.00G(R)	12/13/00 17:00:04	17:26:15	
00121317.35G(R)	12/13/00 17:35:46	17:51:32	
00121409.54G(R)	12/14/00 09:54:16	10:00:00	scan +-10 degrees at 1 deg/sec.
00121410.00G(R)	12/14/00 10:00:03	10:29:46	vertical test
00121410.50G(R)	12/14/00 10:50:49	10:56:40	Test 3
00121410.57G(R)	12/14/00 10:57:25	10:58:12	
00121410.58G(R)	12/14/00 10:58:29	10:58:37	
00121410.59G(R)	12/14/00 10:59:12	11:00:01	
00121411.00G(R)	12/14/00 11:00:03	11:29:38	
00121411.30G(R)	12/14/00 11:30:13	11:42:03	
00121411.42G(R)	12/14/00 11:42:32	11:44:41	Test 4
00121411.45G(R)	12/14/00 11:45:10	11:51:57	
00121411.52G(R)	12/14/00 11:52:49	11:52:49	
00121411.53G(R)	12/14/00 11:53:15	11:58:04	
00121411.59G(R)	12/14/00 11:59:47	12:00:00	
00121412.00G(R)	12/14/00 12:00:56	12:16:28	
00121412.16G(R)	12/14/00 12:17:01	12:17:57	
00121414.29G(R)	12/14/00 14:29:29	14:30:45	Test 5
00121414.33G(R)	12/14/00 14:33:51	14:47:12	Test 6
00121414.47G(R)	12/14/00 14:47:44	14:47:54	
00121414.51G(R)	12/14/00 14:51:56	15:00:01	
00121415.00G(R)	12/14/00 15:00:04	16:00:00	Test 7,8-16:11,9-16:31,10-16:55
00121416.00G(R)	12/14/00 16:00:03	17:00:00	Test 11-17:20,12-17:45
00121417.00G(R)	12/14/00 17:00:03	18:00:00	Test 13-11:41,14-12:02
00121418.00G(R)	12/14/00 18:00:03	18:09:38	
00121418.09G(R)	12/14/00 18:09:59	18:10:07	
00121418.17G(R)	12/14/00 18:18:01	18:46:46	
00121511.14G(R)	12/15/00 11:14:07	11:38:41	Test 15-12:14
00121511.41G(R)	12/15/00 11:41:26	11:47:31	
00121511.48G(R)	12/15/00 11:48:03	11:49:45	
00121511.50G(R)	12/15/00 11:50:37	11:51:04	
00121511.51G(R)	12/15/00 11:52:00	11:52:59	
00121511.53G(R)	12/15/00 11:53:19	11:59:21	
00121512.00G(R)	12/15/00 12:00:27	12:02:33	
00121512.02G(R)	12/15/00 12:02:59	12:03:42	
00121512.04G(R)	12/15/00 12:04:22	12:05:10	
00121512.06G(R)	12/15/00 12:06:05	12:06:59	
00121512.07G(R)	12/15/00 12:07:20	12:14:40	
00121512.15G(R)	12/15/00 12:15:47	12:17:35	
00121512.17G(R)	12/15/00 12:17:54	12:24:06	
00121512.24G(R)	12/15/00 12:24:44	13:00:01	
00121513.00G(R)	12/15/00 13:00:04	13:47:42	
00121513.48G(R)	12/15/00 13:48:29	14:00:00	
00121514.00G(R)	12/15/00 14:00:02	14:12:01	
00121514.14G(R)	12/15/00 14:14:34	14:15:18	
00121514.16G(R)	12/15/00 14:17:02	14:17:28	
00121514.17G(R)	12/15/00 14:17:57	14:24:23	Car generated dust-14:17
00121514.24G(R)	12/15/00 14:24:59	14:30:11	

00121514.30G(R)	12/15/00 14:30:27	14:30:48	
00121514.31G(R)	12/15/00 14:31:37	14:35:26	Suburban generated dust-14:31
00121514.35G(R)	12/15/00 14:35:43	14:36:01	
00121514.36G(R)	12/15/00 14:36:54	14:38:44	
00121514.39G(R)	12/15/00 14:39:05	14:58:49	
00121514.59G(R)	12/15/00 14:59:04	14:59:09	
00121515.01G(R)	12/15/00 15:01:19	15:29:30	
00121515.30G(R)	12/15/00 15:30:06	16:00:02	
00121516.00G(R)	12/15/00 16:00:04	16:47:59	
00121516.48G(R)	12/15/00 16:48:48	17:00:01	
00121517.00G(R)	12/15/00 17:00:04	17:19:39	
00121517.32G(R)	12/15/00 17:32:52	17:44:42	
00121604.50G(R)	12/16/00 04:50:18	05:00:01	
00121605.00G(R)	12/16/00 05:00:04	05:09:01	
00121605.09G(R)	12/16/00 05:09:45	05:29:10	
00121605.42G(R)	12/16/00 05:42:10	06:00:01	
00121606.00G(R)	12/16/00 06:00:03	06:02:20	
00121606.02G(R)	12/16/00 06:02:57	06:48:22	
00121606.49G(R)	12/16/00 06:49:34	07:00:00	
00121607.00G(R)	12/16/00 07:00:03	07:57:29	
00121607.57G(R)	12/16/00 07:57:48	07:57:53	
00121607.58G(R)	12/16/00 07:58:53	08:00:00	
00121608.00G(R)	12/16/00 08:00:03	08:03:09	
00121608.03G(R)	12/16/00 08:03:43	08:03:51	
00121608.04G(R)	12/16/00 08:04:19	09:00:00	
00121609.00G(R)	12/16/00 09:00:03	10:00:02	
00121610.00G(R)	12/16/00 10:00:04	10:01:22	
00121610.01G(R)	12/16/00 10:01:54	10:36:23	
00121611.00G(R)	12/16/00 11:00:44	11:47:14	
00121611.47G(R)	12/16/00 11:47:59	11:48:25	
00121611.49G(R)	12/16/00 11:50:00	11:50:15	
00121611.50G(R)	12/16/00 11:50:50	11:51:06	
00121611.51G(R)	12/16/00 11:51:48	12:00:00	
00121612.00G(R)	12/16/00 12:00:03	12:10:28	
00121612.10G(R)	12/16/00		NO Data
00121612.11G(R)	12/16/00 12:11:15	12:11:26	
00121612.19G(R)	12/16/00 12:19:42	12:24:22	
00121612.25G(R)	12/16/00 12:25:08	12:42:28	
00121612.43G(R)	12/16/00 12:43:11	13:00:02	
00121613.00G(R)	12/16/00 13:00:04	14:00:02	
00121614.00G(R)	12/16/00 14:00:04	14:03:29	
00121614.05G(R)	12/16/00 14:05:47	15:00:00	
00121615.00G(R)	12/16/00 15:00:02	16:00:01	
00121616.00G(R)	12/16/00 16:00:04	17:00:02	
00121617.00G(R)	12/16/00 17:00:05	17:53:32	
00121617.56G(R)	12/16/00 17:56:38	17:56:46	
00121617.57G(R)	12/16/00 17:57:11	17:57:39	
00121617.58G(R)	12/16/00 17:58:32	17:59:03	
00121618.06G(R)	12/16/00 18:06:33	18:17:45	
00121618.18G(R)	12/16/00 18:18:25	18:22:33	
00121809.56G(R)	12/18/00 09:56:41	10:00:01	
00121810.00G(R)	12/18/00 10:00:03	10:08:35	
00121810.08G(R)	12/18/00 10:08:54	10:17:41	

Appendix B. Description of the 10-Second Meteorological, DustTrak, and SF_6 File

The validated 10-second average meteorological, tracer gas and DustTrak data are contained in an Excel spreadsheet.
The following is an excert from the spreadsheet.
The data for each parameter are presented in columns
There is some header information with serial numbers of the DustTrak instruments and some calculations performed on each column of data, including minimum, maximum, average, median and number of data points
The first column is the start time of the 10-second averaging period.
Columns 2-9 are the DustTrak data in milligrams per cubinc meter.
Columns 10-14 are the wind, temperature and dew point data from the background, upwind meteorological station.
Column 15 is the tracer gas data in parts per trillion.
Columns 16-33 include the meteorological data from all three heights on the downwind tower.
Column 34 includes control numbers used for the processing
During the evening periods, the downwind tower was lowered for security reasons. Meteorological data were voided from the downwind tower when the tower was down.

1	2	3	4	5	6	7	8	9	10	11	12	13	14	15	16	17	18	19	20	21	22	23	24	25	26	27	28	29	30	31	32	33	34
From Met_mass_data\all_data																																	
	PM10_BG	PM2.5_BG	PM-10_2m	PM-2.5_2m	PM-10_5m	PM-2.5_5m	PM-10_10m	PM-2.5_10m																									
Serial Number:	21879	21911	21955	21569	21975	21908	21976	21912																									
Time constant (seconds):	10	10	10	10	10	10	10	10		12/14 SF6 release rate was 400g/hr																							
Log Interval (mm:ss):	0:10	0:10	0:10	0:10	0:10	0:10	0:10	0:10		12/15 and 12/16 SF6 release rate was 200g/hr																							
All Data																														corrected			
min	0.010	0.005	-0.003	0.003	0.000	0.004	0.004	0.009	0.2	0.0	0.0	0.1	-18.6	0.0	0.2	0.0	0.0	0.0	0.0	0.0	0.0	0.0	0.0	9.5	0.1	0.0	0.6	-1.7	-0.9	-117.5	0.0	0.0	
max	73.685	8.047	59.378	3.125	23.119	6.720	29.000	7.770	13.3	360.0	99.7	29.2	12.7	34976.6	9.5	360.0	98.7	10.1	360.0	62.5	10.2	360.0	80.6	22.6	23.3	99.1	25.8	1.0	0.6	491.7	0.9	0.7	
median	0.084	0.074	0.128	0.094	0.065	0.076	0.051	0.076	1.3	92.5	6.7	13.6	4.0	96.4	1.2	107.4	3.2	2.1	261.6	4.3	1.6	245.4	4.5	15.6	6.5	74.6	7.5	-0.1	0.0	-18.3	0.1	0.0	
average	0.115	0.090	0.188	0.089	0.111	0.086	0.089	0.090	2.3	143.8	7.6	13.3	2.7	1727.0	1.6	148.1	4.6	2.7	212.5	5.4	2.3	205.2	5.6	16.4	9.3	67.7	10.2	-0.1	-0.1	53.7	0.1	0.0	
No. points	5024	5087	3691	3692	5635	5636	5331	5675	45579	45579	45579	44521	44521	4816	27308	27308	27308	7053	7053	7053	6280	6280	6280	3111	16461	26745	26714	7053	26745	26745	7053	26745	
		mg/m^3	mg/m^3	mg/m^3	mg/m^3	mg/m^3	mg/m^3	mg/m^3	m/sec	deg	deg	deg C	deg C	corrected	m/sec	deg	deg	m/sec	deg	deg	m/sec	deg	deg	deg C	deg C	percent	deg C	m/sec	m/sec	W/m^2	m/sec	m/ces	
Start Time	PM10_BG	PM2.5_BG	PM-10_2m	PM-2.5_2m	PM-10_5m	PM-2.5_5m	PM-10_10m	PM-2.5_10m	WS-2BG	WD-2BG	SgTht-BG	T-BG	DP-BG	SF6(ppt)	WS-2DW	WD-2DW	gTht-2DW	WS-10DW	WD-10DW	Tht-10DW	WS-5DW	WD-5DW	gTht-5DW	T10DW	T2DW	RH	RH-T	VWS10	VWS2	netRAD	sigW10	sigW2	
12/13/00 9:20:00									2.056	102.4	11.12	10.37	9.27																				2
12/13/00 9:20:10									1.894	110.4	5.856	10.35	9.33																				2
12/13/00 9:20:20									2.176	110.7	4.625	10.33	9.38																				2
12/13/00 9:20:30									1.971	101.4	6.899	10.33	9.42																				2
12/13/00 9:20:40									1.804	91.9	7.22	10.37	9.44																				2
12/13/00 9:20:50									1.539	107.2	9.7	10.42	9.46																				2
12/15/00 11:04:30	0.156	0.146	0.164	0.139	0.148	0.145	0.126	0.172	1.104	160.8	15.49	14.93	11.86	347	1.326	211.3	9.5								13.68	63.72	14.68		-0.012	252.9		0.037	2
12/15/00 11:04:40	0.159	0.144	0.164	0.14	0.149	0.146	0.13	0.17	1.232	134.2	8.66	14.96	11.84	347	1.296	203.1	6.352								13.69	63.88	14.67		-0.08	252.5		0.03	2
12/15/00 11:04:50	0.157	0.147	0.166	0.14	0.147	0.147	0.127	0.168	1.321	136.6	9.76	15.03	11.85	346	1.18	201.8	7.46								13.7	64.07	14.69		-0.051	252.2		0.041	2
12/15/00 11:05:00	0.168	0.146	0.16	0.139	0.156	0.147	0.126	0.169	1.245	132.3	18.81	14.98	11.85	345	1.3	201.4	24.23								13.72	64.39	14.68		-0.126	251.9		0.081	2
12/15/00 11:05:10	0.155	0.147	0.158	0.137	0.155	0.148	0.129	0.169	1.108	140.7	8.77	14.88	11.85	345	1.129	245.2	7.1								13.76	64.59	14.7		-0.103	252.1		0.125	2
12/15/00 11:05:20	0.155	0.146	0.158	0.14	0.155	0.148	0.125	0.17	1.484	151.7	8.5	14.86	11.82	344	1.052	239.7	6.013								13.75	64.63	14.73		-0.039	251.3		0.042	2
12/15/00 11:05:30	0.153	0.147	0.16	0.139	0.149	0.147	0.126	0.166	1.351	157.1	9.72	14.83	11.84	345	1.215	244	3.011								13.74	64.41	14.72		0.033	250.4		0.075	2
12/15/00 11:05:40	0.156	0.147	0.17	0.139	0.149	0.149	0.127	0.17	1.091	152.5	13.47	14.87	11.85	344	0.954	237.8	5.914								13.73	64.19	14.75		0.017	249.2		0.069	2
12/15/00 11:05:50	0.154	0.146	0.159	0.137	0.153	0.146	0.126	0.17	1.125	157.9	19.8	14.96	11.84	344	1.21	211.4	20.74								13.74	64.82	14.76		-0.251	248.6		0.164	2
12/15/00 11:06:00	0.154	0.147	0.169	0.14	0.149	0.148	0.129	0.165	1.313	153.4	18.94	15.08	11.86	345	1.599	179.4	12.7								13.78	65.18	14.76		-0.255	248.7		0.113	2
12/15/00 11:06:10	0.151	0.15	0.161	0.139	0.15	0.148	0.125	0.17	1.693	200.2	14.62	15.24	11.86	345	1.655	176.5	2.035								13.85	64.7	14.81		-0.194	249.4		0.097	2
12/15/00 11:06:20	0.159	0.147	0.159	0.136	0.146	0.145	0.127	0.171	1.903	202	9.4	15.42	11.92	344	1.475	162.5	4.131								13.9	64.31	14.84		-0.094	250.2		0.08	2
12/15/00 11:06:30	0.154	0.146	0.16	0.136	0.152	0.146	0.129	0.17	2.373	203.8	9.83	15.48	11.98	341	1.531	159.3	5.53								13.95	64.26	14.86		-0.119	250.3		0.059	2
12/18/00 15:55:40									0.219	296.8	0																						2
12/18/00 15:55:50									0.219	296.8	0																						2
12/18/00 15:56:00									0.219	296.8	0																						2
12/18/00 15:56:10									0.219	296.8	0																						2
12/18/00 15:56:20									0.219	296.8	0																						2

Appendix C. Description of Hourly Meteorological Data Files

The validated hourly average meteorological data for the background site are contained in an Excel spreadsheet.

The spreadsheet is HRLYMET.xls.

The following is an excert from the spreadsheet.

The data for each parameter are presented in columns.

There is some header information with some calculations performed on each column of data, including minimum, maximum, average, median and number of data points.

The first column is the start time of the 1-hour averaging period.

The second column is the end time of the 1-hour averaging period.

The next five columns contain the wind speed, direction sigma theta, temperature and dew point data.

Begin time	End Time	WS (m/sec)	WD (deg)	SigTheta (Deg)	T (deg C)	DP (deg C)
	min	0.5	1.1	5.9	0.3	-9.8
revised 4/30/2001	max	8.6	359.2	101.5	28.5	15.2
from DVP_BG_MET\	averge	2.0	146.9	42.9	13.8	4.5
Five_10sec…	median	1.5	96.5	38.5	13.6	5.0
	count	840	840	716	840	840
11/13/00 13:00	11/13/00 14:00	1.5	338.3	52.5	18.2	-3.5
11/13/00 14:00	11/13/00 15:00	1.4	324.2	41.6	18.6	-3.5
11/13/00 15:00	11/13/00 16:00	1.2	226.4	84.1	18.8	-2.5
11/13/00 16:00	11/13/00 17:00	1.5	127.8	57.3	17.2	-1.5
11/13/00 17:00	11/13/00 18:00	1.7	33.6	57.0	14.3	-1.1
11/13/00 18:00	11/13/00 19:00	1.9	269.2	32.1	12.8	4.9
12/18/00 0:00	12/18/00 1:00	6.6	70.0		19.2	-4.1
12/18/00 1:00	12/18/00 2:00	6.6	66.8		18.0	-5.1
12/18/00 2:00	12/18/00 3:00	5.9	69.2		17.2	-6.3
12/18/00 3:00	12/18/00 4:00	7.0	64.2		16.8	-7.8
12/18/00 4:00	12/18/00 5:00	7.9	73.2		16.6	-9.2
12/18/00 5:00	12/18/00 6:00	7.5	82.3		16.2	-9.6
12/18/00 6:00	12/18/00 7:00	6.9	87.9		16.1	-9.8
12/18/00 7:00	12/18/00 8:00	6.6	90.2		16.2	-9.4
12/18/00 8:00	12/18/00 9:00	7.2	85.5		17.0	-8.4
12/18/00 9:00	12/18/00 10:00	7.2	86.5		18.0	-7.3
12/18/00 10:00	12/18/00 11:00	8.4	79.9		19.6	-6.3
12/18/00 11:00	12/18/00 12:00	8.5	78.7		20.7	-5.4
12/18/00 12:00	12/18/00 13:00	8.6	78.0		21.1	-5.1

Appendix D. Details from Model Simulations

In the text, we depicted examples of the model calculations designed to simulate various features of the optical scattering from the generated dust clouds. More simulation results are shown below. In Figure D-1, the changes in the backscatter extinction as a function of number density of 10 μm particles are shown for the visible (523 nm) and near-infrared (1046 nm) wavelengths for two values of complex refractive index. The complex index of refraction represents the absorption of the particles and can vary widely for crustal materials. Figure D-2 shows the simulations as a function of particle size for two concentrations.

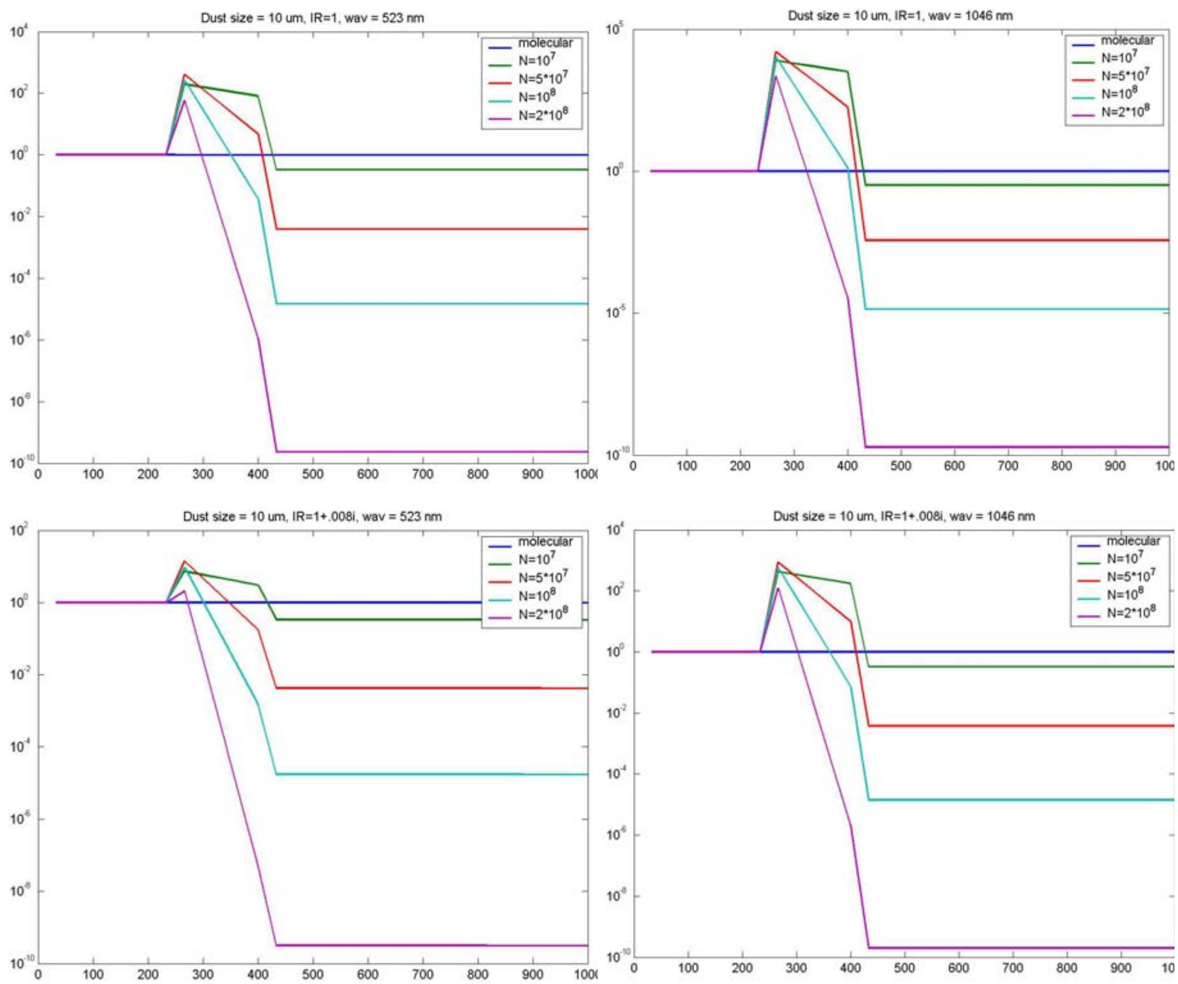

Figure D-1. Simulation model of the scattering from 10 μm dust showing backscatter and extinction expected for both wavelengths at several different particle concentrations in the upper panels. The two lower panels show the same results, except they show dependence on complex index of refraction typical for crustal materials.

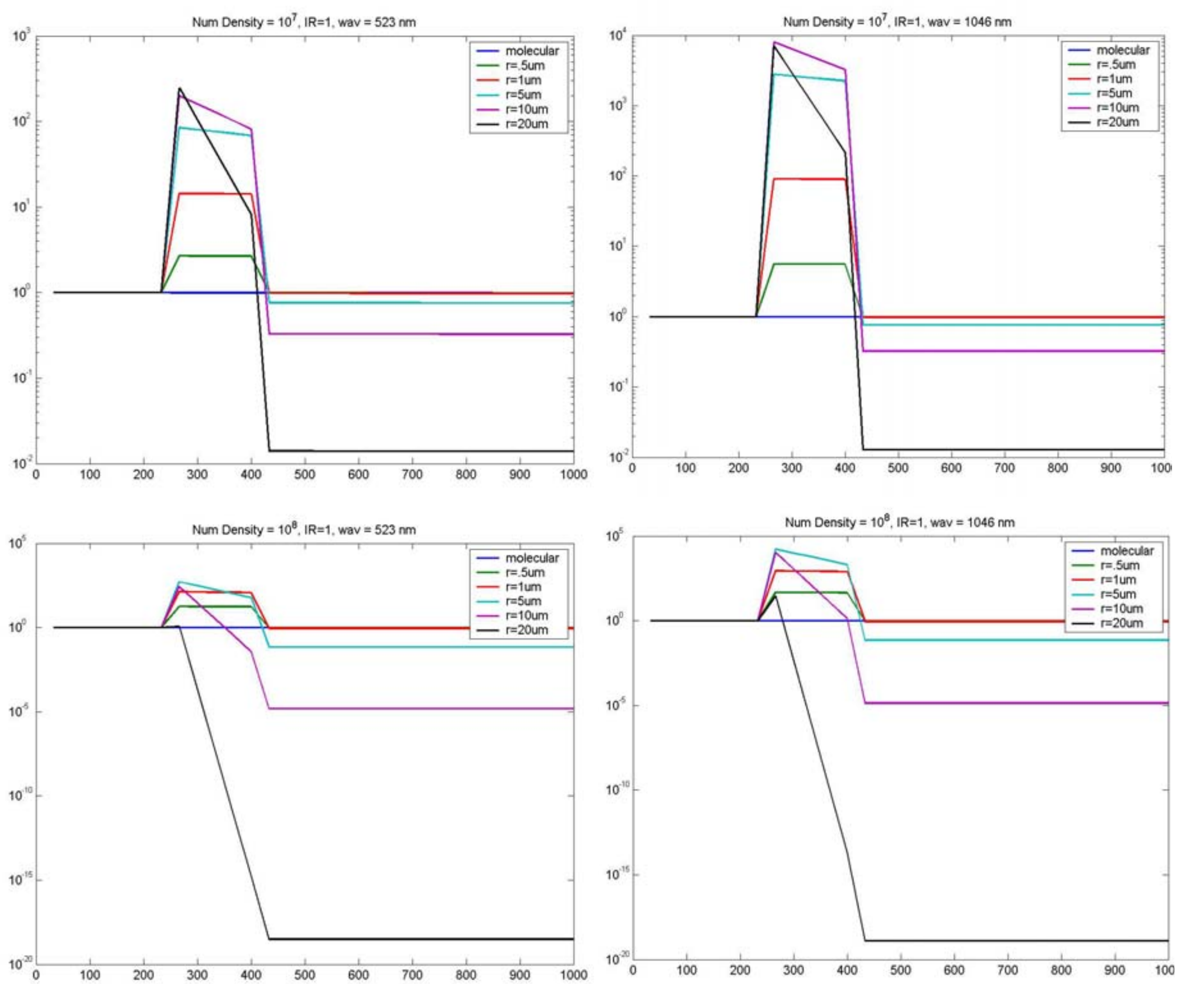

Figure D-2. Calculations of the backscatter and extinction for the two wavelengths show the dependence on the particle size. The upper panels show values for particle concentration of 10^7 m^{-3} and the lower panels show values for particle concentration of 10^8 m^{-3}.

The effect of changing the value of the complex refractive index for the two wavelengths and two particle concentrations is shown in Figure D-3. The extinction does not depend on the magnitude of the complex refractive index but the scattered intensity depends strongly on it. The same dependence on the particle concentration and wavelength is observed as shown in the preceding simulations.

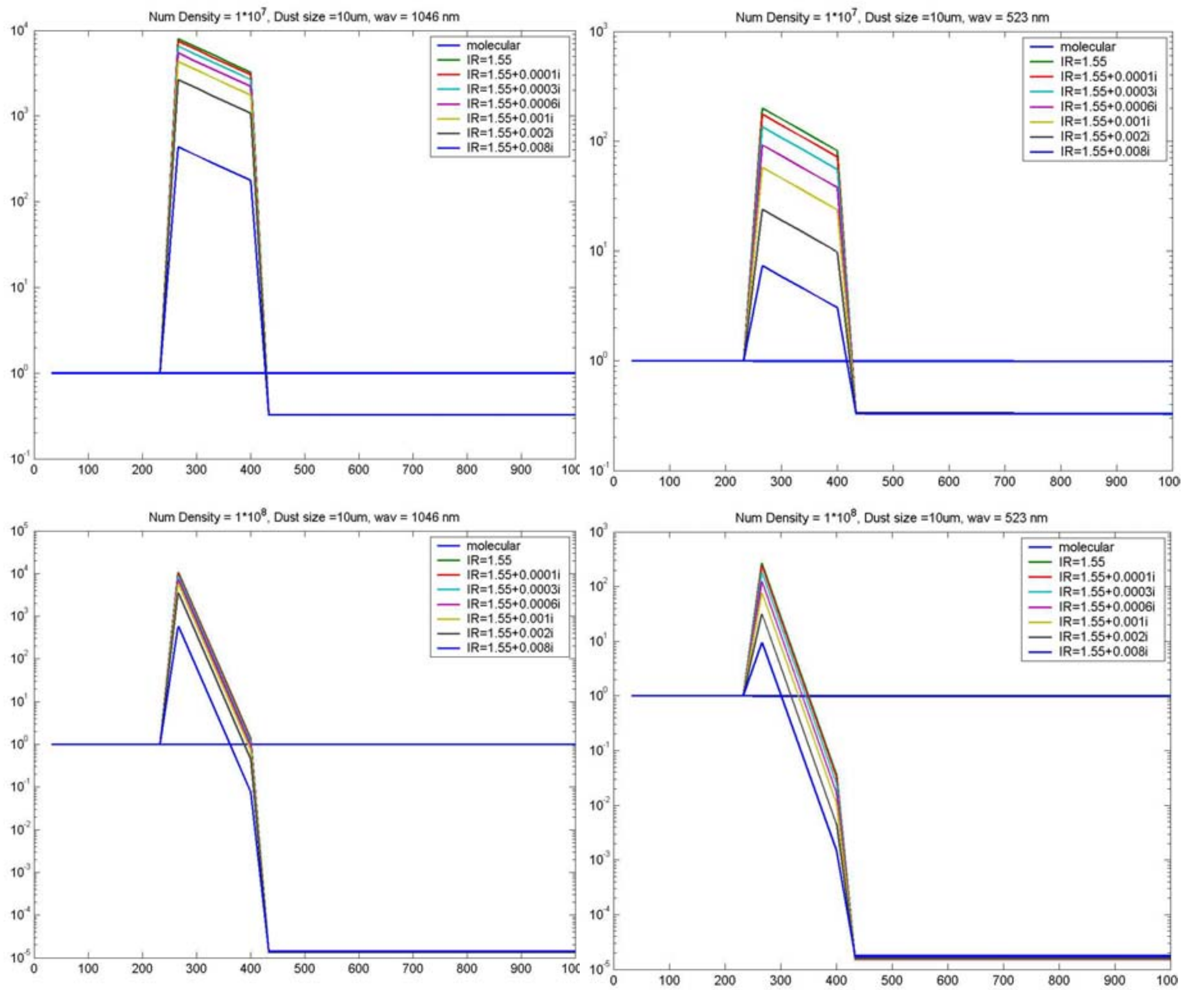

Figure D-3. The dependence of the backscatter on the absorption due to increasing complex refractive index is displayed for the two wavelengths and for two particle number densities.

In addition to those examples of field tests results presented in Figures D-1, D-2 and D-3, the results in Figures D-4, D-5, D-6, D-7, D-8, and D-9 show several example cases from the measurements during the pilot study that can be compared with these simulations.

The result in Figure D-4 shows a small puff of about 0.5 kg of sieved dirt from the field. The 0^o and $+10^o$ azimuth directions show the drift of the dust cloud to the right in the background wind. The feature at 450 m at $+10^o$ azimuth is due to scattering from a row of scrub bush and the -10^o azimuth plots show that no change is observed along a clear path. If we compare the backscatter at around 280 m at 0^o azimuth angle in Figure D-4 with the simulation result in Figure D-2, it suggests that the observed scattering feature is due to small amount ($< 10^7$ /m^3) of fine particles (<1μm) in the air.

Figure D-5 shows the results from Test #2 for both wavelengths at azimuth scan angles of -5^o (left), -2.5^o, 0^o, $+2.5^o$, and $+5^o$ (right). The test consisted of 5.5 kg of sieved dust being released at 16:31. If we compare the result with the simulation in Figure D-2 and D-1, it indicates that the feature of strong scattering and extinction is due to small amount ($< 10^7$ /m^3) of larger size particles (> 1μm) in the air.

Figure D-6 shows results from Test #10 of a slow drift and slow dissipation of a 5 kg dust cloud. The comparison with the simulation in Figure D-2 suggests that large amount ($> 10^7$ /m^3) of the larger size particles (~ 10 μm) are present.

Figure D-7 shows the dust cloud generated by vehicle on an east-west path during Test #19. The scattering observed is explained by the amount of small size particles stirred up by vehicle.

Figure D-8 shows the backscatter and extinction from the white powder (calcium carbonate) from Test #7. Because the atmospheric condition is very stable and calm during this test, we can set the laser beam staring through the generated dust plume without scanning, as this permits the study of the processes of dissipating and settling of the plume material. The scattering peaks in both red and green signals at about 500 meters are due to scattering from a row of scrub bush, the scattering peaks at about 250 meters are due to generated dust plume. The result showing here is very interesting because the process of settling out of larger size particles can be clearly observed. We compared with the simulation results in Figure D-2. The larger size particles (~ 10μm) that are responsible for most of the extinction settled out in 40 seconds, however, the smaller size particles (between 1 μm and 10 μm), which contribute to most of the scattering, will stay in the air for several minutes. The backscatter signal after one minute is most likely due to the scattering from the remaining fine mode particles (<1 μm), which stay in the atmosphere for a longer time.

In Figure D-9, results from Test #13 show the response of the green and NIR channel from soil generated dust in the upper four panels. Also, the process of settling out of larger size particles can be clearly observed. The lower left panel shows the dust cloud at 10^o elevation angle being blown back over the instrument location. The lower right panel shows the ratios of the green/NIR signals that are useful in describing the changes in the particle properties, in this case it is due to changes in concentration.

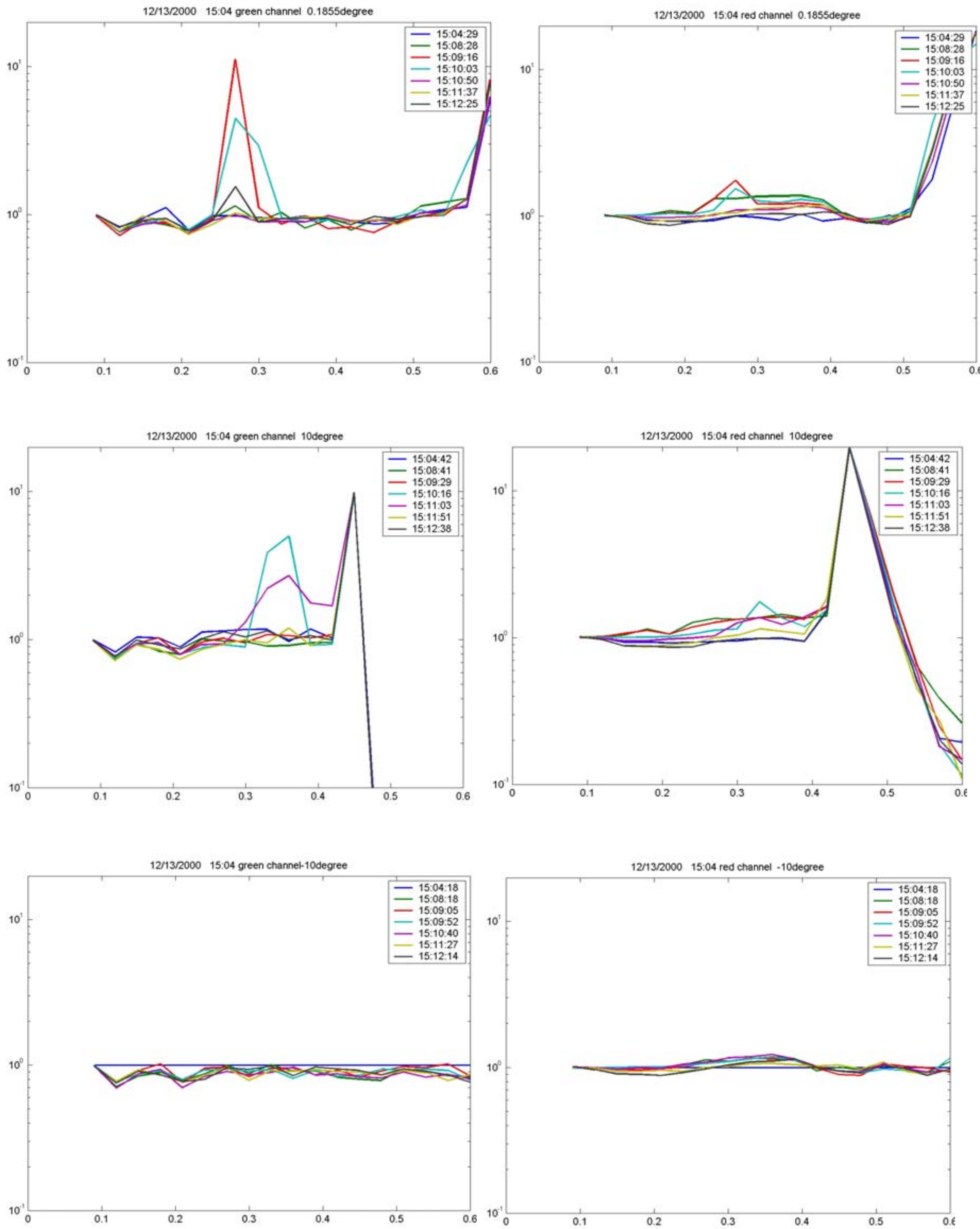

Figure D-4. Results from Test #1, a small puff of about 0.5 kg of sieved dirt from the field. The 0^o and $+10^o$ azimuth directions show the drift of the dust cloud to the right in the background wind. The feature at 450 m at $+10^o$ azimuth is due to scattering from a row of scrub bush and the -10^o azimuth plots show that no change is observed along a clear path.

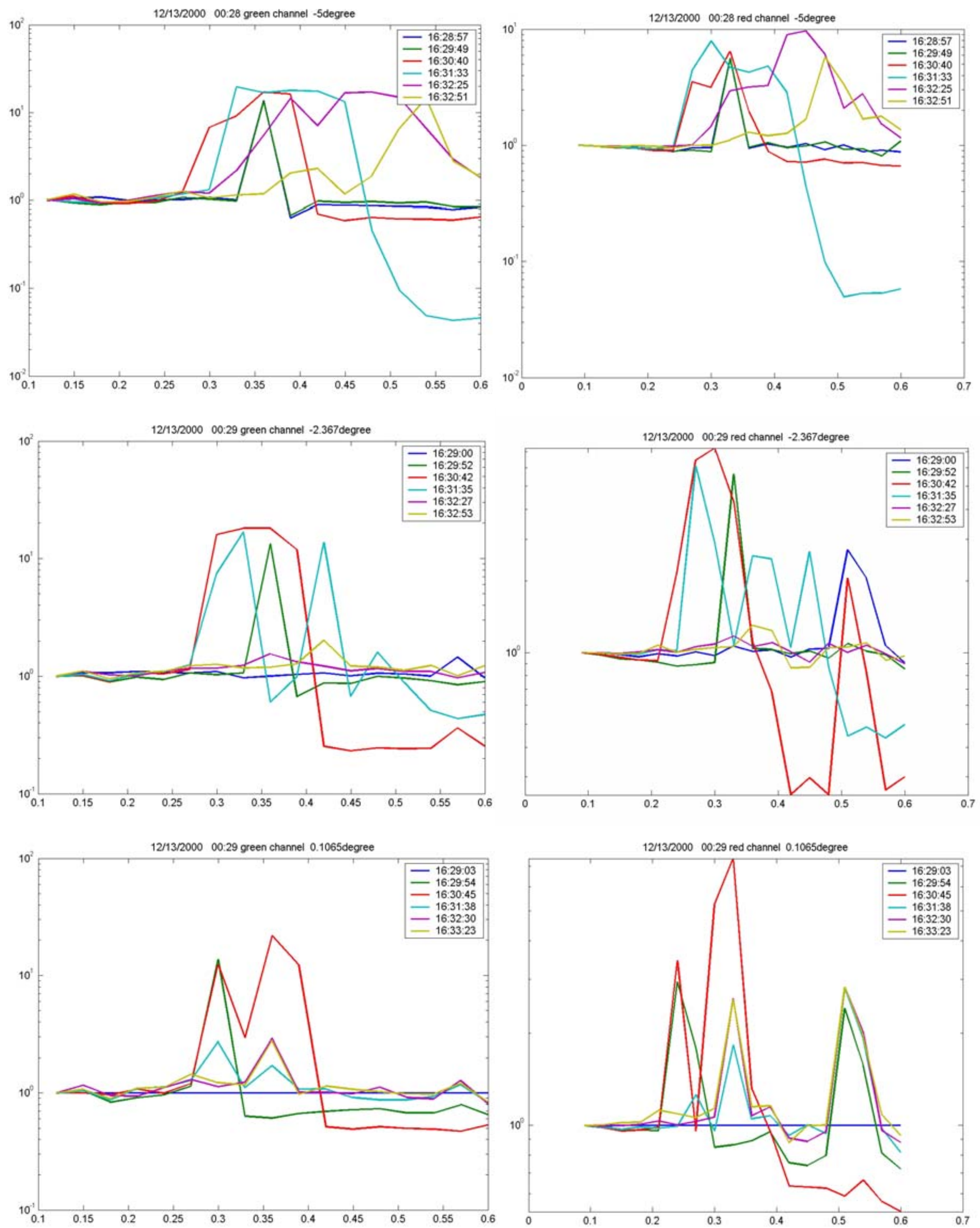

Figure D-5. The results from Test #2 are shown for both wavelengths at azimuth scan angles of -5^{o} (left), -2.5^{o}, 0^{o}, $+2.5^{o}$, and $+5^{o}$ (right). The test consisted of 5.5 kg of sieved dust being released at 16:31.

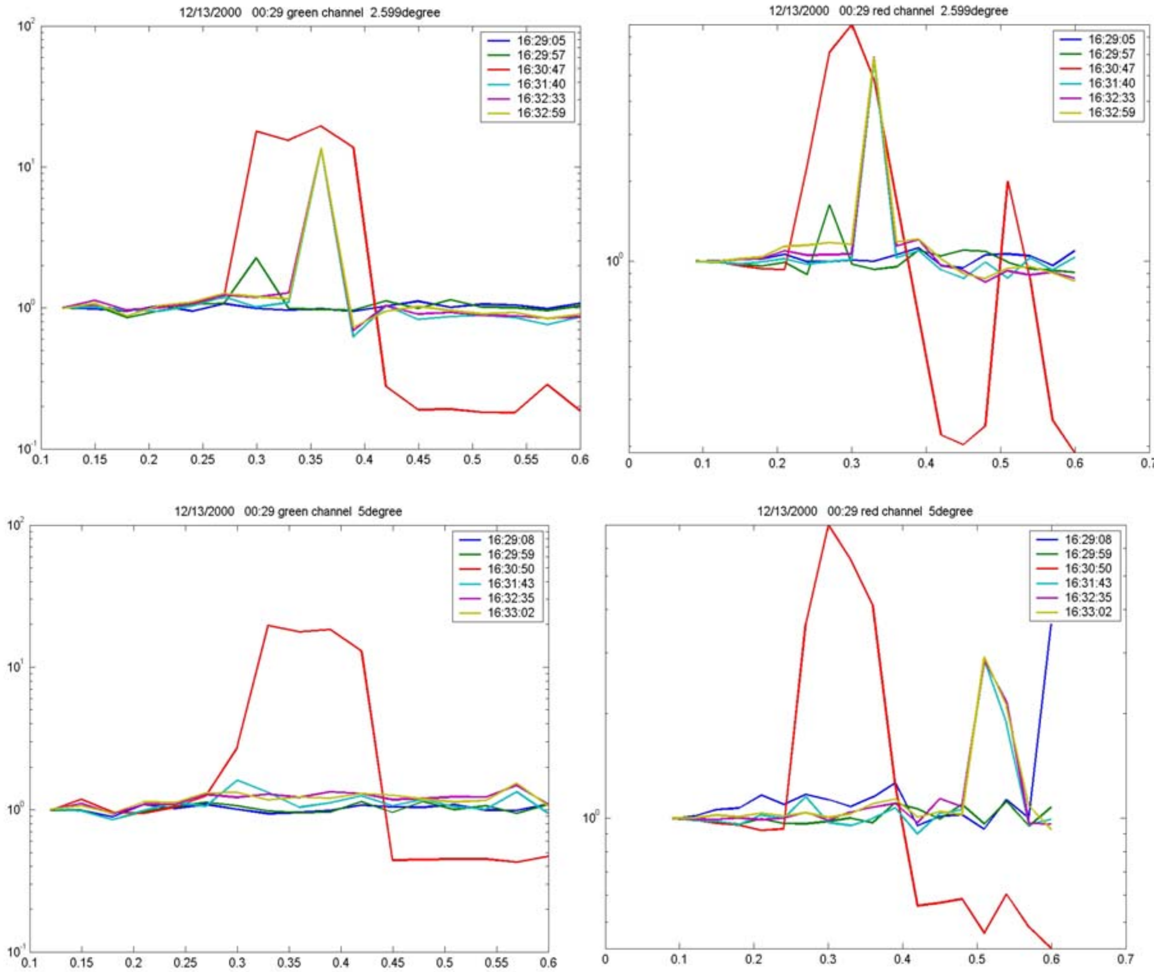

Figure D-5. (Contd.) The results from Test #2 are shown for both wavelengths at azimuth scan angles of -5^o (left), -2.5^o, 0^o, $+2.5^o$, and $+5^o$ (right). The test consisted of 5.5 kg of sieved dust being released at 16:31.

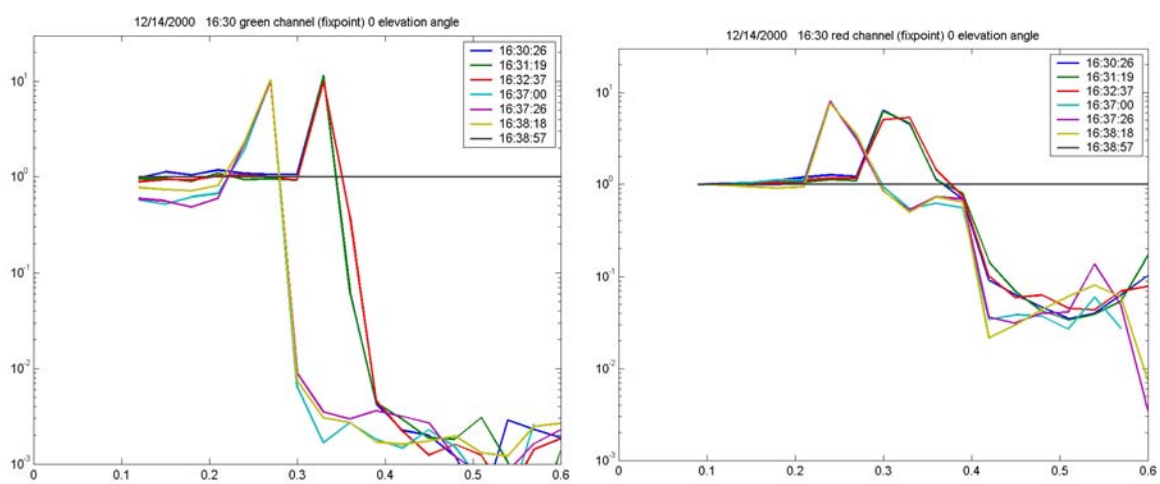

Figure D-6. Results from Test #10 show a slow drift and slow dissipation of a 5 kg dust cloud. The time gap is while scans were made at higher elevation angles.

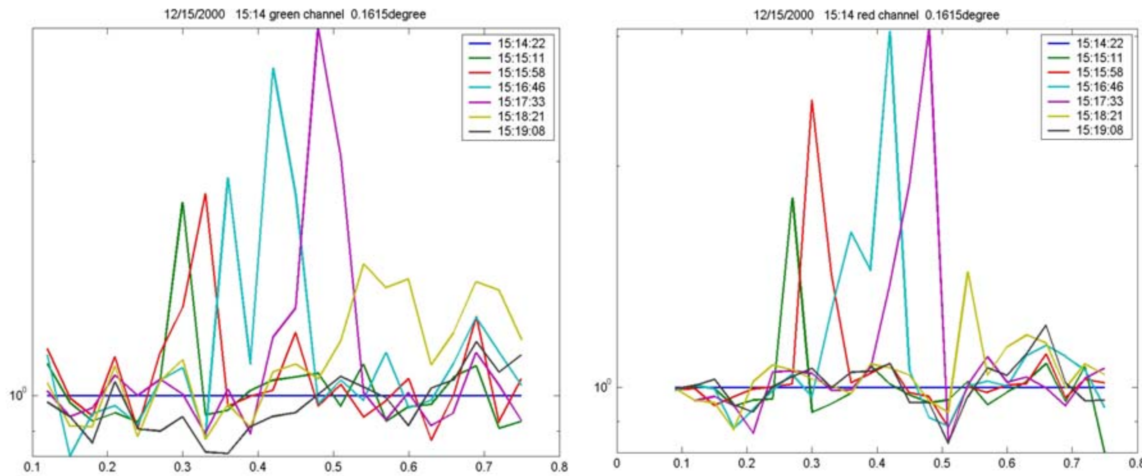

Figure D-7. The dust cloud generated by vehicle on an east-west path during Test #19 was irregular and most dust of small size particles being stirred up by the vehicle as evidenced by predominate backscatter signal at both wavelengths.

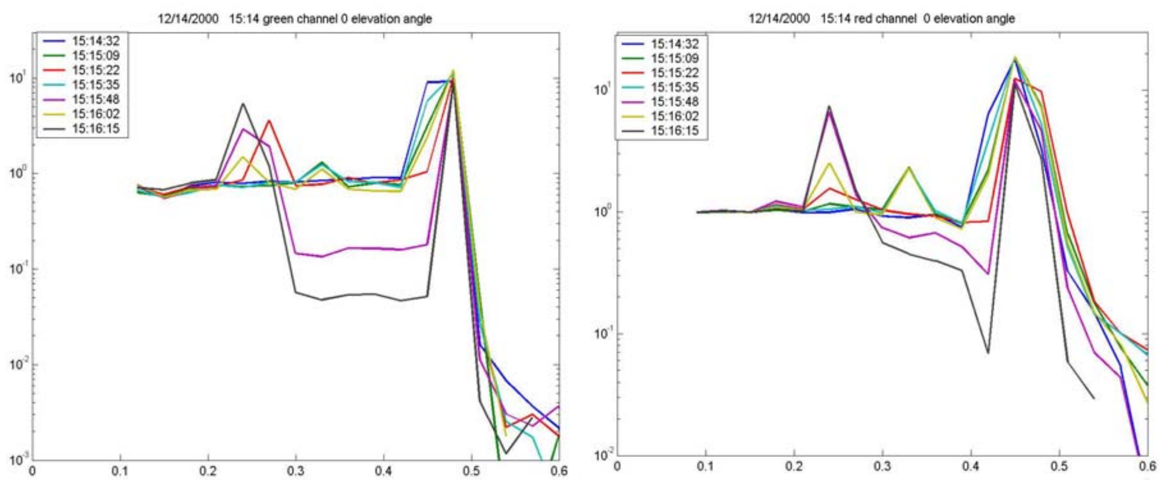

Figure D-8. Results from Test #7 show the backscatter and extinction from the white powder (calcium carbonate).

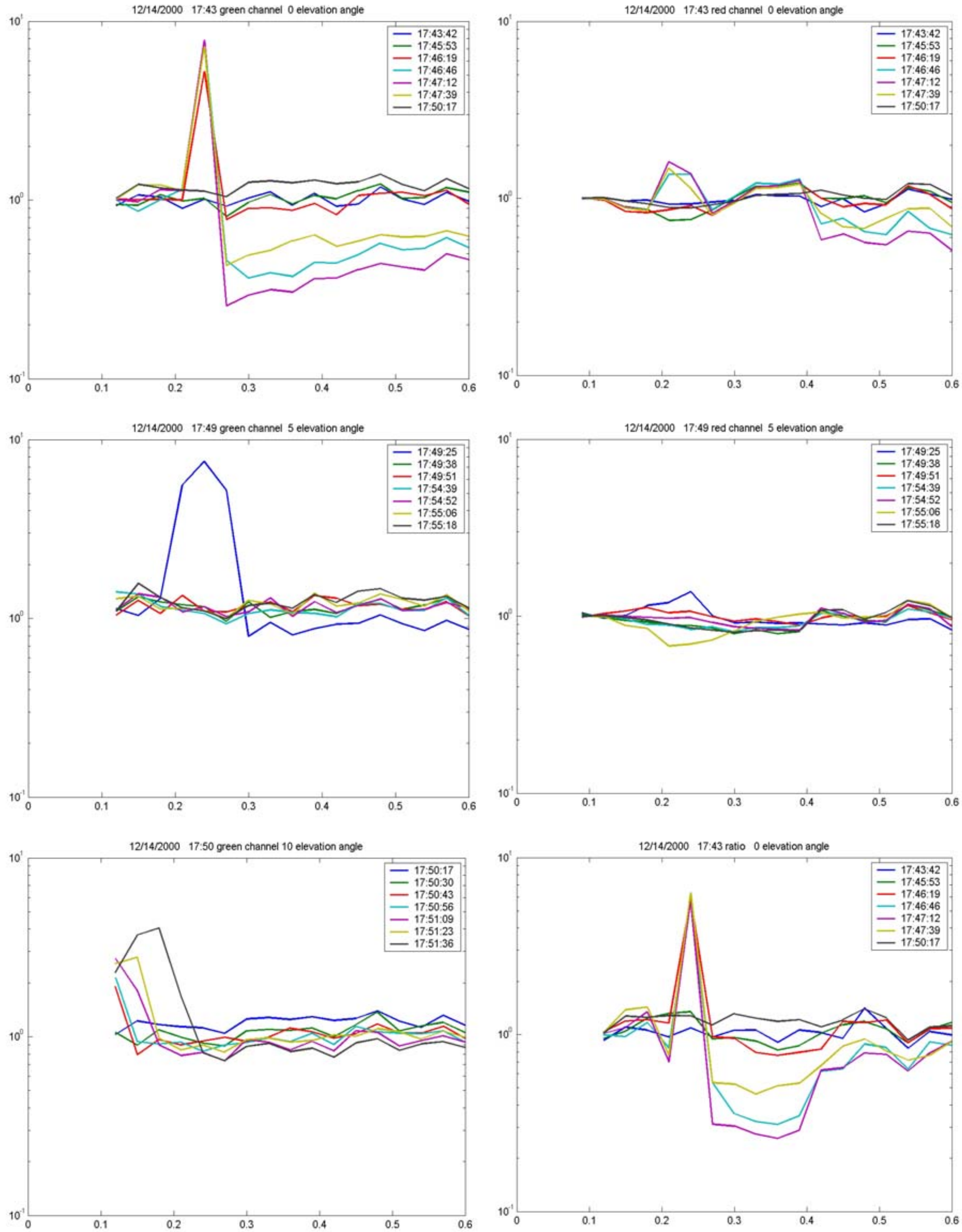

Figure D-9. Results from Test #13 show the response of the green and NIR channel in the upper four panels. The lower left panel shows the dust cloud at 10^{o} elevation angle being blown back over the instrument location. The lower right panel shows the ratios of the green/NIR signals that are useful in describing the changes in the particle properties, in this case it is due to changes in concentration.

Appendix E. Details of Events from the Main Study

Table E-1. Summary of meteorological conditions during the test period.

Date	AVE WS m/s	MAX WS m/sec	AVE WD Deg	Min T Deg C	MAX T Deg C	AVE T Deg C	AVE SR watt/cm^2
8-Dec	6.7	10.3	53.0	12.3	21.9	16.5	137.1
9-Dec	3.6	7.3	148.6	4.9	18.3	11.5	136.7
10-Dec	1.9	5.7	111.6	0.6	11.6	6.2	97.3
11-Dec	2.8	9.9	176.9	-0.2	13.2	5.8	129.8
12-Dec	2.2	6.3	166.2	0.9	15.4	7.8	133.3
13-Dec	1.6	3.5	152.9	-2.3	15.2	6.0	132.0
14-Dec	1.9	4.5	136.9	1.4	8.8	5.2	ISD
15-Dec	2.5	6.8	118.2	0.1	12.5	5.3	140.5
17-Dec	1.6	5.0	176.0	-1.4	17.6	7.4	133.6
18-Dec	2.8	6.5	89.7	-2.0	20.6	9.5	139.1
19-Dec	1.6	2.7	119.1	0.1	22.2	9.5	137.5

ISD= Insufficient data to calculate an average

Table E-2. Summary of the measurement tests that were conducted with the lidar scanning artificially created atmospheric dust plumes.

Test #	Date	Time	Test Type	Soil Type	Amount	Size	Comments
Test #1	12/12/2001	11:33	Scan 30^o@1^o/s	UCR Dust	838 gm	<425 micron	
Test #2	12/12/2001	11:49		UCR Dust	1 kg	<425 micron	
Test #3	12/12/2001	12:00		UCR Dust	1 kg	<425 micron	Dust generator above chamber
Test #4	12/12/2001	14:25	Scan 30^o@1^o/s	UCR Dust		<425 micron	1.9^o elevation
Test #5	12/12/2001	14:27		UCR Dust	2.45 kg	<75 micron	
Test #6	12/12/2001	15:02		UCR Dust	0.29 kg	<75 micron	
Test #7	12/12/2001	20:15	Chamber Test	CaCO3	~1 mg	2 micron	
Test #8	12/12/2001	20:20	Chamber Test	CaCO3	~2-3 mg	2 micron	
Test #9	12/12/2001	20:42	Chamber Test	UCR Dust	pinch	<75 micron	
Test #10	12/12/2001	20:48	Chamber Test	CaCO3	5 mg	2 micron	
Test #1	12/13/2001	10:26	Scan(1.6^o) 16^o@1^o/sec	CaCO3	2.5 kg	2micron	
Test #2	12/13/2001	10:42		CaCO3	2.5 kg	2micron	moved home position
Test #3	12/13/2001	10:58		CaCO3	2.5 kg	2micron	Test failed, program died
Test #4	12/13/2001	11:06		CaCO3	2.5 kg	2micron	
Test #5	12/13/2001	11:45	Fix point move elevation angle	CaCO3	2.5 kg	2micron	100 sec release
Test #6	12/13/2001	12:22	Fix point move elevation angle	CaCO3	2.5 kg	10micron	
Test #7	12/13/2001	12:39	Fix point move elevation angle	CaCO3	2.5 kg	10micron	Release till 12:41:00
Test #8	12/13/2001	12:55	Scan(1^o) 10^o@1^o/sec	CaCO3	2.5 kg	10micron	Release till 12:56:20
Test #9	12/13/2001	13:08		CaCO3	2.5 kg	15micron	Release till 13:09:15
Test #10	12/13/2001	13:18		CaCO3	2.5 kg	15micron	Release till 13:19:56
Test #11	12/13/2001	13:30		CaCO3	2.5 kg	8micron	Release till 13:32:50
Test #12	12/13/2001	13:43	Scan(1^o) 20^o@1^o/sec	CaCO3	2.5 kg	4micron	Release till 13:45:00
Test #13	12/13/2001	13:57		CaCO3	2.5 kg	0.7micron	Release till 13:58:35
Test #14	12/13/2001	14:09		CaCO3	2.5 kg	50%@200um 50%larger	Release till 14:10:00
Test #15	12/13/2001	14:20		CaCO3	2.5 kg	100micron	Release till 14:21:25
Test #16	12/13/2001	14:36		CaCO3	2.0kg	1kg@2um 1kg@15um	Release till 14:37:00
Test #17	12/13/2001	14:48		CaCO3	2.0kg	1kg@0.7um 1kg@10um	Release till 14:50:00
Test #18	12/13/2001	14:58		CaCO3	2.0kg	1kg@4um 1kg@100um	Release till 14:58:30
Test #19	12/13/2001	16:27		UCR dust	0.587kg	< 75 micron	Release till 16:28:30
Test #10	12/16/2001	7:09	Horiz scan 14o@1o/sec	UCR dust	1.5kg	< 75 micron	
	12/16/2001	7:11	Horiz scan 10o@1o/sec				
Test #11	12/16/2001	7:15	Horiz scan 10o@1o/sec	UCR dust	1.5kg	< 75 micron	
Test #12	12/16/2001	7:25		UCR dust	1.5kg	< 75 micron	
Test #13	12/16/2001	8:10		local dirt	1.5kg	< 425 micron	
Test #14	12/16/2001	8:16	Horiz scan 20o@1o/sec	CaCO3	1.5 kg	8 micron	
Test #15	12/16/2001	8:28		CaCO3	1.5 kg	15 micron	
	12/16/2001	8:32					Dust generator above chamber
Test #16	12/16/2001	8:34		CaCO3	1.5 kg	4 micron	
Test #17	12/16/2001	8:57		CaCO3	1.5 kg	0.7 micron	
Test #18	12/16/2001	9:08		CaCO3	1.5 kg	15 micron	
Test #18	12/16/2001	9:17		CaCO3	1.5 kg	4 micron	
Test #19	12/16/2001	9:21		CaCO3	1.5 kg	100 micron	
Test #20	12/16/2001	9:24		CaCO3	1.5 kg	10 micron	
till 10:05	12/19/2001	8:00	Vertical profile 30o				
Test #38	12/19/2001	10:15	horiz star (0.9o)	CaCo3	300 g	4 micron	
Test #39	12/19/2001	10:18		CaCo3	300 g	75 micron	
Test #40	12/19/2001	10:25		Kearney	300 g	< 425 micron	
Test #41	12/19/2001	10:27		Kearney	1.5kg	< 425 micron	
Test #42	12/19/2001	10:39		CaCo3	600 g	0.7 micron	
Test #43	12/19/2001	10:45		CaCo3	600 g	10 micron	
Test #44	12/19/2001	10:50		CaCo3	300 g	0.7 micron	
Test #45	12/19/2001	11:04		CaCo3	600 g	4 micron	
Test #46	12/19/2001	11:11		CaCo3	600 g	300g@4um 300g@15um	
Test #47	12/19/2001	11:14		CaCo3	600 g	15 micron	
Test #48	12/19/2001	11:16		Shafter	600 g	< 70 micron	
Test #49	12/19/2001	11:27		CaCo3	600 g	15 micron	
Test #50	12/19/2001	11:30		CaCo3	600 g	100 micron	
Test #51	12/19/2001	11:35		CaCo3	600 g	200 micron	
Test #52	12/19/2001	11:40		CaCo3	600 g	100 micron	
Test #53	12/19/2001	11:45		CaCo3	600 g	4 micron	
Test #54	12/19/2001	11:48		Westside	900 g	< 425 micron	
Test #55	12/19/2001	11:51		Westside	900 g	< 425 micron	
	12/19/2001						
	12/19/2001	11:55	truck generate dust				
	12/19/2001	11:58	car generate dust				
	12/19/2001	12:43	truck generate dust				change elevation during test
	12/19/2001	13:23	back to fixpoint				
	~~12/19/2001~~	~~13:31~~	~~Vertical profile @28o~~				

Table E-3. Calibration tests performed on December 17, 2001

Test #	Date	Time	Test Type	Soil Type	Amount	Size	DT Ave mg/m3
Test #1	12/17/2001	5:28	Into Chamber	CaCO3	50 mg	0.7 micron	0.61
	12/17/2001	5:30	Open chamber				
Test #2	12/17/2001	5:35	Into Chamber	CaCO3	800 mg	0.7 micron	7.33
	12/17/2001	5:37	Open chamber				
Test #3	12/17/2001	5:48	Into Chamber	CaCO3	50 mg	2 micron	1.17
	12/17/2001	5:50	Open chamber				
Test #4	12/17/2001	5:55	Into Chamber	CaCO3	800 mg	2 micron	7.63
	12/17/2001	5:57	Open chamber				
Test #5	12/17/2001	6:01	Into Chamber	CaCO3	50 mg	4 micron	1.70
	12/17/2001	6:02	Open chamber				
Test #6	12/17/2001	6:06	Into Chamber	CaCO3	800 mg	4 micron	8.48
	12/17/2001	6:08	Open chamber				
Test #7	12/17/2001	6:12	Into Chamber	CaCO3	50 mg	8 micron	1.82
	12/17/2001	6:13	Open chamber				
Test #8	12/17/2001	6:16	Into Chamber	CaCO3	800 mg	8 micron	5.33
	12/17/2001	6:17	Open chamber				
Test #9	12/17/2001	6:25	Into Chamber	CaCO3	50 mg	10 micron	2.07
	12/17/2001	6:27	Open chamber				
Test #10	12/17/2001	6:31	Into Chamber	CaCO3	800 mg	10 micron	5.13
	12/17/2001	6:33	Open chamber				
Test #11	12/17/2001	6:40	Into Chamber	CaCO3	50 mg	15 micron	1.20
	12/17/2001	6:42	Open chamber				
Test #12	12/17/2001	6:46	Into Chamber	CaCO3	800 mg	15 micron	3.24
	12/17/2001	6:48	Open chamber				
Test #13	12/17/2001	6:54	Into Chamber	CaCO3	50 mg	100 micron	
	12/17/2001	6:56	Open chamber				
Test #14	12/17/2001	6:58	Into Chamber	CaCO3	800 mg	100 micron	2.44
	12/17/2001	7:00	Open chamber				
Test #15	12/17/2001	7:08	Into Chamber	CaCO3	50 mg	100 micron	0.47
	12/17/2001	7:10	Open chamber				
Test #16	12/17/2001	7:14	Into Chamber	Az Road Dust	50 mg		0.49
	12/17/2001	7:16	Open chamber				
Test #17	12/17/2001	7:20	Into Chamber	Az Road Dust	200 mg		1.73
	12/17/2001	7:21	Open chamber				
Test #18	12/17/2001	7:30	Into Chamber	Az Road Dust	800 mg		10.58
	12/17/2001	7:32	Open chamber				
Test #19	12/17/2001	7:39	Into Chamber	UCR dust	50 mg	< 75 micron	0.77
	12/17/2001	7:41	Open chamber				
Test #20	12/17/2001	7:46	Into Chamber	UCR dust	200 mg	< 75 micron	0.74
	12/17/2001	7:48	Open chamber				
Test #21	12/17/2001	7:54	Into Chamber	UCR dust	800 mg	< 75 micron	1.80
	12/17/2001	7:56	Open chamber				
Test #22	12/17/2001	8:04	Into Chamber	Shafter	50 mg		0.17
	12/17/2001	8:06	Open chamber				
Test #23	12/17/2001	8:10	Into Chamber	Shafter	200 mg		0.50
	12/17/2001	8:12	Open chamber				
Test #24	12/17/2001	8:17	Into Chamber	Shafter	800 mg		1.88
	12/17/2001	8:19	Open chamber				
Test #25	12/17/2001	8:27	Into Chamber	Westside	50 mg		0.22
	12/17/2001	8:29	Open chamber				
Test #26	12/17/2001	8:33	Into Chamber	Westside	200 mg		0.48
	12/17/2001	8:35	Open chamber				
Test #27	12/17/2001	8:40	Into Chamber	Westside	800 mg		1.59
	12/17/2001	8:42	Open chamber				
Test #28	12/17/2001	8:49	Into Chamber	Kearney	50 mg		0.25
	12/17/2001	8:51	Open chamber				
Test #29	12/17/2001	8:57	Into Chamber	Kearney	200 mg		0.11
	12/17/2001	8:58	Open chamber				
Test #30	12/17/2001	9:02	Into Chamber	Kearney	800 mg		1.55
	12/17/2001	9:03	Open chamber				
	12/17/2001						

Table E-4. Lidar calibration tests performed on December 19, 2001.

Test #	Date	Time	Test Type	Soil Type	Amount	Size	DT Ave mg/m3
Test #1	12/19/2001	4:42	Into Chamber	CaCO3	50 mg	0.7 micron	1.01
	12/19/2001	4:43	Open chamber				
Test #2	12/19/2001	4:48	Into Chamber	CaCO3	200 mg	0.7 micron	0.80
	12/19/2001	4:49	Open chamber				
Test #3	12/19/2001	4:55	Into Chamber	CaCO3	800 mg	0.7 micron	0.49
	12/19/2001	4:56	Open chamber				
Test #4	12/19/2001	5:02	Into Chamber	CaCO3	50 mg	2 micron	0.74
	12/19/2001	5:03	Open chamber				
Test #5	12/19/2001	5:08	Into Chamber	CaCO3	200 mg	2 micron	1.73
	12/19/2001	??	Open chamber				
Test #6	12/19/2001	5:20	Into Chamber	CaCO3	800 mg	2 micron	5.57
	12/19/2001	5:21	Open chamber				
Test #7	12/19/2001	5:26	Into Chamber	CaCO3	50 mg	4 micron	1.52
	12/19/2001	5:27	Open chamber				
Test #8	12/19/2001	5:33	Into Chamber	CaCO3	200 mg	4 micron	1.54
	12/19/2001	5:34	Open chamber				
Test #9	12/19/2001	5:37	Into Chamber	CaCO3	800 mg	4 micron	3.73
	12/19/2001	5:38	Open chamber				
Test #10	12/19/2001	5:43	Into Chamber	CaCO3	50 mg	10 micron	1.16
	12/19/2001	5:44	Open chamber				
Test #11	12/19/2001	5:49	Into Chamber	CaCO3	200 mg	10 micron	1.89
	12/19/2001	5:50	Open chamber				
Test #12	12/19/2001	5:54	Into Chamber	CaCO3	800 mg	10 micron	3.00
	12/19/2001	5:55	Open chamber				
Test #13	12/19/2001	6:40	Into Chamber	CaCO3	50 mg	15 micron	0.81
	12/19/2001	6:41	Open chamber				
Test #14	12/19/2001	6:04	Into Chamber	CaCO3	200 mg	15 micron	1.00
	12/19/2001	6:05	Open chamber				
Test #15	12/19/2001	6:08	Into Chamber	CaCO3	800 mg	15 micron	1.91
	12/19/2001	6:09	Open chamber				
Test #16	12/19/2001	6:13	Into Chamber	Az Road dust	50 mg		0.35
	12/19/2001	6:14	Open chamber				
Test #17	12/19/2001	6:17	Into Chamber	Az Road dust	200 mg		0.75
	12/19/2001	6:18	Open chamber				
Test #18	12/19/2001	6:21	Into Chamber	Az Road dust	800 mg		3.31
	12/19/2001	6:22	Open chamber				
Test #19	12/19/2001	6:26	Into Chamber	UCR dust	50 mg	< 425 micron	0.32
	12/19/2001	6:27	Open chamber				
Test #20	12/19/2001	6:30	Into Chamber	UCR dust	200 mg	< 425 micron	0.49
	12/19/2001	6:31	Open chamber				
Test #21	12/19/2001	6:34	Into Chamber	UCR dust	800 mg	< 425 micron	0.65
	12/19/2001	6:35	Open chamber				
Test #22	12/19/2001	6:38	Into Chamber	Kearney	50 mg		0.19
	12/19/2001	6:39	Open chamber				
Test #23	12/19/2001	6:43	Into Chamber	Kearney	200 mg		0.20
	12/19/2001	6:44	Open chamber				
Test #24	12/19/2001	6:46	Into Chamber	Kearney	800 mg		0.53
	12/19/2001	6:47	Open chamber				
Test #25	12/19/2001	6:51	Into Chamber	Kearney	3.2 g		1.23
	12/19/2001	6:52	Open chamber				
Test #26	12/19/2001	6:59	Into Chamber	Westside	50 mg		0.09
	12/19/2001	7:00	Open chamber				
Test #27	12/19/2001	7:03	Into Chamber	Westside	200 mg		0.13
	12/19/2001	7:04	Open chamber				
Test #28	12/19/2001	7:07	Into Chamber	Westside	800 mg		0.32
	12/19/2001	7:08	Open chamber				
Test #29	12/19/2001	7:12	Into Chamber	Westside	3.2 g		0.81
	12/19/2001	7:13	Open chamber				
Test #30	12/19/2001	7:18	Into Chamber	Shafter	200 mg		0.07
	12/19/2001	7:19	Open chamber				
Test #31	12/19/2001	7:22	Into Chamber	Shafter	800 mg		0.10
	12/19/2001	7:23	Open chamber				
Test #32	12/19/2001	7:25	Into Chamber	Shafter	3.2 g		0.54
	12/19/2001	7:26	Open chamber				
Test #33	12/19/2001	7:32	Into Chamber	CaCO3	50 mg	0.7 micron	0.13
	12/19/2001	7:33	Open chamber				
Test #34	12/19/2001	7:37	Into Chamber	CaCO3	200 mg	0.7 micron	0.13
	12/19/2001	7:38	Open chamber				
Test #35	12/19/2001	7:41	Into Chamber	CaCO3	800 mg	0.7 micron	1.54
	12/19/2001	7:42	Open chamber				
Test #36	12/19/2001	7:47	Into Chamber	CaCO3	50 mg	2 micron	0.87
	12/19/2001	7:48	Open chamber				
Test #37	12/19/2001	7:52	Into Chamber	CaCO3	200 mg	2 micron	1.14
	12/19/2001	7:53	Open chamber				

A Climet optical particle counter was used to measure the concentrations of the particles in 16 size groups covering the range from the accumulation mode (0.5 μm) through part of the course size range (10 μm). The instrument results for measurements on $CaCO_4$ powders of three sizes, 0.7, 4 and 15 mm, are shown in Figure E-1. Table E-5 provides an example of measurements obtained on particle size during a part of the tests on 19 December 2002.

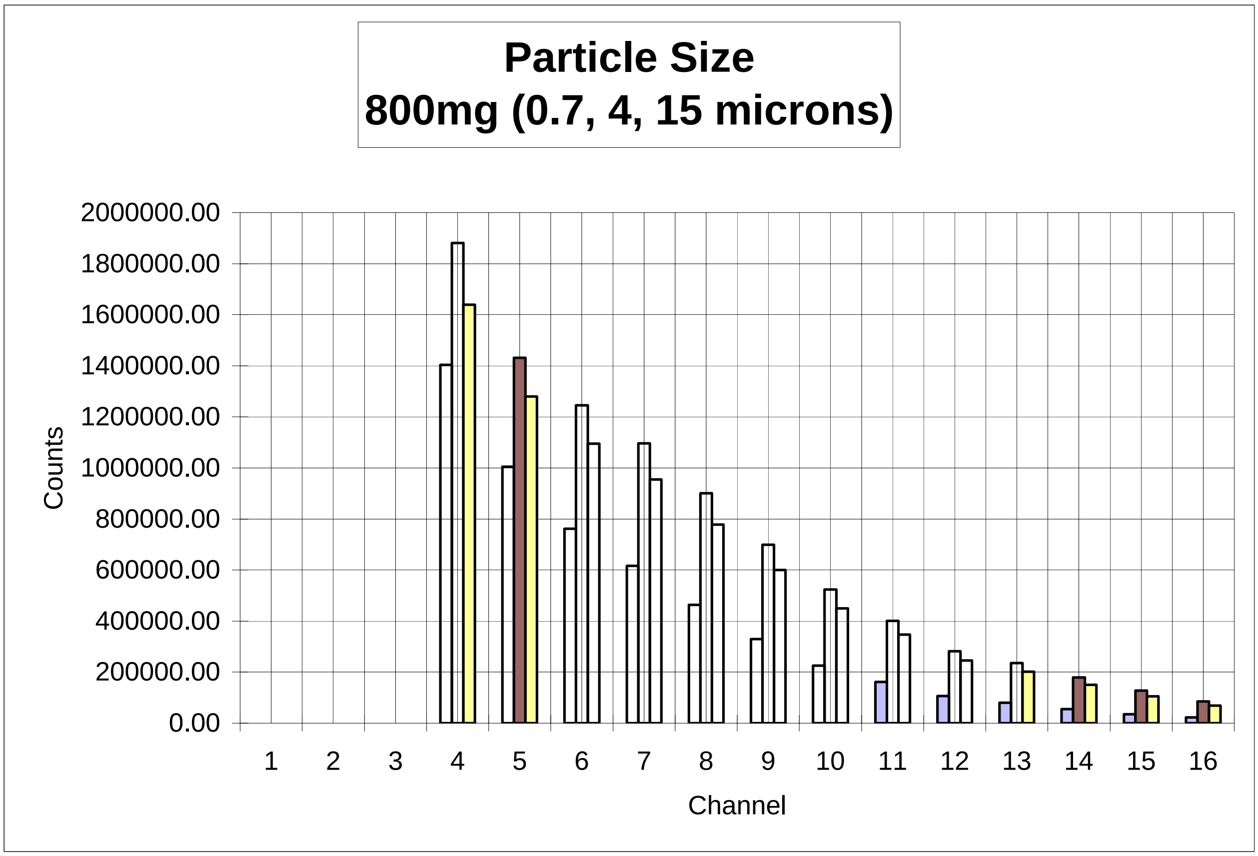

Figure E-1. Example of the Climet Data on particle size from 19 December 2002.

Table E-5. Data list from the Climet particle spectrometer on 19 December 2002.

A	Test	micron																			
08:01:43,DEM		,4	1.26	42.2	60.4	385598	254553	188459	151445	113198	78734	52363	35863	23327	14708	7886	3932	1855	713	258	9
08:00:43,DEM		,4	1.23	42.6	59.6	450915	305553	229482	186455	141417	100365	68222	48151	31767	20561	11557	6057	2959	1213	441	17
07:59:43,DEM		,4	1.22	42.6	60.8	512155	357049	272034	224037	172893	125293	88057	63842	43448	29898	18170	10373	5562	2463	993	39
07:58:43,DEM		,4	1.18	42.2	61.6	586696	419165	324703	269951	211865	157873	115310	87320	61253	45179	30323	19556	11740	6147	2850	125
07:57:43,DEM		,4	1.25	42.2	61.2	207148	131927	96683	78082	59947	44075	32123	24340	17049	12808	8829	5876	3713	2125	1098	55
07:56:43,DEM		,4	1.16	41.8	61.6	173197	77889	57515	48440	40244	33474	27893	23824	21510	20266	18775	17065	15221	12880	10276	748
07:55:43,DEM		,4	1.24	41.0	62.8	160732	88482	61221	48300	36530	27016	20124	15927	12428	10014	7741	6078	4672	3379	2406	173
07:54:43,DEM		,4	1.18	41.0	62.8	548629	367458	266957	210428	153361	104646	69897	49223	33384	22495	13440	7662	4008	1864	689	28
07:53:43,DEM	#37~200mg	2,4	1.18	41.0	62.4	1029459	747456	567209	457432	341809	240851	165920	120303	81446	60118	39396	24593	14688	7603	3501	158
07:52:43,DEM		,4	1.21	41.0	62.8	96916	45847	29134	22242	16658	12292	9180	7068	5314	3994	2752	1865	1220	667	351	17
07:51:43,DEM		,4	1.22	40.6	63.2	103674	46122	27088	19349	13495	9170	6330	4616	3390	2351	1487	958	588	316	158	7
07:50:43,DEM		,4	1.17	40.6	64.0	196759	108263	71683	54205	38069	25289	16488	11360	7792	5071	2978	1718	953	447	205	9
07:49:43,DEM		,4	1.20	40.2	63.6	529304	346048	245877	191653	138479	93162	61016	41974	28074	18499	10682	5890	3009	1333	529	21
07:48:43,DEM	#36~50mg	2,4	1.22	39.8	64.4	954423	671424	495052	393063	288167	198656	132877	93801	62256	43592	27069	15940	8880	4346	1900	83
07:47:43,DEM		,4	1.17	40.2	63.2	99382	48960	32397	25379	19485	14711	11093	8703	6443	4895	3405	2278	1392	765	359	15
07:46:43,DEM		,4	1.16	40.2	64.0	69453	23613	10709	6638	4106	2654	1852	1384	1035	752	496	346	214	122	68	3
07:45:43,DEM		,4	1.21	40.6	64.0	118612	55043	32897	23959	16604	11078	7238	5077	3521	2318	1392	840	491	256	109	5
07:44:43,DEM		,4	1.23	40.2	63.2	224313	123642	81464	61689	44019	29723	19604	13530	9329	6176	3684	2218	1247	629	282	13
07:43:43,DEM		,4	1.25	41.0	62.8	749767	495182	354580	278473	203599	140126	93276	65242	43443	30074	18537	11054	6312	3166	1423	65
07:42:43,DEM	#35~800mg	0.7,4	1.26	41.4	60.8	1403470	1E+06	761356	616188	463261	329343	226148	161432	106819	80439	54547	35420	22232	12759	6833	369
07:41:43,DEM		,4	1.24	41.4	60.0	107583	63506	48813	41384	33915	27023	21095	16752	12196	9794	7185	5129	3567	2237	1294	76
07:40:43,DEM		,4	1.19	41.0	60.8	66277	28583	17251	12881	9465	6799	4875	3753	2836	2107	1454	954	599	338	161	8
07:39:43,DEM		,4	1.23	41.0	61.2	98525	49688	32706	25324	18806	13484	9553	7210	5422	3918	2645	1748	1074	579	255	11
07:38:43,DEM	#34~200mg	0.7,4	1.27	40.6	62.0	179387	105131	74177	59084	44795	32711	23751	18160	13696	10220	7058	4967	3332	2003	1111	61
07:37:43,DEM		,4	1.25	40.2	63.6	68630	30781	19406	14899	11306	8341	6306	4934	3814	2865	2024	1410	945	575	328	19
07:36:43,DEM		,4	1.19	39.8	64.8	71415	31707	19647	14798	11040	8032	5857	4522	3401	2486	1651	1040	614	314	147	5
07:35:43,DEM		,4	1.18	39.8	66.4	82359	38876	24888	19145	14418	10431	7594	5846	4450	3196	2076	1335	776	367	149	6
07:34:43,DEM		,4	1.18	39.4	65.2	95252	47909	32007	24822	18645	13643	9915	7668	5816	4231	2851	1863	1137	599	275	12
07:33:43,DEM	#33~50mg	0.7,4	1.19	39.0	65.6	123547	66208	45492	35999	27468	20278	14945	11524	8864	6691	4694	3247	2118	1248	665	34
07:32:43,DEM		,4	1.24	38.6	66.4	60035	23898	13778	10200	7657	5784	4500	3648	2922	2301	1655	1130	734	421	212	11
07:31:43,DEM		,4	1.21	37.8	67.6	59841	22943	13017	9434	7068	5327	4080	3306	2638	1984	1376	936	578	316	140	6
07:30:43,DEM		,4	1.16	37.4	68.4	63145	24996	14346	10499	7900	5967	4602	3696	2893	2161	1465	995	594	316	140	6
07:29:43,DEM		,4	1.14	37.0	69.2	72853	32444	20903	16376	12794	9813	7582	5972	4614	3360	2280	1429	827	445	212	9
07:28:43,DEM		,4	1.18	36.6	70.0	87996	44993	32109	26557	21770	17235	13532	10871	8443	6228	4085	2554	1468	714	319	12

07:27:43,DEM				,4	1.15	36.2	71.2	146175	94296	77103	68104	58457	47997	38533	31469	24389	18465	12477	7941	4523	2069	849	31
07:26:43,DEM	#32	3.2g Shafter	<425	,4	1.25	35.4	71.2	229085	170794	148785	135671	119822	102234	85456	72249	57721	46670	34801	24434	15927	8794	4077	185
07:25:43,DEM				,4	1.18	35.4	71.6	63295	21996	10698	6951	4820	3613	2903	2462	2102	1736	1310	948	621	364	176	9
07:24:43,DEM				,4	1.16	35.4	71.2	78403	33951	21199	16542	13263	10448	8225	6595	5156	3832	2595	1660	1007	471	192	6
07:23:43,DEM	#31	800mg Shafter	<425	,4	1.16	35.8	70.4	138081	86199	70196	62215	53746	44706	36332	29977	23789	18560	13231	8891	5582	2976	1327	54
07:22:43,DEM				,4	1.24	35.4	72.4	74917	31386	19213	15026	12404	10375	8764	7524	6134	5050	3819	2748	1861	1059	548	25
07:21:43,DEM				,4	1.16	35.0	74.0	67196	22999	10986	7069	4885	3603	2843	2320	1903	1511	1130	840	545	306	157	5
07:20:43,DEM				,4	1.30	34.2	75.2	77919	31296	18247	13666	10485	8175	6367	5173	4081	3049	2123	1372	825	415	201	9
07:19:43,DEM	#30	200mg Shafter	<425	,4	1.22	33.0	76.0	120324	68958	52745	45438	38453	31812	26072	21916	17849	14282	10654	7635	5019	2937	1418	69
07:18:43,DEM				,4	1.18	32.6	76.0	76201	29188	15692	11043	8048	6075	4664	3748	2996	2326	1626	1097	692	363	158	6
07:17:43,DEM				,4	1.17	31.8	75.2	83448	33818	19536	14433	10751	8068	6164	4957	3902	2918	2022	1301	787	404	170	6
07:16:43,DEM				,4	1.30	31.4	73.6	97076	44135	28199	21998	17043	12942	9820	7652	5843	4232	2730	1741	999	511	217	7
07:15:43,DEM				,4	1.24	31.8	74.0	120942	63361	45191	37238	30018	23219	17815	14037	10636	7679	5009	3147	1759	843	343	13
07:14:43,DEM				,4	1.20	31.4	72.8	197903	129846	105176	91956	77130	62068	48868	39302	30168	22880	15592	9894	5655	2674	1080	40
07:13:43,DEM	#29	3.2g Westside	<425	,4	1.20	31.8	72.4	365798	290926	255522	231866	202667	170900	141978	119841	94145	77925	59843	43510	29154	16784	8305	378
07:12:43,DEM				,4	1.21	32.2	74.8	97093	45722	30997	25491	21306	18083	15448	13553	11366	9812	8143	6551	5054	3526	2199	135
07:11:43,DEM				,4	1.27	32.6	76.0	85670	34858	19918	14805	11013	8184	6104	4736	3677	2710	1795	1102	630	318	131	5
07:10:43,DEM				,4	1.25	32.6	76.4	92415	40782	25522	19805	15416	11752	8976	7121	5553	4040	2661	1663	935	443	180	7
07:09:43,DEM				,4	1.26	32.6	76.0	125707	69165	51136	43235	35430	28052	21885	17698	13793	10272	6922	4332	2448	1124	426	16
07:08:43,DEM	#28	800mg Westside	<425	,4	1.24	32.2	75.2	166799	106829	86359	75721	64486	52907	43050	35775	28791	22893	16746	11594	7408	4037	1820	81
07:07:43,DEM				,4	1.24	32.2	74.4	87120	36612	21819	16508	12744	9744	7603	6187	4920	3862	2821	2036	1405	825	463	24
07:06:43,DEM				,4	1.22	33.0	72.4	91184	37496	21787	16163	11945	8708	6445	5081	3832	2822	1807	1152	640	299	118	4
07:05:43,DEM				,4	1.20	33.0	71.2	103106	46186	29241	22579	17344	13055	9822	7693	5856	4199	2724	1615	884	405	169	6
07:04:43,DEM	#27	200mg Westside	<425	,4	1.22	33.0	70.8	132591	71439	51794	42974	34909	27428	21364	17159	13374	10191	7026	4601	2852	1469	624	27
07:03:43,DEM				,4	1.22	34.2	72.4	86800	33889	18794	13412	10001	7469	5756	4589	3602	2671	1914	1263	802	417	189	8
07:02:43,DEM				,4	1.22	33.8	75.2	88811	34237	18827	13396	9863	7314	5456	4293	3317	2386	1546	969	530	257	108	4
07:01:43,DEM				,4	1.21	32.6	74.4	95109	38190	21918	16066	12176	9232	7066	5592	4349	3221	2163	1363	756	365	149	6
07:00:43,DEM	#26	50mg Westside	<425	,4	1.17	33.0	73.6	112154	53712	35847	28910	23380	18457	14602	11899	9425	7247	5057	3295	1979	1018	456	17
06:59:43,DEM				,4	1.16	33.0	71.2	86637	30828	15116	10013	6878	5018	3861	3139	2536	1888	1321	893	571	297	138	5
06:58:43,DEM				,4	1.19	33.8	70.0	83620	30301	15204	10145	7193	5282	4133	3365	2728	2101	1492	1010	610	301	131	5
06:57:43,DEM				,4	1.21	34.6	71.2	80737	30831	16723	11846	8723	6560	5000	4005	3211	2425	1683	1098	648	310	136	5
06:56:43,DEM				,4	1.21	34.6	73.2	82792	33180	18936	14027	10579	7985	6245	5086	4111	3133	2163	1450	903	468	199	8
06:55:43,DEM				,4	1.20	33.8	73.6	84373	33679	19181	14075	10688	8160	6375	5129	4186	3172	2222	1499	935	516	239	12
06:54:43,DEM				,4	1.22	33.8	73.6	95473	41296	25575	19840	15594	12190	9477	7587	5945	4431	3067	1937	1228	644	283	12
06:53:43,DEM				,4	1.19	33.8	73.6	275501	200744	171126	153314	131623	107300	84329	66962	48943	36960	24825	15021	8194	3630	1315	47
06:52:43,DEM	#25	3.2g Kearney	<425	,4	1.17	33.8	73.6	601005	505889	458949	423489	375061	318558	263209	219225	164189	1E+05	1E+05	72614	47721	26527	12660	582

06:51:43,DEM		,4	1.25	33.8	75.2	88055	30759	14899	9693	6679	4802	3794	3130	2545	1977	1479	1058	660	365	156	6
06:50:43,DEM		,4	1.17	33.4	75.6	90275	31486	14636	9110	6116	4360	3296	2669	2177	1663	1210	844	540	264	104	4
06:49:43,DEM		,4	1.27	33.0	75.6	94805	33760	16767	11158	7826	5684	4433	3572	2839	2218	1594	1133	763	480	296	20
06:48:43,DEM		,4	1.19	32.6	76.8	196676	121094	93759	79817	65121	50530	38163	29278	21361	15531	9946	5849	3163	1377	495	18
06:47:43,DEM #24	800mg Kearney	<425,4	1.17	32.2	76.0	471282	371432	319872	285354	242297	195409	153771	123239	91202	71625	51035	34231	21164	11170	4913	209
06:46:43,DEM		,4	1.25	31.8	75.2	124126	60024	41041	33716	27897	23028	19156	16099	12377	10362	8127	6067	4179	2493	1311	60
06:45:43,DEM		,4	1.27	32.6	74.4	124427	58092	36891	28345	21474	15905	11611	8842	6575	4689	2985	1733	963	430	167	6
06:44:43,DEM #23	200mg Kearney	<425,4	1.19	33.0	74.4	225711	145259	113258	95945	78113	60175	45444	35754	27155	20322	13837	9017	5400	2658	1053	41
06:43:43,DEM		,4	1.23	33.4	74.8	89222	29531	12775	7537	4828	3330	2628	2179	1811	1421	1047	750	469	254	108	4
06:42:43,DEM		,4	1.20	33.0	75.6	89482	29887	13151	8062	5160	3664	2869	2403	2025	1586	1204	852	583	317	142	6
06:41:43,DEM		,4	1.23	33.0	75.6	90559	31967	15390	9887	6599	4613	3524	2838	2249	1762	1260	896	587	291	137	4
06:40:43,DEM		,4	1.21	32.6	74.8	140618	71348	47374	36766	27612	20020	14392	10896	8039	5720	3605	2130	1133	486	180	7
06:39:43,DEM #22	50mg Kearney	<425,4	1.24	33.0	75.6	296451	197292	152236	126951	100409	75501	56249	44113	33226	25347	17510	11509	6790	3368	1430	57
06:38:43,DEM		,4	1.25	32.6	76.0	116465	54732	36382	28972	23114	18438	14868	12322	9471	7820	6055	4408	2945	1648	746	31
06:37:43,DEM		,4	1.21	32.6	76.0	89408	30433	14307	9122	6224	4517	3562	2943	2434	1941	1418	971	649	344	164	8
06:36:43,DEM		,4	1.20	32.6	75.6	209281	134529	107510	93057	77402	61935	48265	38454	28604	21745	14621	8967	4801	2078	665	24
06:35:43,DEM #21	800mg UCR	<425,4	1.19	32.6	75.2	638594	528861	471592	429175	374025	313886	257696	215260	163638	1E+05	1E+05	74650	48527	26272	11716	488
06:34:43,DEM		,4	1.30	32.6	76.0	86659	28235	12400	7551	4860	3413	2658	2218	1835	1444	1052	720	459	246	107	5
06:33:43,DEM		,4	1.25	32.6	76.8	90136	30456	14045	8830	5875	4187	3232	2621	2111	1619	1184	796	503	252	121	5
06:32:43,DEM		,4	1.17	32.6	76.8	182037	108452	82642	69852	57033	44939	34461	27204	20515	15280	10092	5997	3156	1223	383	13
06:31:43,DEM #20	200mg UCR	<425,4	1.25	32.2	75.6	438395	344551	296976	265482	227879	188801	153645	127586	98420	80469	60030	41648	25903	12926	5284	208
06:30:43,DEM		,4	1.20	32.2	76.4	89371	32095	16145	10816	7583	5442	4177	3343	2636	1999	1386	943	582	290	141	6
06:29:43,DEM		,4	1.19	31.8	75.6	96247	38096	21541	15462	11335	8429	6381	4929	3869	2833	1858	1159	666	321	145	7
06:28:43,DEM		,4	1.24	31.4	75.2	144043	78549	56491	46312	36848	28565	21654	16905	12892	9507	6121	3619	1860	741	257	8
06:27:43,DEM #19	50mg UCR	<425,4	1.16	31.4	74.8	321778	238546	200049	175631	147704	120271	95887	78552	61319	48837	35021	23300	13591	6119	2173	79
06:26:43,DEM		,4	1.14	31.4	74.0	97024	42286	26158	19941	15424	11963	9296	7450	5881	4523	3162	2116	1304	663	285	11
06:25:43,DEM		,4	1.26	31.4	74.0	112186	53922	36700	29406	23089	17467	12876	9739	7156	4970	3098	1886	1050	505	210	9
06:24:43,DEM		,4	1.23	31.4	73.6	207906	136737	111226	96143	79181	61774	45580	34284	24585	16797	9643	5117	2430	1002	401	14
06:23:43,DEM		,4	1.21	31.4	73.2	661259	532007	471732	424754	362695	294090	227363	176902	123228	94927	63860	38552	20021	8014	2442	72
06:22:43,DEM #18	800mg AZ Road	,4	1.26	31.8	74.4	2014630	1E+06	1E+06	1E+06	1128984	976318	813614	676617	511440	4E+05	4E+05	272084	2E+05	1E+05	48201	###
06:21:43,DEM		,4	1.20	31.4	74.8	81272	29986	15618	10696	7621	5486	4080	3194	2507	1844	1251	820	524	279	137	6
06:20:43,DEM		,4	1.19	31.4	74.4	93489	39960	24382	18402	13841	10301	7696	5916	4506	3187	2027	1220	703	368	169	8
06:19:43,DEM		,4	1.28	31.4	74.0	208098	136965	109745	94185	76978	59879	44800	34018	24445	17373	10602	5869	2759	1035	331	12
06:18:43,DEM #17	200mg AZ Road	<425,4	1.16	31.8	74.4	677054	559201	491071	440015	374300	304019	238404	189778	136645	1E+05	74854	47971	27011	12029	4344	140
06:17:43,DEM		,4	1.26	31.8	72.0	97001	43279	28017	22062	17565	13875	10904	8838	6701	5203	3648	2371	1407	681	268	10
06:16:43,DEM		,4	1.18	33.0	74.0	91740	35251	19635	13755	9705	6808	4887	3707	2766	1942	1265	838	488	262	115	5

06:15:43,DEM		,4	1.19	33.0	72.4	184528	105154	75035	59984	45270	32446	22641	16439	11763	8005	4676	2548	1275	500	181	6
06:14:43,DEM #16	50mg AZ Road	<425,4	1.17	33.8	71.6	429998	303486	237633	197768	155121	115770	83508	62790	45589	33189	21264	12870	6970	3131	1194	45
06:13:43,DEM		,4	1.17	34.2	70.4	125989	61934	40745	31472	23447	16913	11975	8958	6589	4647	3044	1891	1117	535	238	10
06:12:43,DEM		,4	1.30	35.4	73.2	129091	62445	41076	31617	23444	16445	11378	8285	6034	4114	2551	1528	903	459	223	9
06:11:43,DEM		,4	1.22	35.4	73.6	220735	133987	98655	79540	60183	42292	28813	20780	14625	9850	5834	3291	1694	828	380	16
06:10:43,DEM		,4	1.22	35.0	74.0	658530	496297	400466	336471	263088	191724	134763	98863	67440	49265	31261	18492	9828	4332	1604	58
06:09:43,DEM #15	800 mg	15,4	1.25	35.0	74.0	1639643	1E+06	1E+06	954464	778091	600141	450086	347101	245783	2E+05	2E+05	105574	68308	38192	18401	842
06:08:43,DEM		,4	1.17	35.0	74.8	149112	81175	60564	50793	41419	32850	25781	20722	14936	12235	9298	6800	4676	2790	1461	74
06:07:43,DEM		,4	1.25	34.2	76.0	106699	45325	26168	18761	13369	8959	6142	4393	3161	2181	1309	751	388	171	73	3
06:06:43,DEM		,4	1.21	33.8	75.6	430043	302406	235731	194703	150280	107411	73971	53286	36901	25700	15649	8765	4450	1881	649	21
06:05:43,DEM #14	200 mg	15,4	1.17	33.8	75.6	1141364	903078	749179	640912	510974	382260	277357	209210	144886	1E+05	77431	50096	29999	15351	6714	281
06:04:43,DEM		,4	1.22	33.4	75.6	107050	47812	29207	21619	15641	11003	7898	6002	4536	3292	2209	1479	895	473	214	10
06:03:43,DEM		,4	1.17	33.4	75.6	125771	60039	37450	28102	20088	13713	9326	6711	4934	3361	2084	1311	761	413	196	8
06:02:43,DEM		,4	1.23	33.4	76.0	363494	243493	182654	147179	110043	76604	51351	36817	25487	17592	10506	5852	2999	1300	509	20
06:01:43,DEM #13	50 mg	15,4	1.23	33.0	75.2	937333	714956	570304	474852	366545	264429	185382	137102	95264	72370	49062	31529	18891	9706	4345	185
06:00:43,DEM		,4	1.22	33.0	75.2	215644	126899	102067	88590	74035	59792	47084	37398	27516	23268	18203	13478	9257	5649	2895	142
05:59:43,DEM		,4	1.19	33.0	74.8	115844	52140	32009	23592	16819	11524	7836	5623	4120	2826	1754	1122	684	383	169	7
05:58:43,DEM		,4	1.10	33.4	74.8	175392	97752	68110	53451	39600	27136	18031	12737	9028	5886	3492	1941	1078	509	219	9
05:57:43,DEM		,4	1.21	33.0	73.2	271983	172275	128206	103229	77561	53665	35949	25380	17704	11643	6698	3700	1913	884	379	15
05:56:43,DEM		,4	1.25	33.4	73.2	836220	630980	514539	433926	339265	246682	172248	125257	84431	63232	41445	24693	13141	5590	1991	68
05:55:43,DEM #12	800 mg	10,4	1.23	33.8	74.8	2388388	2E+06	2E+06	1E+06	1127573	882033	664977	511270	364156	3E+05	2E+05	167832	1E+05	59893	27549	###
05:54:43,DEM		,4	1.24	33.8	76.0	197879	111623	90231	79024	67216	55237	43895	35190	25871	21892	17228	12711	8838	5365	2709	127
05:53:43,DEM		,4	1.18	33.4	73.6	81658	27191	12296	7559	4792	3174	2313	1842	1468	1102	809	556	379	231	128	6
05:52:43,DEM		,4	1.21	34.2	72.8	266390	176827	140450	118496	93724	68162	47126	33870	23478	15586	8867	4616	2237	910	317	12
05:51:43,DEM		,4	1.23	35.4	74.8	662423	527627	447833	390047	316958	238585	171491	127375	87146	63117	39518	22563	11678	4855	1686	55
05:50:43,DEM #11	200 mg	10,4	1.09	35.8	74.0	1080828	873095	763641	678036	564437	442222	334810	260210	183303	1E+05	1E+05	72573	45627	24376	11341	495
05:49:43,DEM		,4	1.28	35.8	73.6	169027	93526	72701	62700	52750	43164	34889	28576	20967	17344	13569	9965	6996	4232	2194	109
05:48:43,DEM		,4	1.14	35.4	74.0	136225	63607	41169	31193	22471	15105	9877	6835	4674	2965	1644	927	529	279	128	6
05:47:43,DEM		,4	1.25	35.0	73.6	183077	98612	70103	55639	41449	28362	18473	12733	8632	5340	2862	1461	774	353	158	7
05:46:43,DEM		,4	1.29	35.0	73.6	301846	192408	148131	122178	93568	66048	44062	30837	20936	13406	7307	3693	1744	721	264	10
05:45:43,DEM		,4	1.20	35.4	72.8	474160	335685	268726	226133	176870	127287	87442	62716	42416	28702	16749	8943	4456	1826	642	21
05:44:43,DEM #10	50 mg	10,4	1.22	35.8	74.8	866542	672033	559896	481512	385525	287639	206827	154457	103561	78539	52944	33472	19471	9720	4250	177
05:43:43,DEM		,4	1.19	35.8	75.6	177538	96350	74699	64911	55156	45609	36770	29616	21126	17559	13421	9613	6345	3605	1717	80
05:42:43,DEM		,4	1.22	35.0	76.0	124934	56320	35337	26550	19239	13126	8783	6224	4507	3077	1908	1213	725	393	170	8
05:41:43,DEM		,4	1.25	34.2	74.8	193626	107443	76627	60868	45541	31290	20459	14343	9932	6420	3647	1990	1111	534	260	12
05:40:43,DEM		,4	1.15	35.0	74.4	366900	243075	187574	153973	117122	81712	54030	37672	25403	16860	9691	5179	2588	1041	435	18

05:39:43,DEM		,4	1.23	34.2	73.2	1138126	906804	752955	641582	505581	368389	256529	185662	120870	89415	57430	33800	18007	7974	3071	114
05:38:43,DEM #9	800 mg	4,4	1.21	33.4	73.6	1880574	1E+06	1E+06	1E+06	901595	699557	524196	401215	282383	2E+05	2E+05	127903	84587	48655	24252	###
05:37:43,DEM		,4	1.26	33.8	74.0	123565	60097	40934	33066	26569	21210	16909	13878	10429	8517	6544	4895	3445	2204	1218	64
05:36:43,DEM		,4	1.21	34.2	74.0	129231	60565	37423	27442	19110	12545	8086	5608	3913	2549	1494	901	483	246	94	4
05:35:43,DEM		,4	1.21	33.8	74.8	733624	536567	415835	337355	250291	169505	109096	74777	48421	33012	19086	10274	4900	1870	595	19
05:34:43,DEM #8	200 mg	4,4	1.15	33.0	73.2	2056941	2E+06	1E+06	1E+06	869514	628947	435289	312773	207755	2E+05	1E+05	72766	42355	20720	8677	353
05:33:43,DEM		,4	1.24	32.6	71.2	184284	112698	86775	72101	56567	42103	30301	22392	15362	11781	8037	5266	3217	1722	844	36
05:32:43,DEM		,4	1.15	32.6	70.8	117583	56210	34670	25327	17684	11450	7297	5073	3564	2349	1461	912	545	290	126	6
05:31:43,DEM		,4	1.20	34.2	71.6	165515	89699	59225	44509	31103	19983	12386	8264	5573	3483	1939	1068	569	274	128	5
05:30:43,DEM		,4	1.31	34.2	70.8	253473	151579	105273	80864	57430	37176	22923	15123	9944	6063	3256	1718	841	368	160	7
05:29:43,DEM		,4	1.27	34.2	71.6	441752	290614	210884	165368	119346	78587	49453	33312	22071	13884	7386	3723	1745	655	216	8
05:28:43,DEM		,4	1.16	33.8	71.2	838655	603706	457389	366987	271569	184934	120043	83054	55170	37164	21326	11322	5584	2284	791	27
05:27:43,DEM #7	50 mg	4,4	1.22	33.4	70.8	1345264	1E+06	814890	670442	508949	357526	242770	173593	116156	85986	55483	33840	19080	9227	3795	153
05:26:43,DEM		,4	1.22	33.4	69.6	93184	38293	20776	14377	9913	6824	4889	3726	2854	2108	1437	1007	628	357	180	8
05:25:43,DEM		,4	1.18	33.8	68.4	107953	47923	27681	19406	13376	9005	6170	4522	3388	2444	1618	1064	648	345	161	7
05:24:43,DEM		,4	1.18	34.2	68.0	146445	72645	44478	32136	22215	14578	9645	6839	5025	3436	2177	1375	842	453	201	9
05:23:43,DEM		,4	1.21	34.2	69.2	399432	244798	165772	124003	85758	54912	34160	22880	15575	10158	5773	3164	1661	775	333	14
05:22:43,DEM		,4	1.25	34.2	69.2	1989217	1E+06	1E+06	922536	683835	470080	309050	212234	138107	1E+05	67834	40254	21136	9245	3436	127
05:21:43,DEM #6	800 mg	2,4	1.21	34.2	68.8	3201076	2E+06	2E+06	2E+06	1298623	957872	673922	487159	334892	3E+05	2E+05	140452	87505	46522	21364	974
05:20:43,DEM		,4	1.19	34.2	69.2	181043	106273	81106	67506	53322	40584	30071	22826	16023	12953	9579	6696	4436	2566	1261	61
05:19:43,DEM		,4	1.17	34.2	68.4	88224	35823	19091	12815	8354	5319	3495	2489	1833	1279	851	541	332	176	78	3
05:18:43,DEM		,4	1.16	35.0	68.8	94970	40158	22317	15258	10110	6380	4093	2890	2069	1435	912	583	363	192	84	4
05:17:43,DEM		,4	1.20	34.6	71.6	110721	51270	30012	20903	13718	8407	5128	3368	2315	1445	844	489	285	156	59	3
05:16:43,DEM		,4	1.23	33.8	72.4	137227	69584	42741	30387	19952	12120	7173	4609	3061	1873	1071	634	351	198	92	4
05:15:43,DEM		,4	1.13	33.8	72.4	192444	107212	69539	50842	34214	21023	12379	7806	5008	2917	1460	777	404	172	74	3
05:14:43,DEM		,4	1.10	33.8	73.6	270754	163171	110180	82308	55992	34377	20099	12668	8042	4651	2320	1161	582	248	107	3
05:13:43,DEM		,4	1.23	33.4	72.4	417478	267368	186365	141286	97403	61161	36041	22797	14515	8557	4179	1904	853	337	138	6
05:12:43,DEM		,4	1.23	33.4	72.0	626070	422329	301630	231916	162322	103744	62568	40370	25697	15442	7767	3732	1627	631	223	8
05:11:43,DEM		,4	1.18	33.8	71.6	813089	566092	411290	320037	227528	147510	91648	60554	38803	24540	13091	6583	3047	1118	357	12
05:10:43,DEM		,4	1.19	33.4	70.8	1055812	765149	569164	449735	325966	217987	140152	95737	62644	42408	24729	13378	6787	2921	1030	36
05:09:43,DEM #5	200 mg	2,4	1.20	33.8	71.2	1539182	1E+06	897759	733869	553408	390761	267893	193008	130686	1E+05	70017	46047	28323	15315	7293	339
05:08:43,DEM		,4	1.20	34.2	71.2	140587	72041	56143	49069	42454	36048	29439	23925	17615	15113	12083	9198	6534	4115	2227	115
05:07:43,DEM		,4	1.10	34.6	70.8	73249	26340	12315	7459	4680	2920	1957	1456	1084	766	492	330	207	113	61	2
05:06:43,DEM		,4	1.25	35.0	70.4	102217	45049	25367	17516	11703	7481	4787	3321	2349	1520	895	517	295	138	67	2
05:05:43,DEM		,4	1.11	34.6	71.2	140915	70601	43543	31697	21885	14217	9023	6184	4360	2759	1558	876	463	201	77	3
05:04:43,DEM		,4	1.25	34.6	71.2	280820	167566	114929	87834	62323	40962	26315	18125	12511	8110	4740	2627	1388	614	249	9

05:03:43,DEM #4	50 mg	2,4	1.19	34.2	71.2	584682	394227	286878	225964	164691	112006	73944	52151	36058	25166	15792	9655	5581	2897	1315	63
05:02:43,DEM		,4	1.18	34.6	71.2	124129	66447	45479	36008	27428	20335	14852	11363	8169	6339	4522	3143	2063	1220	637	34
05:01:43,DEM		,4	1.18	33.8	70.0	83954	31796	16179	10742	7372	5092	3676	2845	2229	1626	1131	758	476	276	142	7
05:00:43,DEM		,4	1.10	34.6	69.6	88741	34755	18010	12138	8208	5651	3991	3038	2324	1711	1172	803	515	287	135	6
04:59:43,DEM		,4	1.23	35.0	69.6	75142	25357	11122	6509	4072	2741	2011	1582	1222	898	618	413	260	148	63	2
04:58:43,DEM		,4	1.24	35.4	70.4	101817	44820	27031	20261	15178	11471	8761	6859	5316	4033	2830	1894	1218	687	325	17
04:57:43,DEM		,4	1.19	34.6	70.8	124451	62365	41636	32865	25531	19595	15044	11918	9240	6957	4831	3271	2019	1115	552	28
04:56:43,DEM #3	800 mg	0.7,4	1.20	34.6	69.6	175310	101947	74127	60831	48844	38594	30146	24508	19367	15227	11379	8228	5786	3702	2182	129
04:55:43,DEM		,4	1.25	34.6	70.0	78188	28087	13226	8393	5475	3682	2673	2019	1543	1141	758	521	330	191	90	4
04:54:43,DEM		,4	1.20	34.6	70.4	85788	32414	16096	10411	6875	4578	3275	2433	1823	1323	874	551	348	183	88	4
04:53:43,DEM		,4	1.06	34.2	70.4	98405	40226	21781	15057	10228	6747	4573	3282	2434	1664	1104	670	417	237	113	4
04:52:43,DEM		,4	1.17	34.2	70.4	121946	54999	31824	22674	15565	10298	6796	4851	3476	2372	1459	894	525	254	110	4
04:51:43,DEM		,4	1.14	33.8	71.6	153383	74839	45603	33367	23241	15640	10500	7523	5230	3523	2184	1360	803	427	197	9
04:50:43,DEM		,4	1.18	33.8	71.2	228532	124071	80917	61094	43538	29597	19924	14171	10136	6995	4482	2803	1726	953	501	22
04:49:43,DEM #2	200 mg	0.7,4	1.15	34.2	69.6	389492	231613	157231	120870	86841	59539	40188	28672	20331	14616	9817	6671	4448	2692	1535	86
04:48:43,DEM		,4	1.21	34.2	70.0	86027	34312	18597	12924	8900	6299	4408	3311	2474	1768	1132	738	459	248	117	5
04:47:43,DEM		,4	1.18	34.2	70.0	99083	43674	25543	18385	13040	9111	6346	4645	3424	2413	1491	935	517	260	112	3
04:46:43,DEM		,4	1.22	34.6	70.0	121780	60445	38539	29100	21280	15006	10449	7643	5553	3812	2356	1400	768	368	156	6
04:45:43,DEM		,4	1.19	34.2	70.0	163352	91754	62536	49126	36850	26801	18903	13995	10240	7241	4673	2940	1747	922	403	19
04:44:43,DEM		,4	1.17	33.8	69.2	229586	141120	101121	80940	61920	45319	32615	24680	18495	13578	9119	6032	3844	2119	1022	49
04:43:43,DEM #1	50 mg	0.7,4	1.20	33.8	69.6	263588	168190	121791	97949	74763	55013	39737	30158	22297	16617	11539	7967	5406	3417	1927	109
04:42:43,DEM		,4	1.15	34.2	68.8	67865	19995	6767	2811	1056	422	263	203	154	111	79	53	39	24	14	

Appendix F
Copies of Manuscripts Prepared for Conference Proceedings

Manuscript F1- Presentation Prepared for the U.S. Environmental Protection Agency's 11th Annual Emission Inventory Conference: Emission Inventories-Partnering for the Future, Atlanta GA, April 16-18, 2002

Evaluation of the Transport and Deposition of Fugitive Dust Using Lidar

Dennis Fitz and David Pankratz
College of Engineering-Center for Environmental Research and Technology
University of California, Riverside
1084 Columbia Avenue, Riverside CA 92507
dfitz@cert.ucr.edu

Russell Philbrick and Guangkun (Homer) Li
Department of Electrical Engineering
The Pennsylvania State University
University Park, PA 16802
crp3@psu.edu

ABSTRACT

Ambient measurements suggest that source inventories of PM_{10} from geologic sources are overestimated by 50 percent or more. This discrepancy may be due to inaccurate emission calculations and/or due to the rapid deposition of PM_{10} after entrainment into the atmosphere. Tests were conducted during December 2000 and December 2001 using a two-wavelength scanning backscatter lidar to investigate PM_{10} deposition rates from artificially generated fugitive dust. Dust was generated by vehicles on unpaved roads and with a blower dispersing known amounts of finely ground calcium carbonate (paint pigment) or native soil. The size and concentration of the resulting dust plumes were monitored for up to a half-hour and a distance of several kilometers. The changes in these dust plumes' characteristics with time, including particle size and density, were estimated from the relationship between backscatter and extinction for the two wavelengths used. The lidar was calibrated using dust of known size distribution and concentration generated in a contained volume during a set of tests conducted in December 2001. A rough approximation of the backscatter and extinction signals has been obtained using model calculations which are based upon Mie theory for spherical particles. These models show that the backscatter signal does not depend strongly on the particle density but does depend strongly upon size and wavelength of the scattering radiation. However, the extinction depends strongly on the concentration and size of the scattering particles but not on the wavelength. Therefore, simultaneous measurements of the backscatter and extinction at two different wavelengths should permit analysis to reveal the approximate settling rates for the various types (i.e., sources) of fugitive dust.

INTRODUCTION

Geologic material is a major component of the airborne particulate matter in the western United States. Airborne particulate matter is an air quality concern because:

- Recent studies have associated increases in airborne particulate matter with increased morbidity and mortality, particularly in elderly and respiratory impaired individuals[1,2,3].

- Reduced visibility due to airborne particulate matter has both degraded the aesthetic beauty of natural views and affects activities such as the scheduled operation of air traffic.
- The changes in optical transmission of the atmosphere due to suspended airborne particulate matter alters the radiative energy balance of the Earth's environment.

Source inventories for PM_{10} and $PM_{2.5}$ show that geologic dust should contribute approximately 50% of the $PM_{2.5}$ in the western United States. Ambient measurements show that material of geologic origin typically contribute approximately 10% to the mass concentration[4]. There are several potential reasons for this discrepancy, the primary ones being inaccurate algorithms and data to calculate emission inventories and uncertainties of the lifetime of PM in the atmosphere.

Our primary objective was to characterize the fate (deposition and transport) of PM emissions originating from mechanical disturbance of the soil. The results from the measurements will be used to validate the accuracy of the algorithms used to determine emission inventories from such sources. The study focused on PM from unpaved roads and agricultural tilling. The tests also included artificially generated dust clouds of material of known size distribution to provide a validation of the analysis of the optical scattering properties and the algorithms for deposition of airborne particulate matter. The results will allow for more accurate assessment of such sources to the regional PM concentrations. These assessments will then aid the formulation of cost-effective PM control strategies.

The overall approach was to

- Evaluate several types of dust generation processes that are expected to be potentially significant sources of geologic material contributing to the PM in the San Joaquin Valley of California.
- Evaluate methods for determining the amount of particulate matter entrained and their fate.

The work was done in a test area where the generation conditions were controlled and where backscatter lidar could be safely used in the scanning mode to characterize the distribution of particulate matter. Tests were conducted by generating PM emissions to simulate emissions from vehicular travel on dirt roads and soil tilling operations. A series of individual test runs was conducted with data collected from real-time measurement methods. During several of these test runs, in addition to the real-time measurements, time-integrated samples were collected during several test periods.

RESEARCH ACTIVITY

Experimental

The study was conducted at the University of California, Riverside, Agricultural Field Station in Moreno Valley, CA. The 720 acre facility is relatively level, except for some raised (~10 feet) dirt roads that run between some of the fields. There were no significant sources of PM around the facility. The project team coordinated with the UCR field site staff regarding any planned field plowing to avoid that activity during periods that tests were performed. The prevailing daytime winds were expected to be from the west during December.

Figure 1 shows the layout for the equipment at the site. A background meteorological station measuring wind speed (WS), wind direction (WD), temperature (T) and dew point (DP) was also located at this site. The meteorological tower provided wind speed and direction at 2, 5, and 10 meters, temperature measurements at 2 and 10 meters, and net radiation measurements at 1.5 meters. The signals from the meteorological sensors were scanned once per second by a Campbell CR10X data logger and processed into ten-second averages.

The SESI scanning micro-pulse lidar (MPL) was located 153 meters upwind of the main dust generator during the pilot study in December 2000. It provided the backscatter signal profiles at two wavelengths and has several features that make it the ideal instrument for mapping the dust clouds to be generated in this program. The instrument has a scanning platform, which can be used to provide a mapping of the airborne particulate matter. The instrument is eye-safe but maintains high sensitivity by using high average power, which is obtained by using a high operating pulse repetition frequency (prf), and the beam is expanded to produce lower energy flux per unit area.

The MPL measures the backscatter signal profiles at 1047 nm in the near infrared (NIR) and 523 nm in the mid-visible spectrum. These wavelengths are most sensitive to scattering from particle sizes in the size range near 1 micron, and they are separated sufficiently to provide some sensitivity to changes in fine particle size distributions.

A high-resolution digital video camera (Sony Digital DCR-VX700) was mechanically coupled to the lidar to document the distribution of the dust generated and to verify the lidar position. Images were taken at each scanning position by the camera mounted on the top of the lidar to follow the path of the laser beam and provide a clear picture of the area being scanned. The scanning lidar with the camera was located upwind of the generation point. The scan covered the region about 10-20° on either side of the centerline from the location of the lidar to the generation point. An inclinometer was mounted on the lidar to measure the elevation angle.

A second video camera was used in the program. It was placed at the location shown in Figure 1. Running simultaneously, these two cameras provided a more complete visual representation of the spatial evolution of the dust clouds.

Most of the dust generation releases were performed using a stationary generator as shown in Figure 2. This device used a 5 horsepower centrifugal blower. Limited testing was carried out using calcium carbonate (~10 µm size) and a fogger (propylene glycol) of the type used to provide special effects for the film industry. For the remaining tests, dust was generated by driving a vehicle (Chevrolet Suburban) along the paths shown in Figure 1. Figure 3 shows the dust generated by this vehicle.

Results and Discussion

The dust generation and measurement instruments were made from 11 to 18 December 2000. Dust was generated and monitored for a total of 22 test periods. Ten-second average meteorological measurements, tracer gas releases and sampling, digital and video camera measurements, and lidar measurements were made during these test periods. Dust was generated and monitored for a total of 22 test periods. These included 11 tests with sieved indigenous soil, 4 tests with the white paint pigment powder, 5 tests with vehicle-generated dust, and 2 tests with the fog generator. Table 1 presents a list of test activities and the time periods that those activities were performed.

Figure 4 shows a typical experiment showing photos of the generation of a dust cloud from the digital video camera mounted on top of the lidar. The dust generation equipment was located about halfway between the lidar and the measurement tower. The lidar was used to automatically make horizontal scans of the test volume, and the elevation angle could be adjusted manually. Using the scanning lidar, the plumes were generally tracked out to 1 km along the path and on radials, which were swept up to ±30º horizontally. The plumes probably could have been tracked much longer, at least along some radials, up to the lidar's maximum range of 20-30 km. Because it was more desirable to obtain data over shorter distances for the pilot study, tracking of plumes was stopped at about 1.5 km.

Figure 5 shows the results of using scene extraction techniques while following the dust cloud. The image obtained with a digital camera was analyzed by removing the background scene by subtracting, pixel by pixel, a background image obtained just before generating the dust plume. After scene extraction is applied, only the signal due to the dust plume is left. The spatial dimensions indicating growth or drift of the cloud can be extracted. It is also possible to determine the optical depth of the cloud relative to the background scene at times and locations where the path is not optically thick.

Figure 6 shows vertical profiles obtained for the visible and near infrared (NIR) channels when the instrument was pointed on an elevation angle of 70^o. The data have been range-corrected for $1/R^2$ (where "R" is the distance from the lidar to the measured plume) dependence, but no other corrections have been applied. Therefore, the telescope form factor is quite noticeable. The top of the planetary boundary layer (PBL) is clearly evident in both the visible and NIR channels. The visible signal is large compared with the NIR signal, and we would expect that most of the contribution to the scattering is by small particles. The shape of the vertical scattering profile is that expected for a well-mixed atmosphere that is relatively clean. The increase in the signal versus altitude is due to two factors, the telescope form factor and the fact that the particles grow larger as the temperature decreases versus altitude. The increase in relative humidity as a function of altitude causes growth in the size of the particles, and since the optical scattering increases approximately with R^6 (where "R" is the radius of the particle) for small particles, we expect to observe more optical scattering near the top of the boundary layer.

Figure 7 shows the returns measured from a target board at a distance of 660 m from the lidar. The measurement was made on four occasions and the results show that no major changes in performance occurred during the period. The differences can be attributed to changes in the path transmission.

Figures 8 and 9 show examples of the measurements from the two wavelengths. The results shown in Figure 8 display the backscatter and the extinction. The backscatter is larger for the NIR channel and the extinction is larger for the visible channel. These differences provide a foundation for using the lidar data to describe and characterize the changes in the airborne particulate matter. Figure 9 shows the large range of changes in backscatter and extinction as the concentration of particles changes during the generation of a very dense cloud using the spinning tire of a vehicle along a 50 m long north-south line. The results are plotted relative to the atmospheric profile immediately before the test to show the dust characteristics more clearly. During the 45-second generation period, the extinction increased and then rapidly decreased again as the larger particles settled quickly, and the fine particle component is observed later. Notice that the extinction reaches a maximum value near the end of the generation period and then decreases rather rapidly. The rapid recovery of the extinction is due to the more rapid settling out of the larger particles; however, the number density is largely composed of smaller particles which stay airborne longer and contribute to the backscatter signal.

The laser signal strength is attenuated after passing the dust cloud. As shown in Figure 8 comparing with the backscatter signal before the dust was generated, the signal strength starts increasing at the front edge of dust plume and forms a peak in the center of cloud. The backscatter coefficient can be estimated from the peak's magnitude. After the laser beam passes through the cloud, there is a sudden drop of backscatter signal due to the attenuation of the laser beam. The extinction coefficient can be estimated by the attenuation amount, which is the signal drop after the laser signal passing through the dust plume. If we assume the dust particles inside the cloud are uniform and spherical, a certain relationship should exist between the values of backscatter and extinction coefficients that correspond to a dust plume with given set of particle sizes. This will allow us to simulate the laser backscatter profile passing through the cloud and specify the dust particle size and density from the analysis of the simulation.

A simple model calculation based upon the scattering theory for spherical particles by Gustov Mie has been used to simulate first order effects observed. Mie theory calculations provide the scattering angle dependence for spherical particles with various indices of refraction[5]. While the dust scattering studied in these experiments cannot be described as associated with spherical particles, it still provides a useful comparison of the scattering properties. In particular, the Mie theory results should provide accurate results for the smaller particles, where shape is less important, and the relationship between the forward and backward scatter intensities (extinction and backscatter) should provide useful insight for this investigation. The theory also provides information on the variations in the absorption of the particles due to their complex index of refraction. The Mie scattering theory used for this investigation is a straightforward application of the scattering intensity in the two polarization planes that comes from directly from electromagnetic theory, and all of the applications here use only the 0^o and 180^o scattering intensity.

Figure 10 shows model calculations of visible and NIR backscatter and extinction for 10μm diameter particles for a variety of concentrations. The calculation simulates a 200-meter-thick uniform dust cloud and calculates values at 30-meter intervals (same as the bin size of the lidar result). The figure shows the differences in backscatter and extinction signals as the density concentration of 10 μm particles changes. It is important to notice that the extinction only depends on the concentration of particles and not the wavelength or absorption. However, the backscatter does depend strongly on the wavelength, but it does not depend on the particle density as long as the dust does not become optically thick.

The calculations shown in Figure 11 demonstrate that the backscatter intensity and the extinction depend on the particle size. The relatively larger backscatter for the NIR wavelength is expected based upon the fact that the longer wavelength allows the particles to remain longer in the Rayleigh scattering range, where the cross-section dependence ($r^6 \sim 2^6 = 64$) results in increased scattering. Increasing the particle size increases the backscatter up to the point where the scattering loss results in an optical thickness that reduces the backscatter signal.

Figure 12 shows one example from the December 2001 test for the case of a 10 μm calcium carbonate cloud containing 600 grams of material. Notice that the magnitude of the backscatter and extinction are similar to the values in the simulation for 10 μm particles shown in Figure 11(a). After release, the backscatter signal does not change very much during the next two minutes (4 profiles) and the extinction is observed to slowly recover. The 10 μm material is sufficiently small that the settling time is slow when compared with the rapid recovery of the extinction from larger dust particles generated by a vehicle in Figure 9.

The experimental backscatter and extinction measurements can now be examined in the context of the simulation calculations. The more difficult task is to use the field measurements to solve the inverse problem and describe the particulate matter properties from the scattering profiles. Our goal is to describe size and distribution of the air borne PM and to show the variation in the settling rate of the particulate matter from various sources. The analysis aimed at developing the inversion algorithm for fully describing the changes in particle size within the generated dust clouds is under way as part of the Ph.D. dissertation of one of us (Guangkun Li) and it is expected to be completed during the coming months.

CONCLUSIONS

Optical scattering measurements using lidar have been examined for each of the several tests using native soil and sized calcium carbonate to generate clouds, and some examples of these results are presented here. The model calculations show that extinction is more dependent on concentration and backscatter is more dependent on particle size. Based on the analysis of results obtained thus far, it is expected that settling rates for generated fugitive dust of various types will be estimated from the lidar data obtained. The preliminary indication is that the rapid settling rate of the larger particles (even when the significant backscatter from the longer airborne small particles is present) results in the lower quantity of fugitive dust as a fraction of emission inventory.

REFERENCE

1 Magari, S.R.; Hauser, R.; Schwartz, J.; Williams, P.L.; Smith, T.J.; and Christiani, D.C. Association of heart rate variability with occupational and environmental exposure to particulate air pollution. *Circulation* 104, 986-991, 2001.

2 Peters, A.; Dockery, D.W.; Muller, J.E.; and Mittleman, M.A. Increased particulate air pollution and the triggering of myocardial infarction. *Circulation* 103, 2810-2815, 2001.

3 Mauderly, J.; Neas, L.; and Schlesinger R. PM monitoring needs related to health effects. *Proceedings of the PM Measurements Workshop*, EPA Report No. 2, Chapel Hill, NC, pp 9-14, July 1998.

4 Watson, J.G., and Chow, J.C. Reconciling Urban Fugitive Dust Emissions Inventory and Ambient Source Contribution Estimates: Summary of Current Knowledge and Needed Research. Document No. 61110.4D2, Desert Research Institute, Reno NV, September 3, 1999.

5 Li, G.; Kizhakkemadam, S.N.; and Philbrick, C.R. Optical scattering by airborne dust particles. Proceeding of the Air Force Optical Transmission Meeting, Hanscom AFB, MA June 2001.

ACKNOWLEDGEMENTS

We wish to thank Patrick Gaffney and the California Air Resources Board for funding this research. We appreciate Tony Taliaferro's assistance in setting up the equipment used in this study. The efforts of Sriram Kizhakkemadam and Gregg O'Marr contributed to the lidar results and were important for the successful data collection.

DISCLAIMER

The statements and conclusions in this report are those of the researchers and universities and not necessarily those of the California Air Resources Board. The mention of commercial products, their source, or their use in connection with material reported herein is not to be construed as actual or implied endorsement of such products.

Figure 1. Lot plot showing measurement equipment layout.

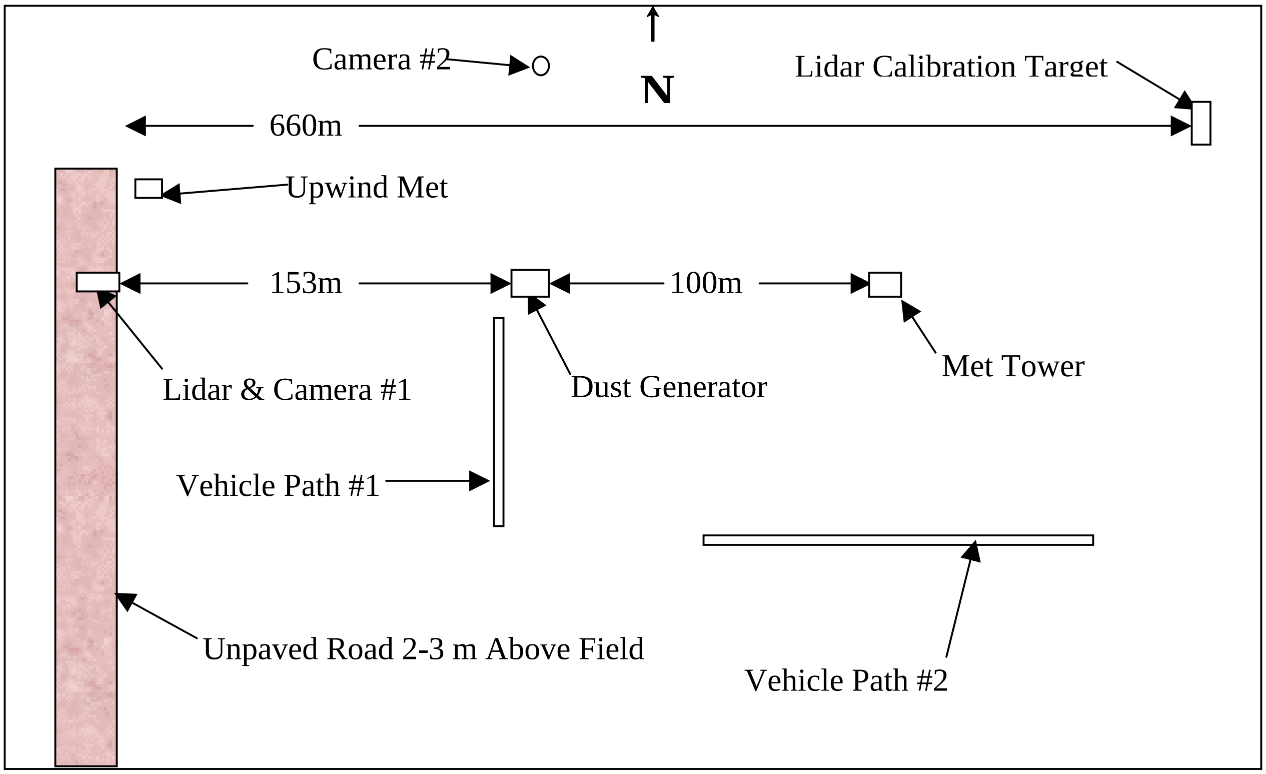

Figure 2. Photograph of centrifugal blower dust generator.

Figure 3. Photograph of vehicular dust.

Figure 4. A set of the digital images selected from Test #2 to illustrate the growth of a dust cloud using the imaging data.

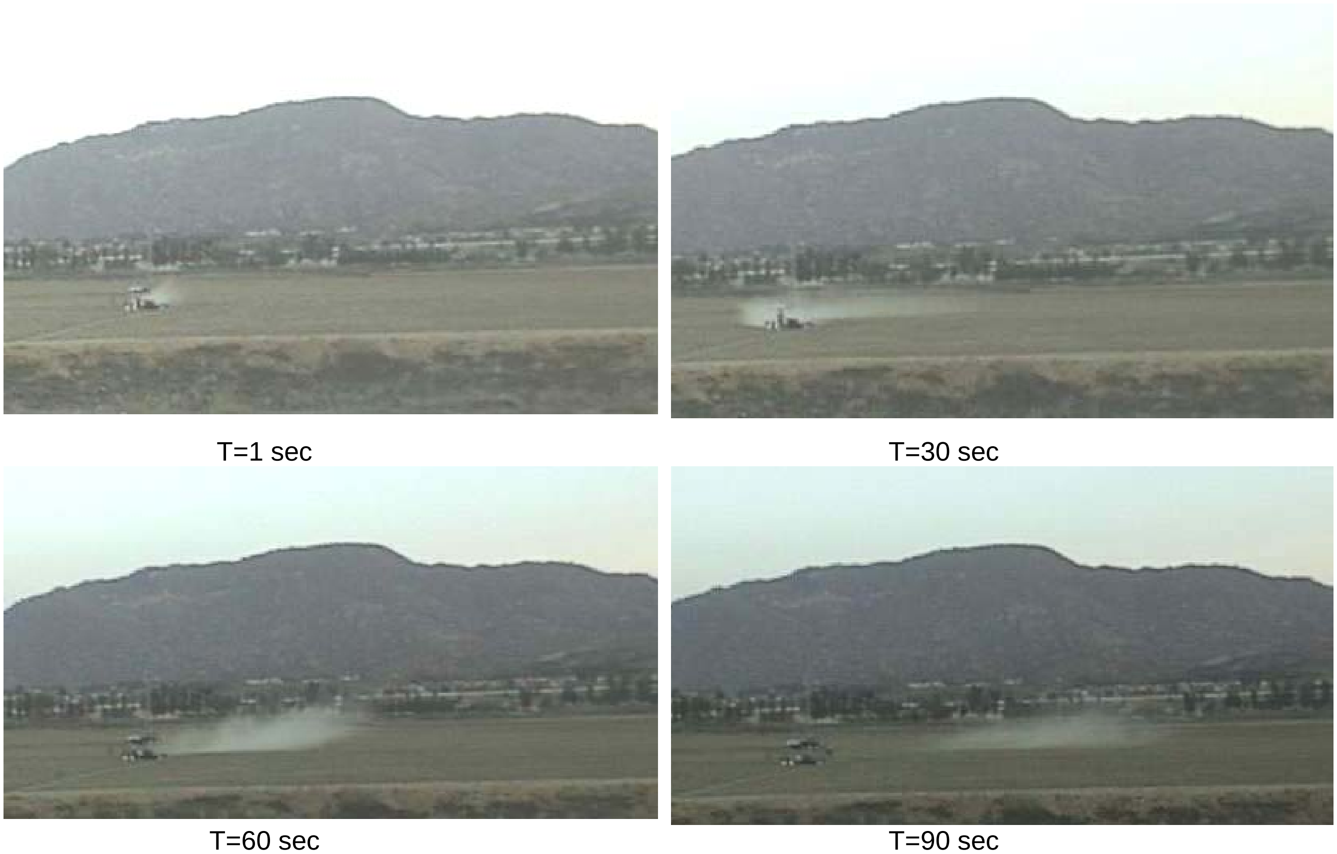

Figure 5. Time sequence of CCD images for Test #18 (dust generated with a vehicle) along with the corresponding background removed images. (a) 14:31:37 (b) 14:32:36 (c)14:32:49 (d) 14:33:14.

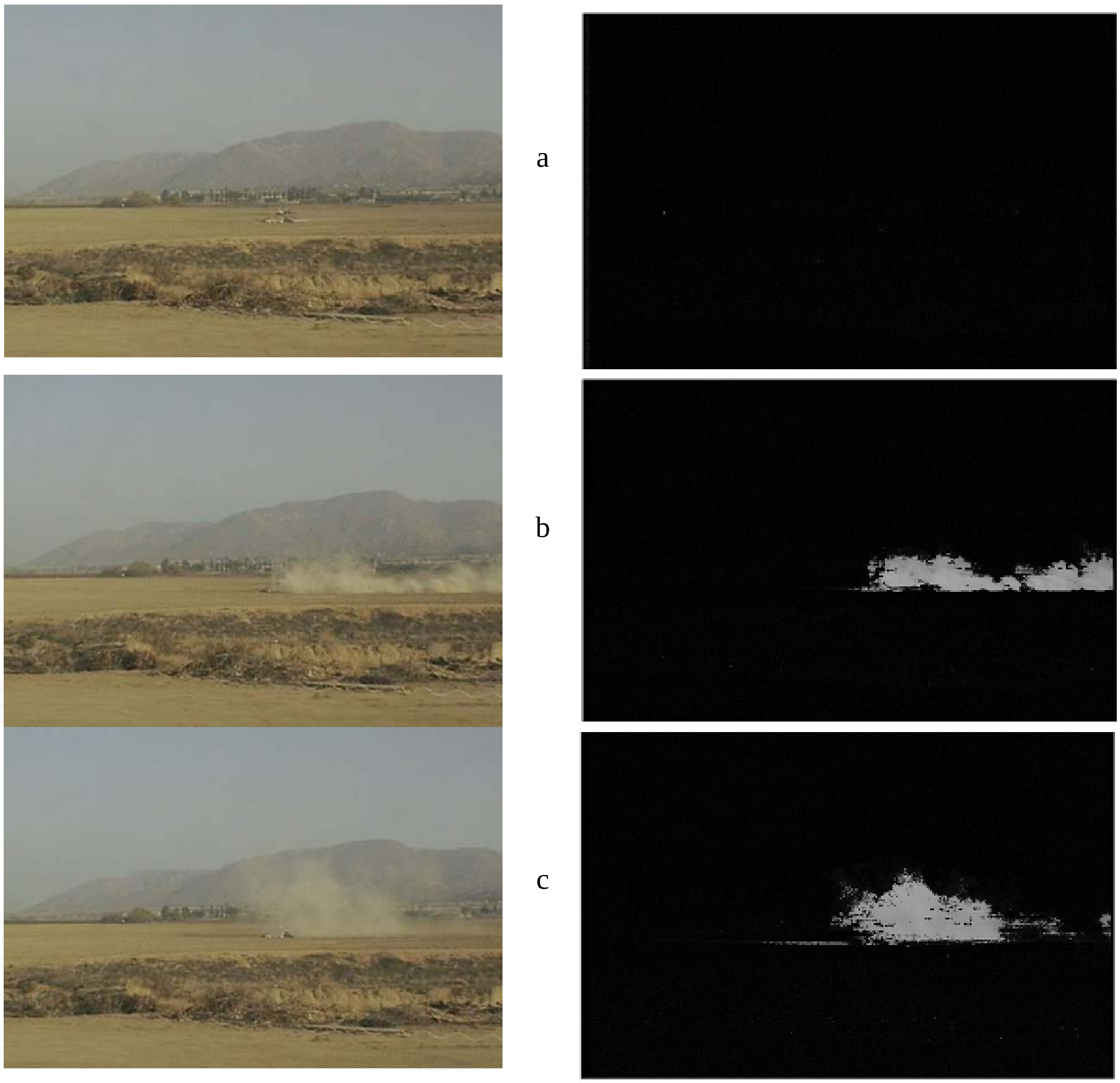

d

Figure 6. Vertical profile (elevation angle 70°) during period of afternoon convection shows the top of the boundary layer near 1300 m.

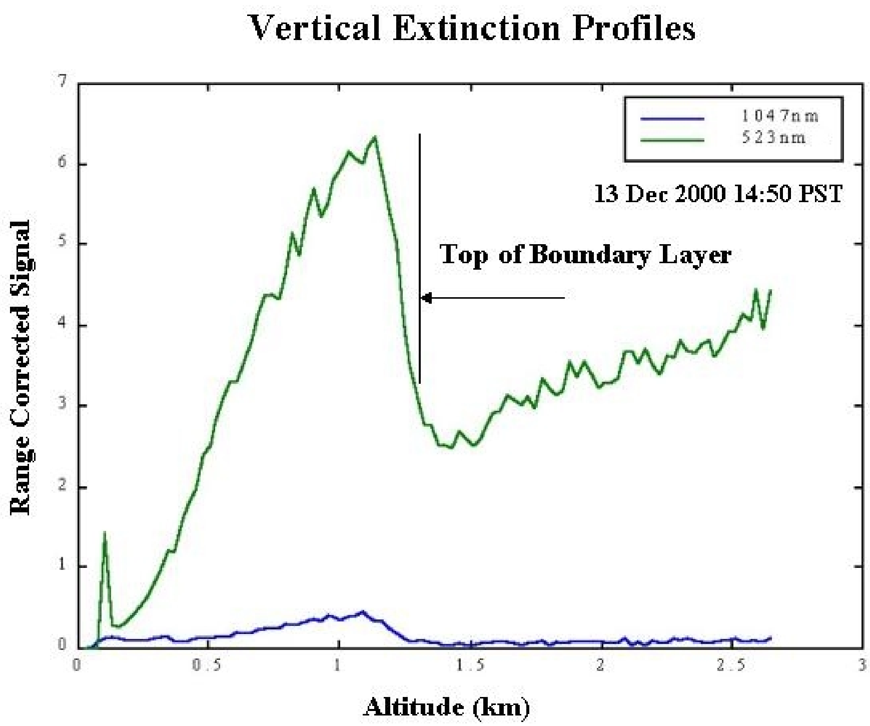

Figure 7. Return from target board at distance of 660 m was used to check the instrument performance and the measure the return as an indication of optical transmission changes.

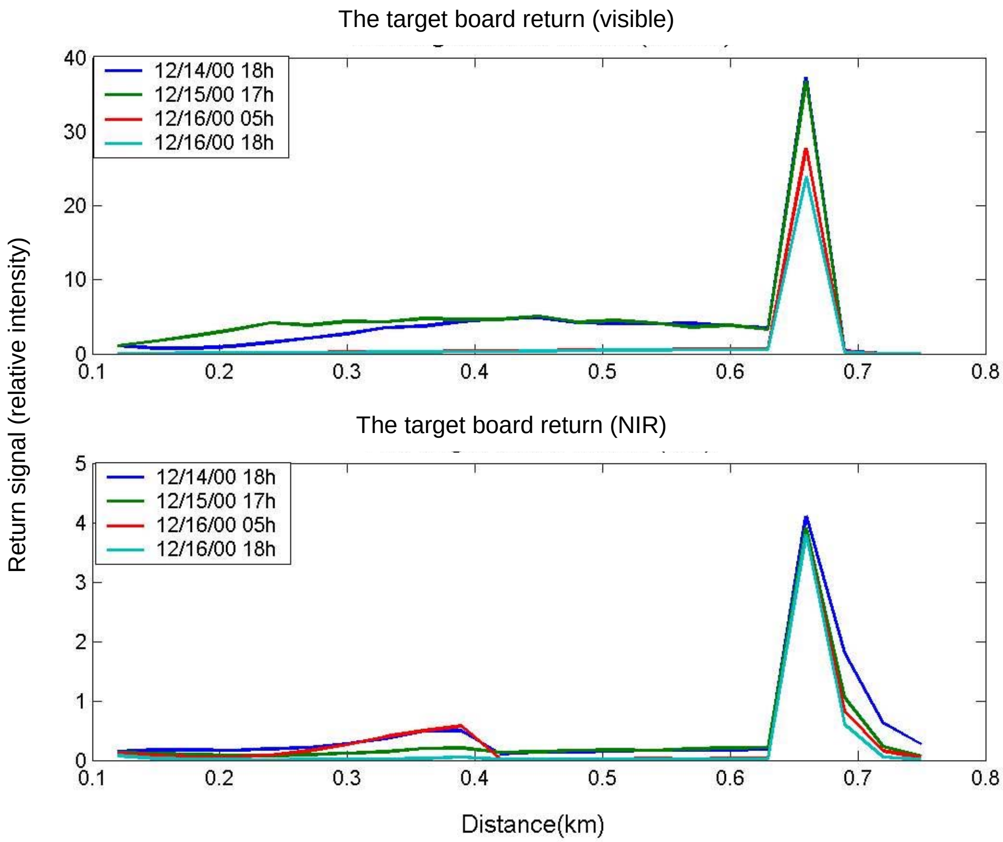

Figure 8. Examples of the raw data profiles from the lidar at the visible and NIR wavelengths during Test #4 show the backscatter and extinction associated with a dust plume at a range of about 500 m.

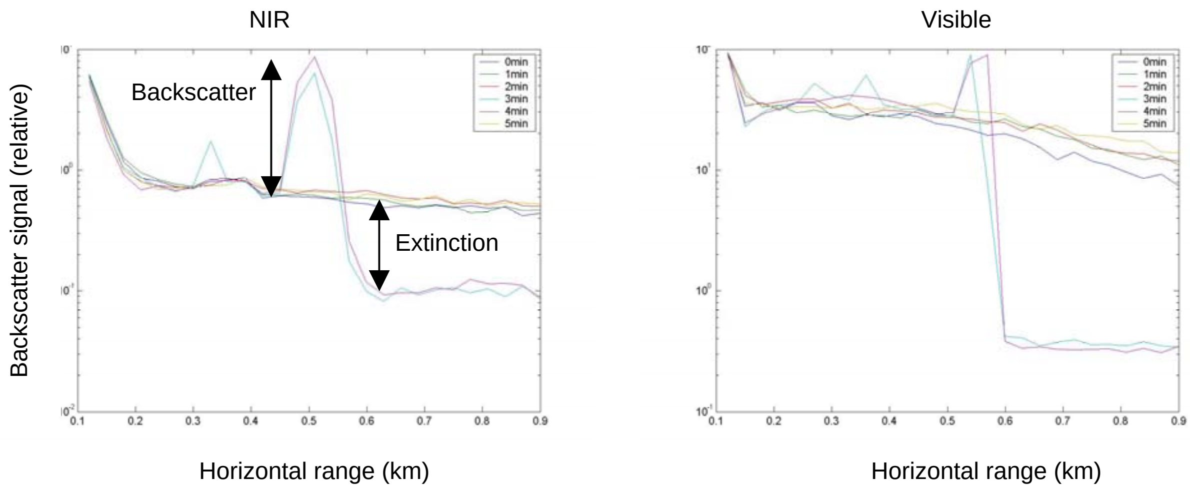

Figure 9. The backscatter and extinction at both visible and NIR wavelengths resulting from vehicle generated dust between 14:32:00 and 14:32:45 during Test #18.

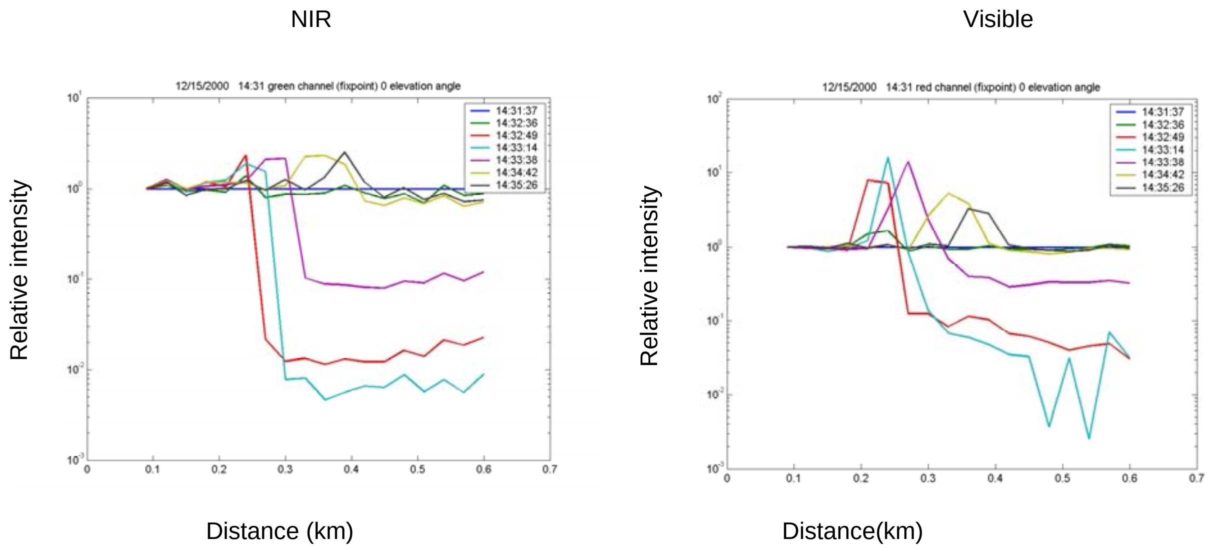

Figure 10. Simulation of the scattering from 10 μm dust for a model calculation shows the expected backscatter and extinction profiles for both wavelengths at several different particle concentrations in the upper panels.

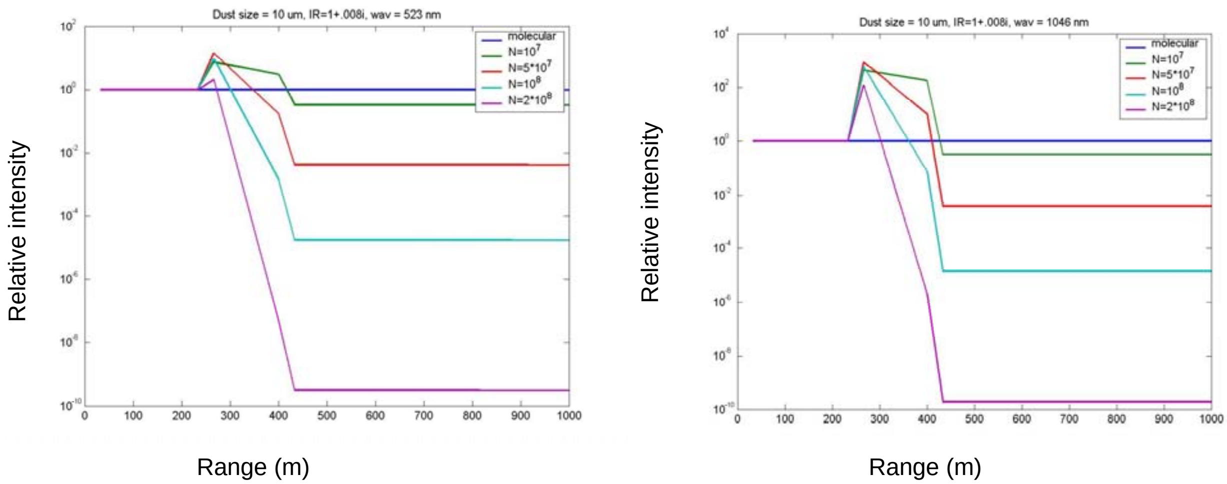

Figure 11. The calculations of the backscatter and extinction profiles for the two wavelengths are shown as the particle size changes. The upper panels show values for particle concentration of 10^7 m^{-3} and the lower panels for concentration of 10^8 m^{-3}.

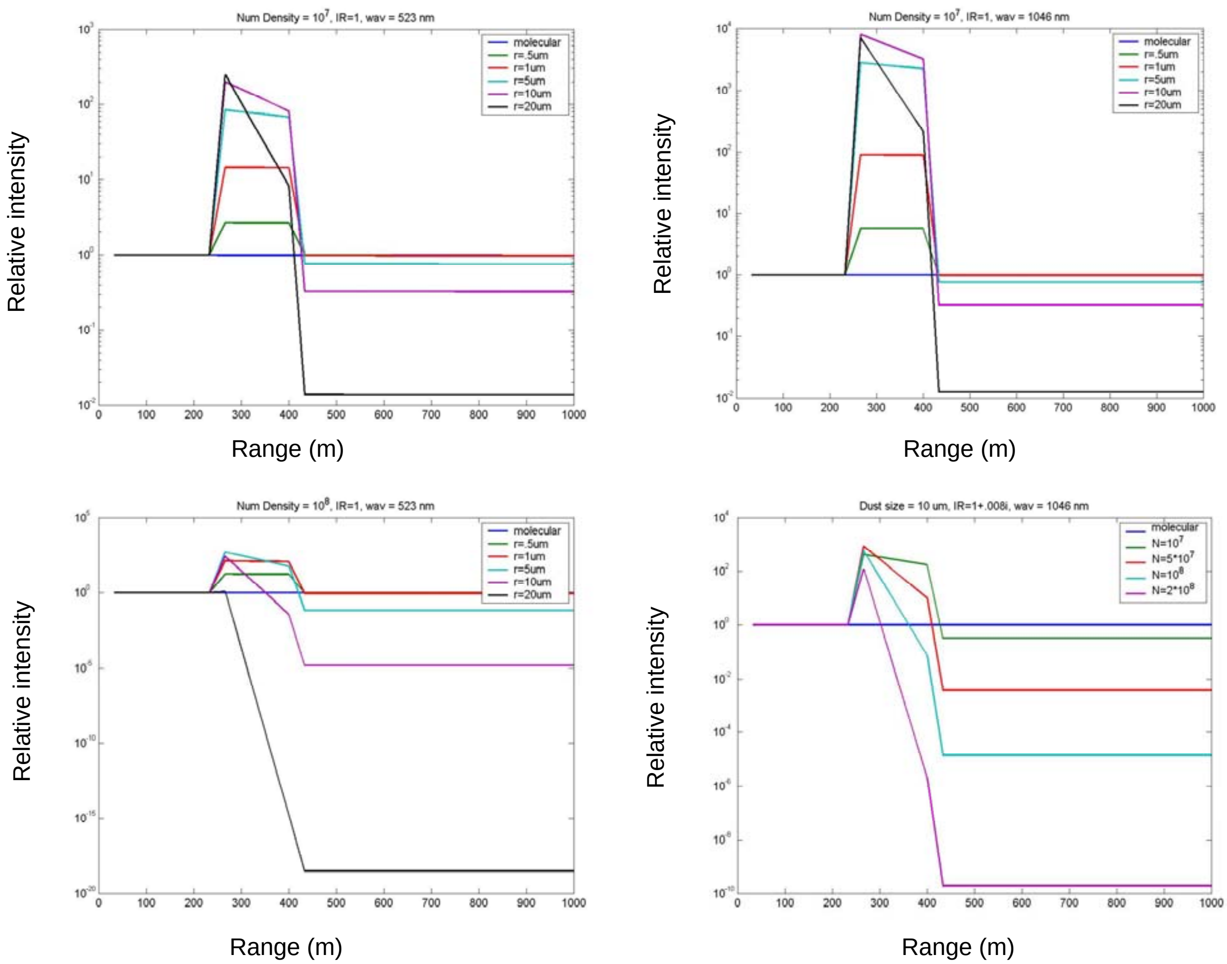

Figure 12. Example of December 2001 test for the case of a 10 µm calcium carbonate cloud containing 600 grams of material.

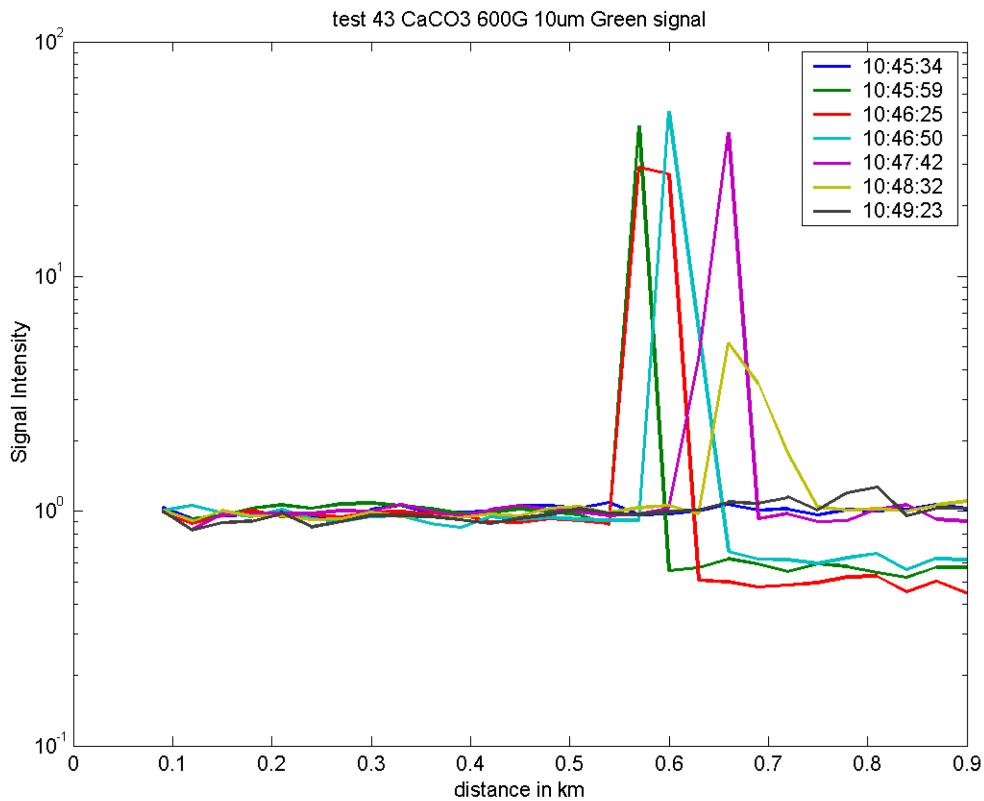

Table 1. Test activities log.

Event	Date	Start Time (hr:mn:sec)	Duration of Release (min:sec)	Release (Kg)	Dust Generation Material
1	12/13/2000	15:08:05	0:05	0.54	Sieved indigenous soil
2	12/13/2000	16:31:00	0:50	5.50	Sieved indigenous soil
3	12/14/2000	10:55:00	1:10	5.00	Sieved indigenous soil
4	12/14/2000	11:40:00	0:50	5.00	Sieved indigenous soil
5	12/14/2000	12:11:00	12:29	22.00	Sieved indigenous soil
6	12/14/2000	14:59:30	1:10	4.42	White paint pigment powder
7	12/14/2000	15:15:30	2:45	5.04	White paint pigment powder
8	12/14/2000	15:46:00	3:15	4.66	White paint pigment powder
9	12/14/2000	16:11:00	1:10	5.00	Sieved indigenous soil
10	12/14/2000	16:31:00	1:30	5.00	Sieved indigenous soil
11	12/14/2000	16:55:00	1:30	5.00	Sieved indigenous soil
12	12/14/2000	17:21:00	1:30	5.00	Sieved indigenous soil
13	12/14/2000	17:45:00	1:30	5.00	Sieved indigenous soil
14	12/15/2000	11:48:00	1:30	1.50	Sieved indigenous soil
15	12/15/2000	12:02:00	1:00	1.45	White paint pigment powder
16	12/15/2000	12:13:00	~20 sec		Suburban; drove around upwind of tower
17	12/15/2000	14:18:00	~20 sec		Suburban; 50 meter line source
18	12/15/2000	14:32:00	~20 sec		Suburban; down/back over 50 meter line (N-S)
19	12/15/2000	15:14:00	~20 sec		Suburban; 150 meter line (E->W)
20	12/15/2000	15:25:00	1:00		one minute "fog" release
21	12/15/2000	15:30:00	1:00		one minute "fog" release
22	12/16/2000	12:15:00	~20 sec		Suburban; N->S line release

Manuscript F-2. 25th Annual Conference on Atmospheric and Radiance Models, Lexington, MA June 25-27, 2002.

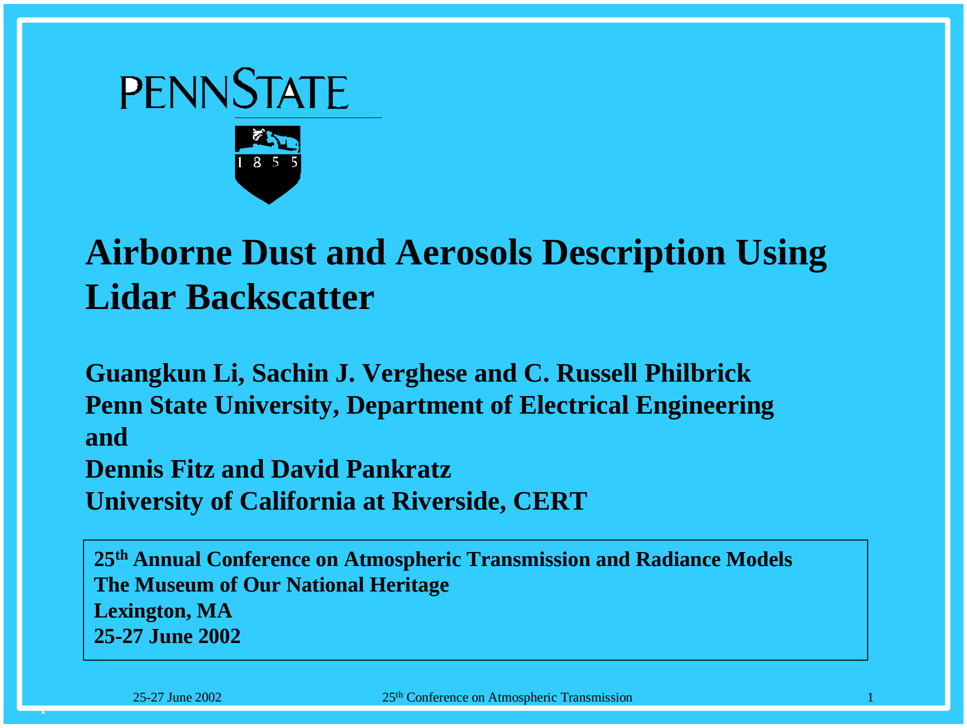

PENNSTATE

1855

Outline

- Introduction to the California Dust Investigation
- Instruments Used
- Chamber Tests
- Measurement Result Examples
- Model Calculations
- Comparisons
- Summary

25-27 June 2002 | 25th Conference on Atmospheric Transmission | 2

Introduction

Research Project: Evaluation of Geologic Dust Entrainment, Removal and Transport Mechanisms

Objective: Investigate the discrepancies between ambient geologic dust measurements and the contributions to source inventories for PM10 and PM2.5.

University of California — Dr. Dennis Fitz
College of Engineering
Center for Environmental Research and Technology (CECERT)
Riverside, CA

Penn State University — Dr. Russell Philbrick
Electrical Engineering Department
University Park, PA

Pilot Study – Conducted 12-18 December 2000
Main Investigation – Conducted 10 - 20 December 2001

Field Site

Field site located 5 miles east of Riverside CA – university farm station

Instrumented Tower

Meteorology properties and particle density and size
Measured at several locations

LIDAR

Scanning Lidar measures particle distributions
Nd:YLF 1047 nm – 523 nm
5-10 μj pulses 1-10 kHz
30 meter range resolution

Portable Digital Lidar *(Dual Wavelength with Scanner)*

System Specifications

Operating Environment Controlled Indoor
Detection Range 30 - 60 km
Laser (dual wavelength) DPSS:Nd:YLF (523.5 nm/1047 nm)
Laser Control Remote Set or RS232
Average Energy VIS: >5 μJ/pulse NIR: >10 μJ/pulse
Pulse Repetition Rate (pulse duration) 1 - 10 kHz (10 ns)
Cassegrain Telescope Diameter (F.O.V.) 0.2 m (- 100 μrad)
Detector APD Photon Counting Module
Scanning Mode Sweep or Stay and Stare
Horizontal Scanning (vertical swiveling) ± 90° (0° - 90°)
Scanning Speed per sec Variable from 0.1° to 30°
Optical Transceiver Dimensions (weight) 33" x 14" x 12" (40 lbs)
Computer Desktop or Laptop PC
Software Windows 95/98 based software
Dual Multichannel Scaler (dimensions) Rack-mountable (19" x 14" x 7")
Data Averaging Time Adjustable from 1 sec to 1 hour
Range Resolution 30 m, 75 m, 150 m, 300 m

25-27 June 2002 — 25th Conference on Atmospheric Transmission — 5

Evaluation of Geologic Dust – California – Dec 2000

Scanning Micro-pulse Lidar

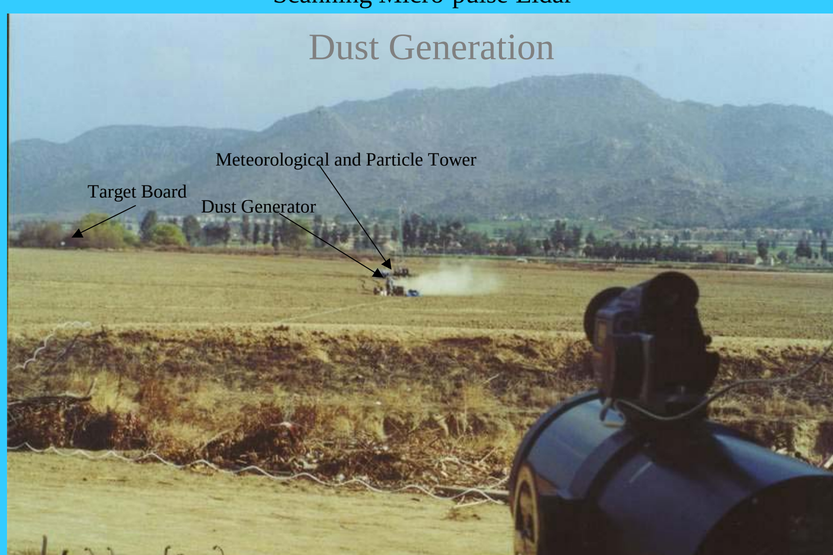

25-27 June 2002 — 25th Conference on Atmospheric Transmission — 6

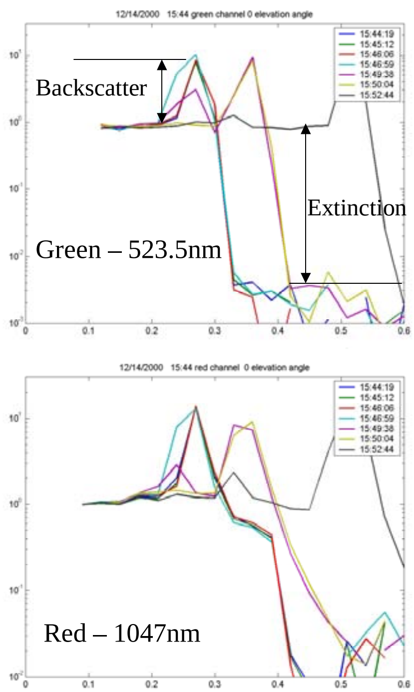

2-λ Backscatter and Extinction

Test #8 Calcium carbonate

10 micron particles – 4.66 kg in 3.2 min

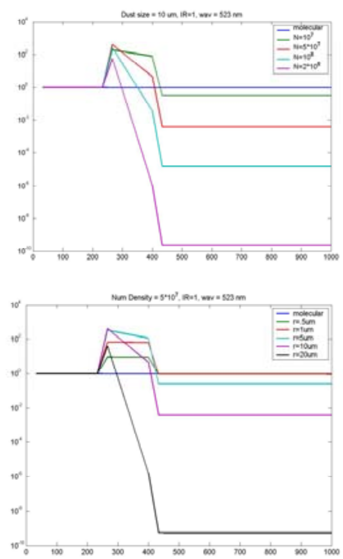

Chamber Test

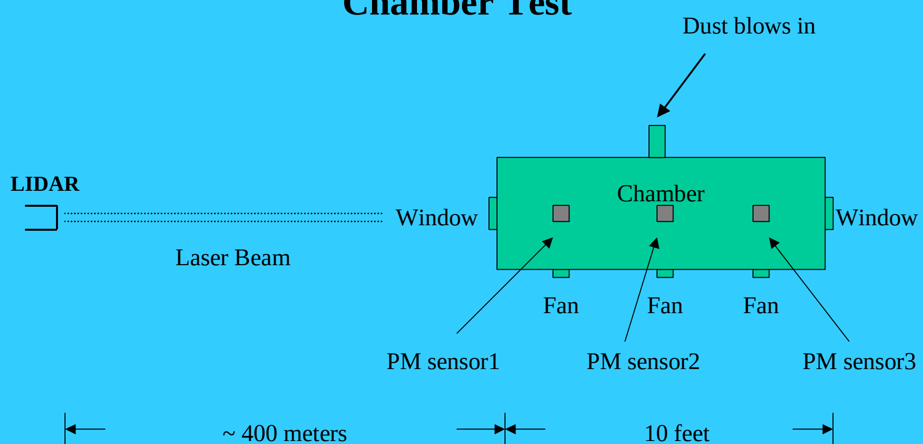

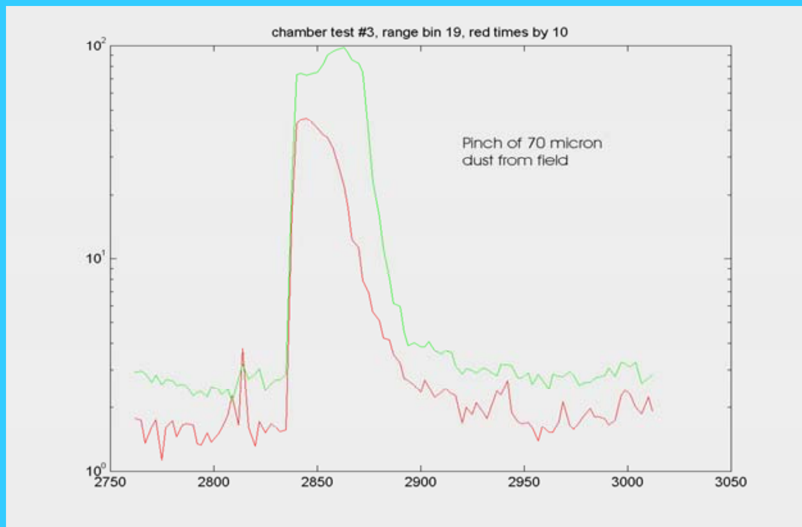
chamber test #3, range bin 19, red times by 10
Pinch of 70 micron
dust from field
10^2
10^1
10^0
2750
2800
2850
2900
2950
3000
3050

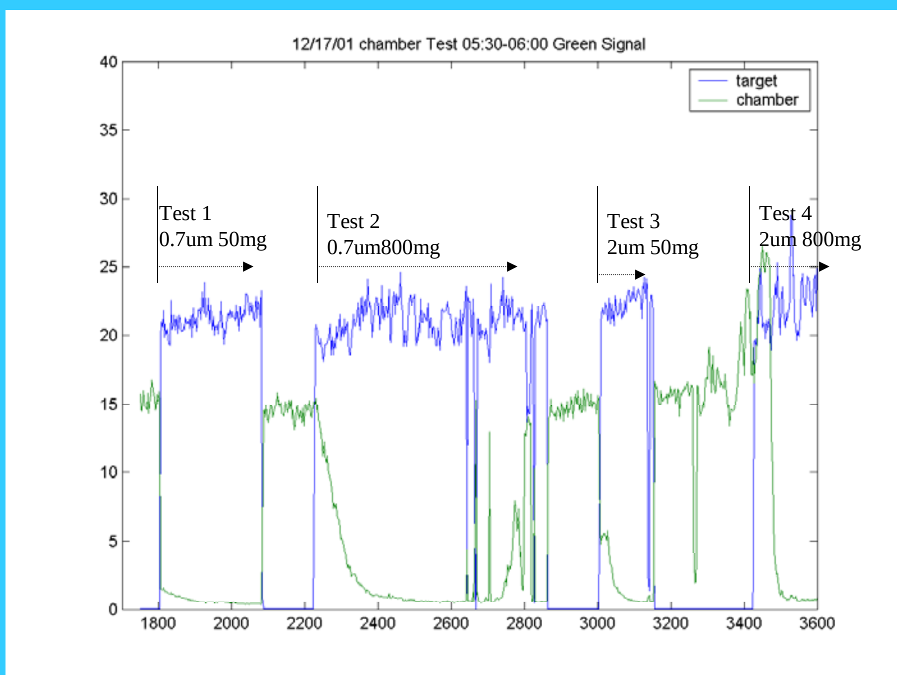
12/17/01 chamber Test 05:30-06:00 Green Signal
target
chamber
Test 1
0.7um 50mg
Test 2
0.7um800mg
Test 3
2um 50mg
Test 4
2um 800mg
40
35
30
25
20
15
10
5
0
1800
2000
2200
2400
2600
2800
3000
3200
3400
3600

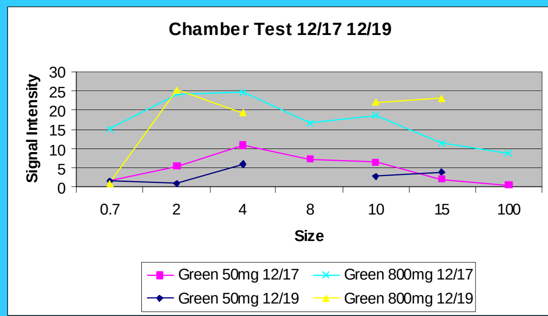

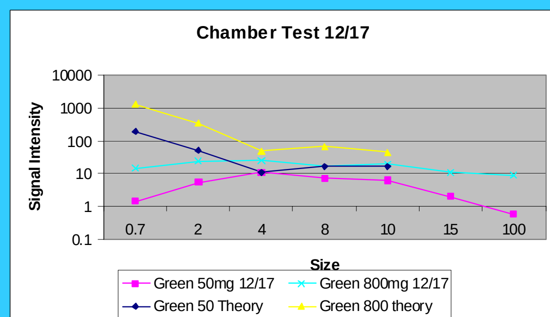

25-27 June 2002 | 25th Conference on Atmospheric Transmission | 11

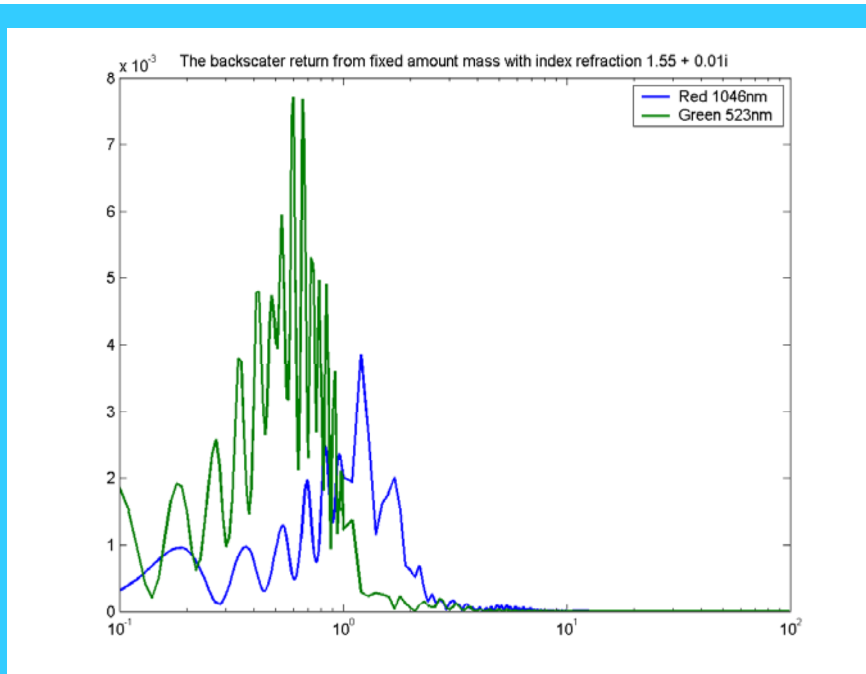

25-27 June 2002 | 25th Conference on Atmospheric Transmission | 12

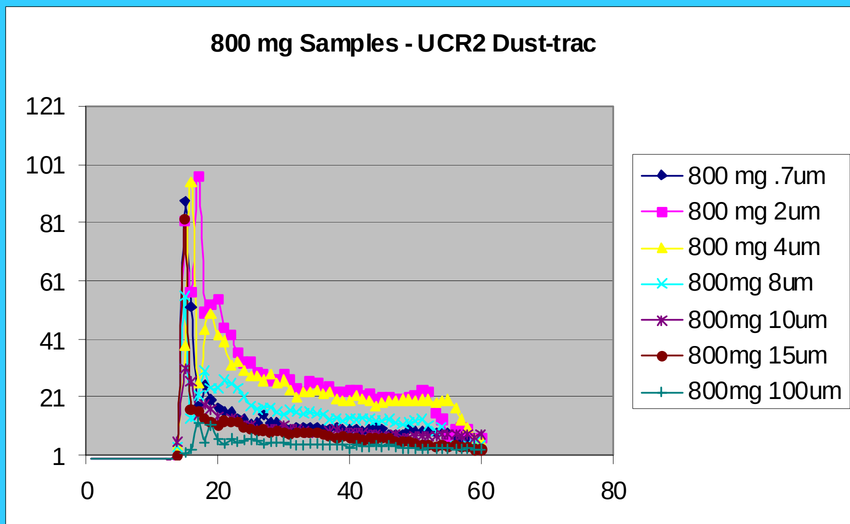
800 mg Samples - UCR2 Dust-trac
121
101
81
61
41
21
1
0
20
40
60
80
800 mg .7um
800 mg 2um
800 mg 4um
800mg 8um
800mg 10um
800mg 15um
800mg 100um

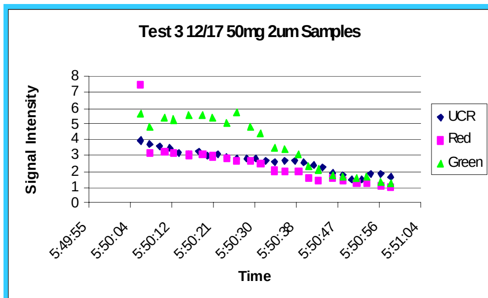
Test 3 12/17 50mg 2um Samples
Signal Intensity
Time
UCR
Red
Green
5:49:55
5:50:04
5:50:12
5:50:21
5:50:30
5:50:38
5:50:47
5:50:56
5:51:04

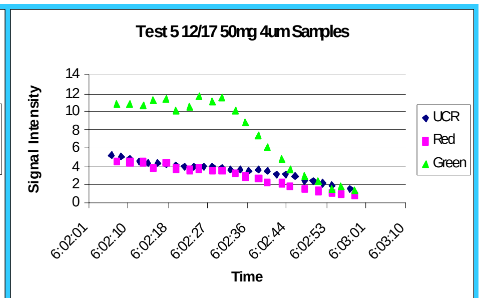
Test 5 12/17 50mg 4um Samples
Signal Intensity
Time
UCR
Red
Green
6:02:01
6:02:10
6:02:18
6:02:27
6:02:36
6:02:44
6:02:53
6:03:01
6:03:10

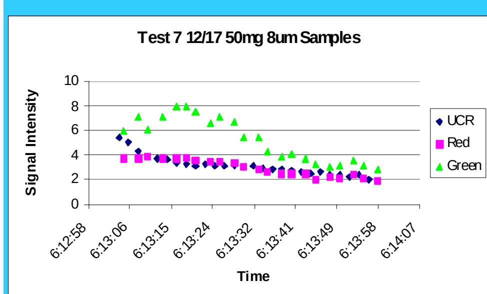
Test 7 12/17 50mg 8um Samples
Signal Intensity
Time
UCR
Red
Green
6:12:58
6:13:06
6:13:15
6:13:24
6:13:32
6:13:41
6:13:49
6:13:58
6:14:07

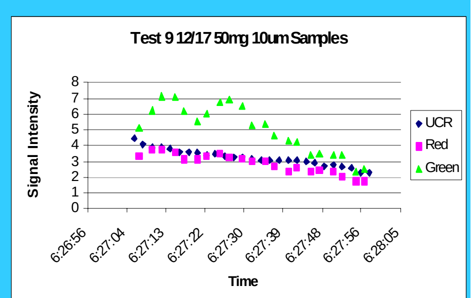
Test 9 12/17 50mg 10um Samples
Signal Intensity
Time
UCR
Red
Green
6:26:56
6:27:04
6:27:13
6:27:22
6:27:30
6:27:39
6:27:48
6:27:56
6:28:05

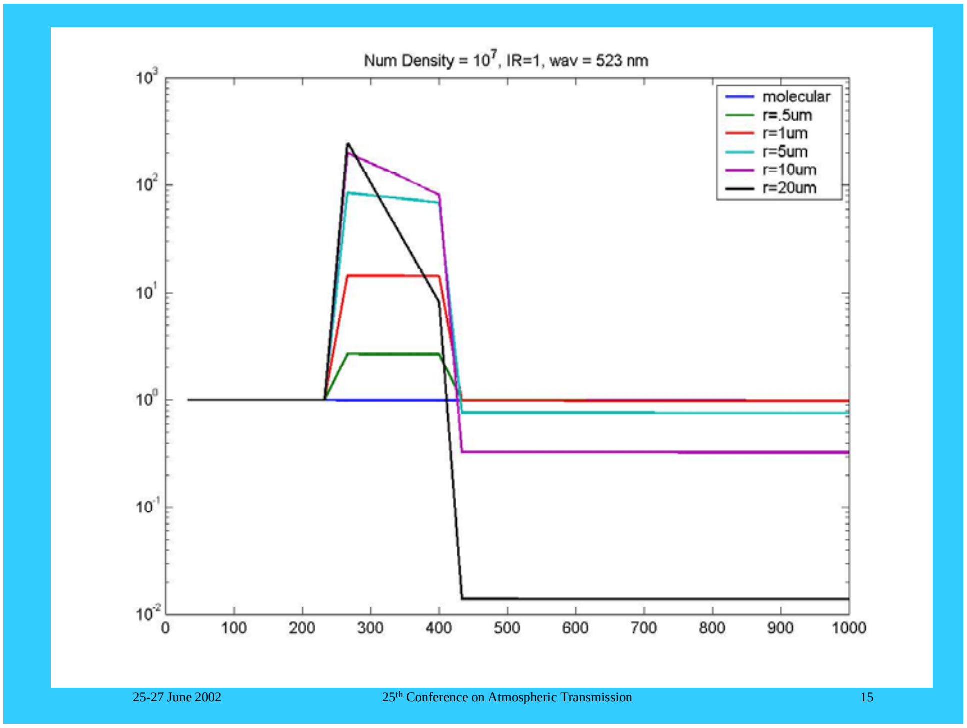
Num Density = 10^7, IR=1, wav = 523 nm
molecular
r=.5um
r=1um
r=5um
r=10um
r=20um
25-27 June 2002
25th Conference on Atmospheric Transmission
15

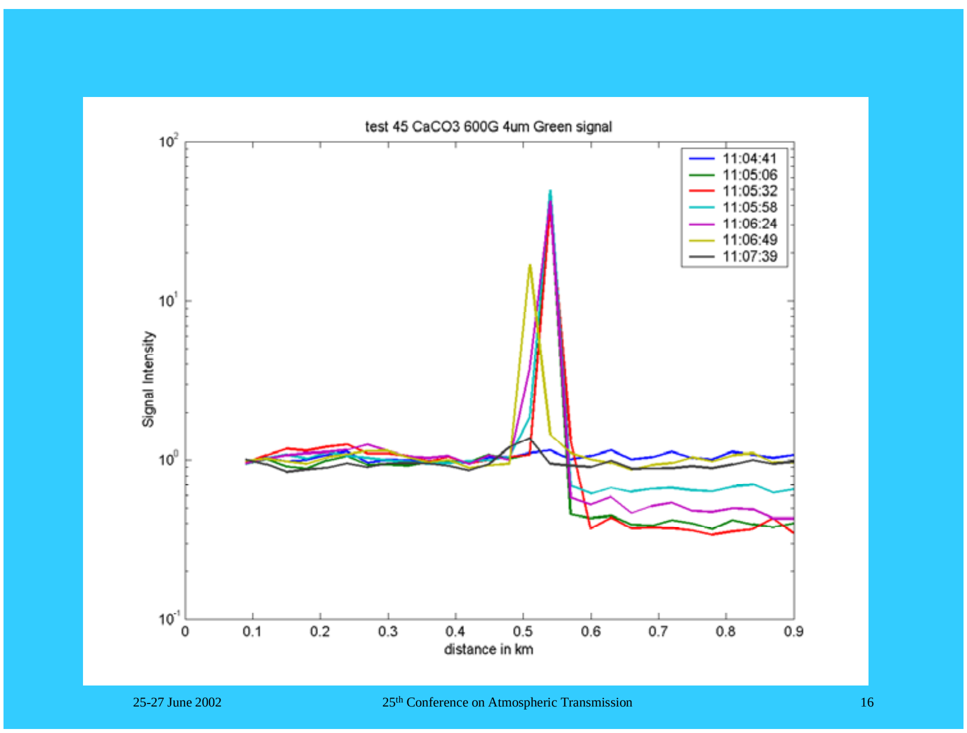
test 45 CaCO3 600G 4um Green signal
11:04:41
11:05:06
11:05:32
11:05:58
11:06:24
11:06:49
11:07:39
Signal Intensity
distance in km
25-27 June 2002
25th Conference on Atmospheric Transmission
16

Time Evolution of Plume

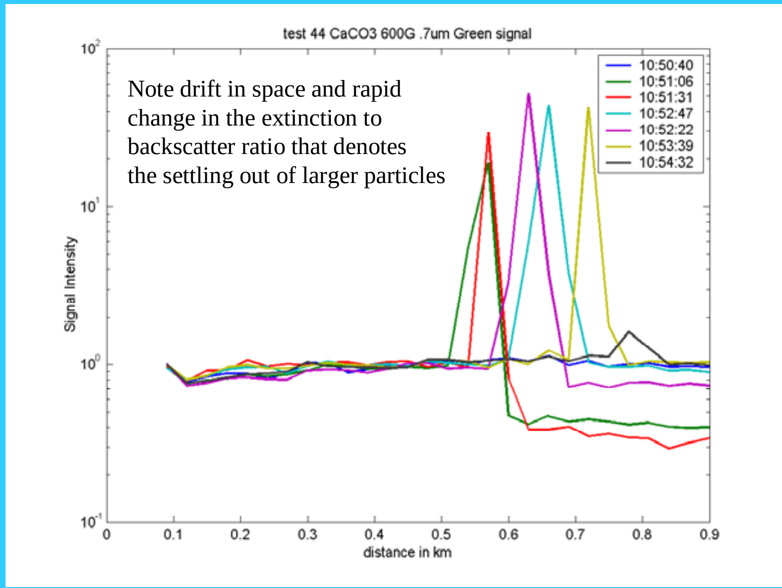

25-27 June 2002 25th Conference on Atmospheric Transmission 17

Particle Size Distribution

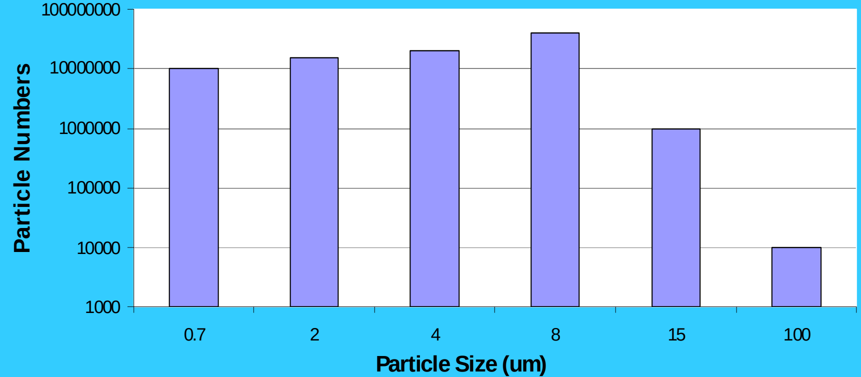

Case 1: Particle size distribution from 0.7um to 10um; Case 2: The 100um was settling out; Case 3: 15 um was settling out; Case 4: 8um was settling out; Case 5: 4um was settling out; Case 2 um was settling out

25-27 June 2002 25th Conference on Atmospheric Transmission 18

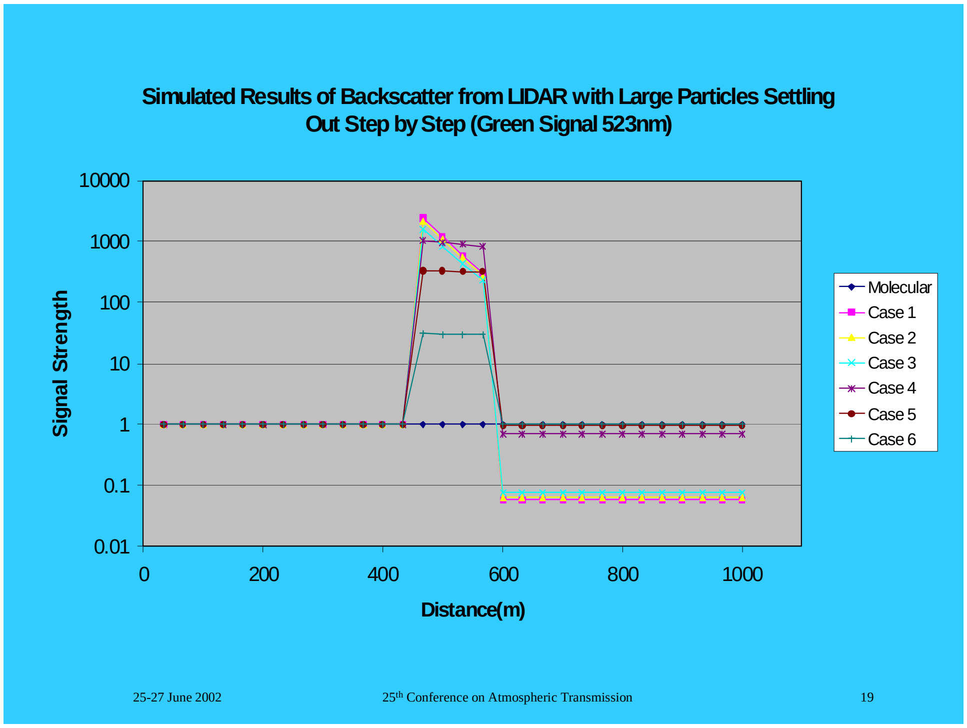
Simulated Results of Backscatter from LIDAR with Large Particles Settling Out Step by Step (Green Signal 523nm)
Signal Strength
10000
1000
100
10
1
0.1
0.01
0
200
400
600
800
1000
Distance(m)
Molecular
Case 1
Case 2
Case 3
Case 4
Case 5
Case 6
25-27 June 2002
25th Conference on Atmospheric Transmission
19

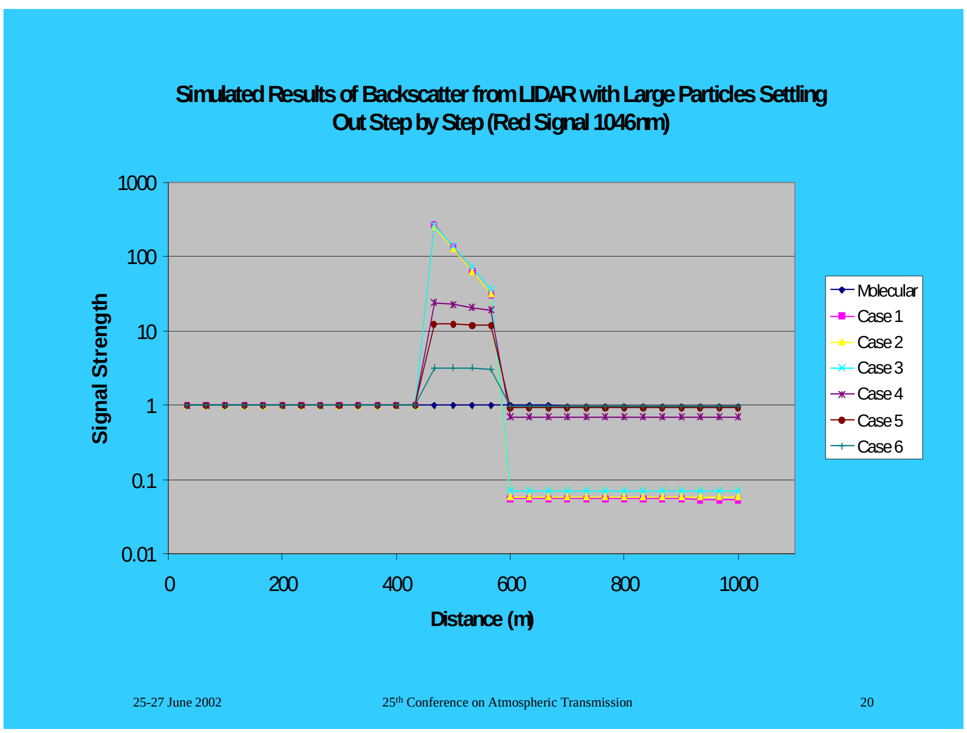
Simulated Results of Backscatter from LIDAR with Large Particles Settling Out Step by Step (Red Signal 1046nm)
Signal Strength
1000
100
10
1
0.1
0.01
0
200
400
600
800
1000
Distance (m)
Molecular
Case 1
Case 2
Case 3
Case 4
Case 5
Case 6
25-27 June 2002
25th Conference on Atmospheric Transmission
20

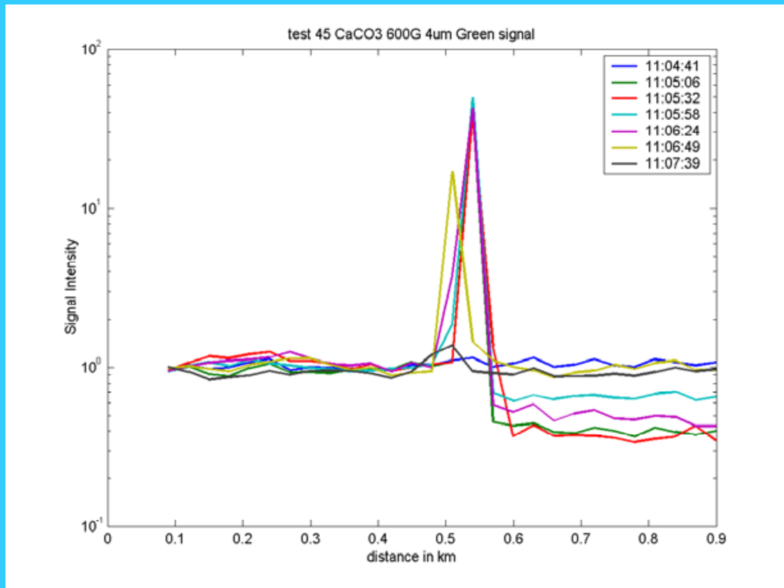

25-27 June 2002 25th Conference on Atmospheric Transmission 21

PENNSTATE
1855

Summary

- Simple model for optical scattering compares favorably
- Extinction can be measured beyond the generated cloud
- Chamber Tests have been used to examine the backscatter versus particle size
- Lidar can be used to measure the settling rate and residence time for various components of the airborne particles in the atmosphere
- Investigations continue on the calculations needed to describe the scattering of dust with T-matrix and other approaches

22 25-27 June 2002 25th Conference on Atmospheric Transmission 22

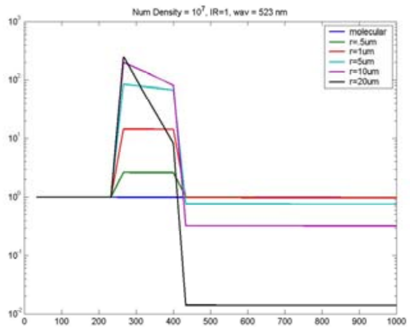

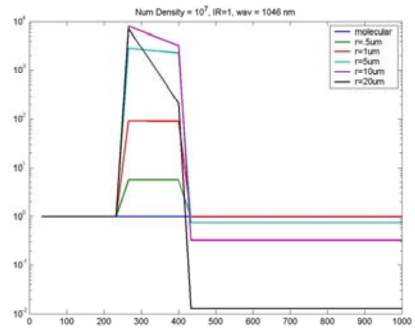

Particle Size

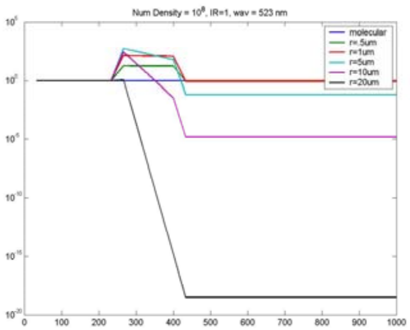

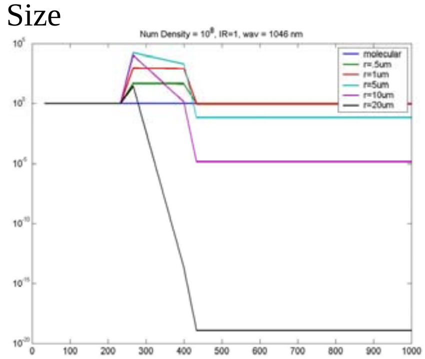

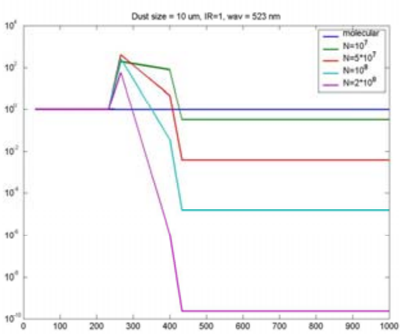

Model Calculation for Dust Cloud

Compare Changing Particle Densities for Different Complex Refractive Index at 523 nm

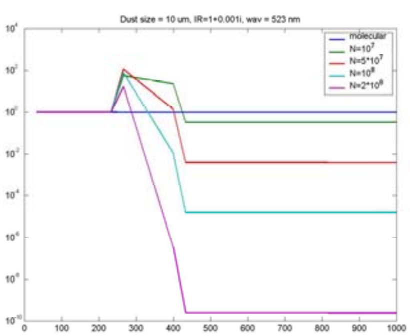

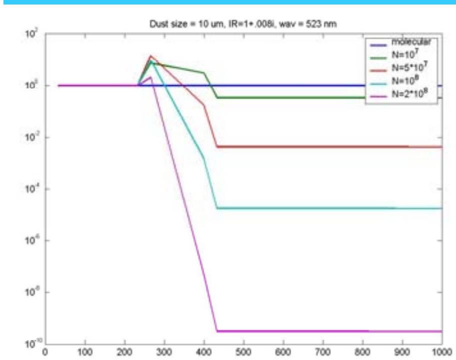

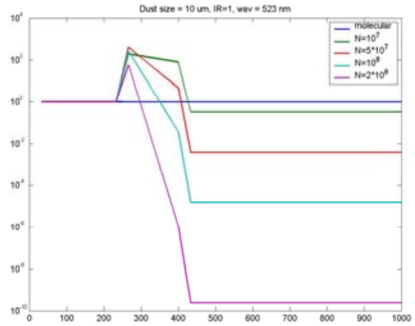

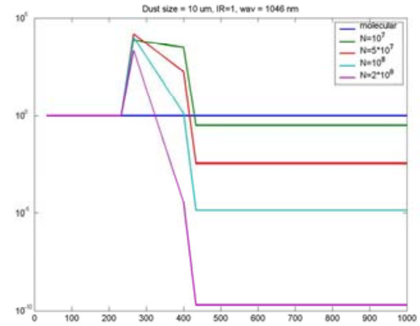

Particle Density

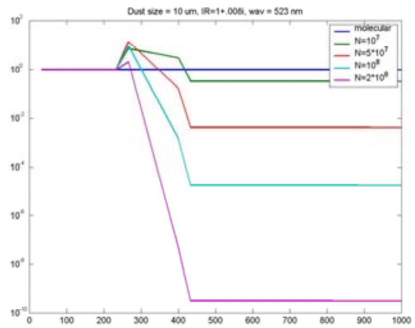

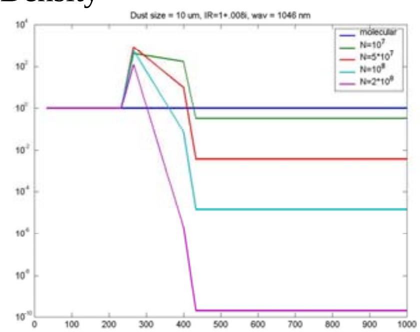

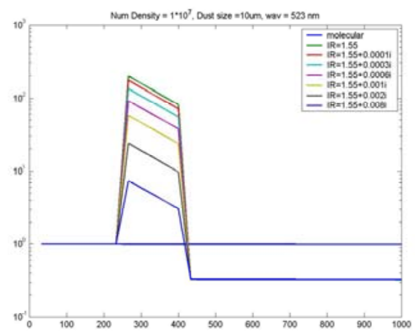

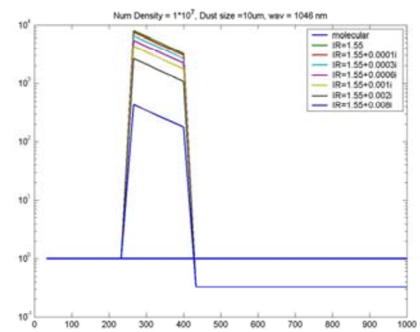

Complex Refractive Index

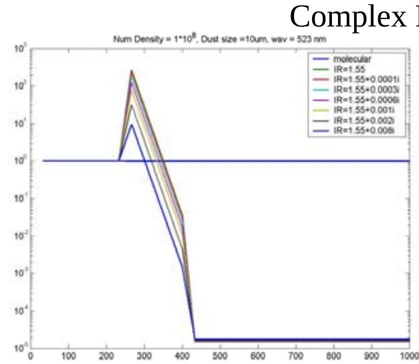

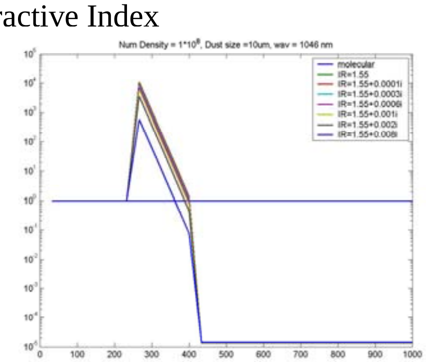

Extinction Efficiency Ratio

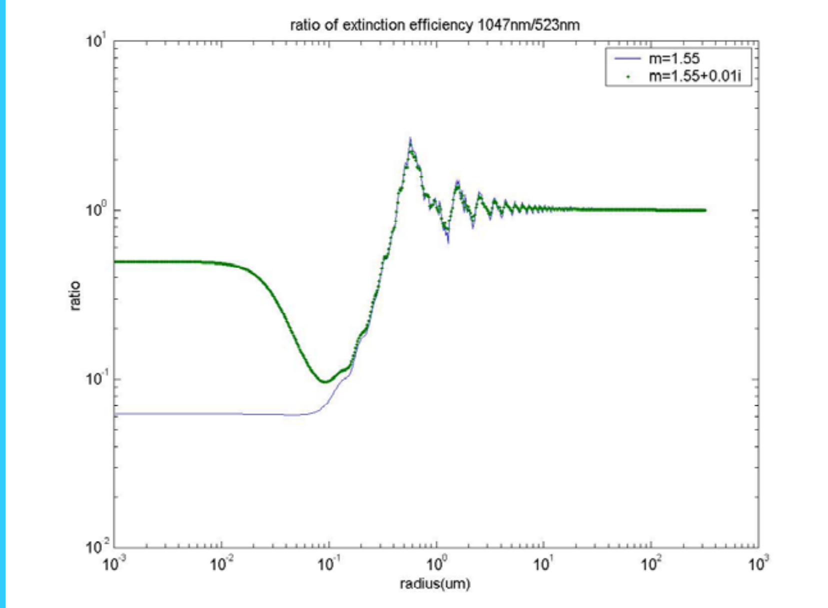

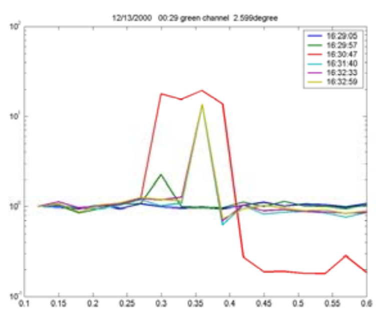

Test #2

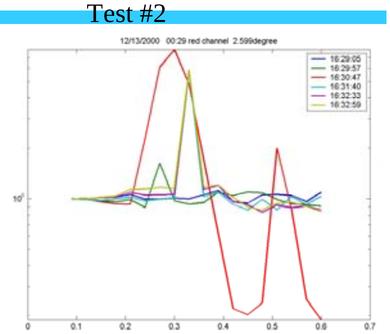

2-λ Backscatter and Extinction

Compare model dust-cloud backscatter and extinction with measured lidar values at 1047 and 523 nm for Test#2 5.0 kg soil

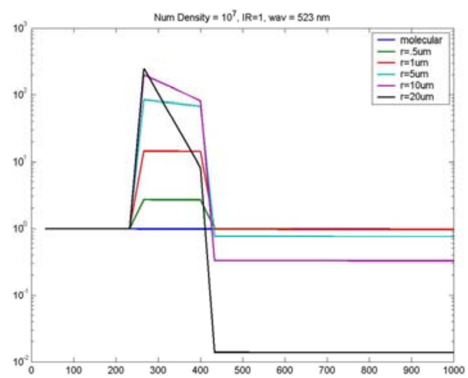

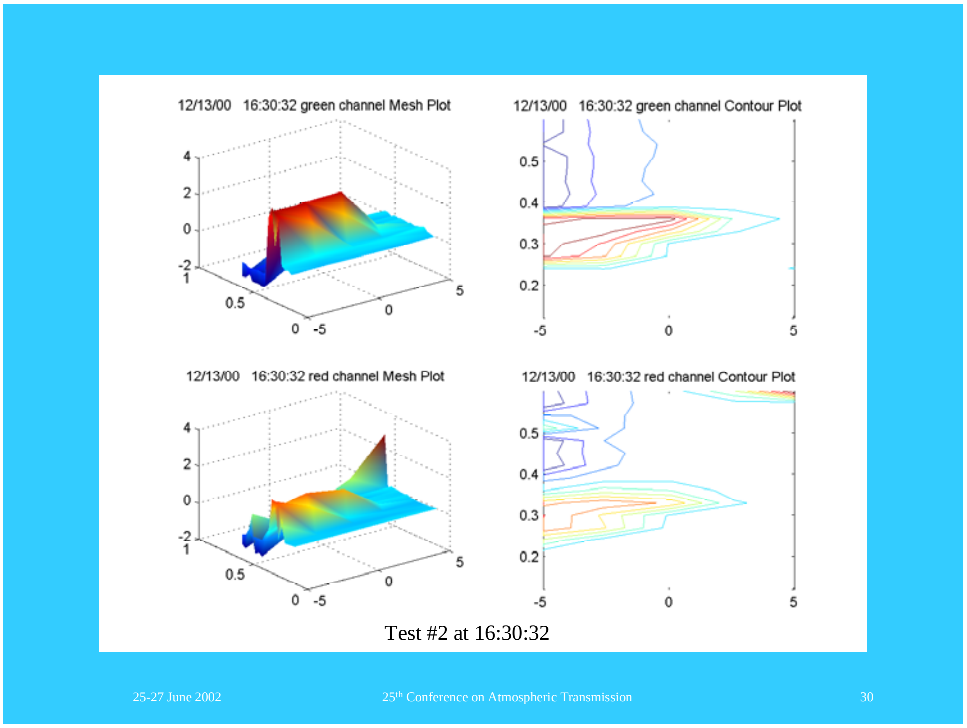
12/13/00 16:30:32 green channel Mesh Plot
12/13/00 16:30:32 green channel Contour Plot
12/13/00 16:30:32 red channel Mesh Plot
12/13/00 16:30:32 red channel Contour Plot
Test #2 at 16:30:32
25-27 June 2002
25th Conference on Atmospheric Transmission
30

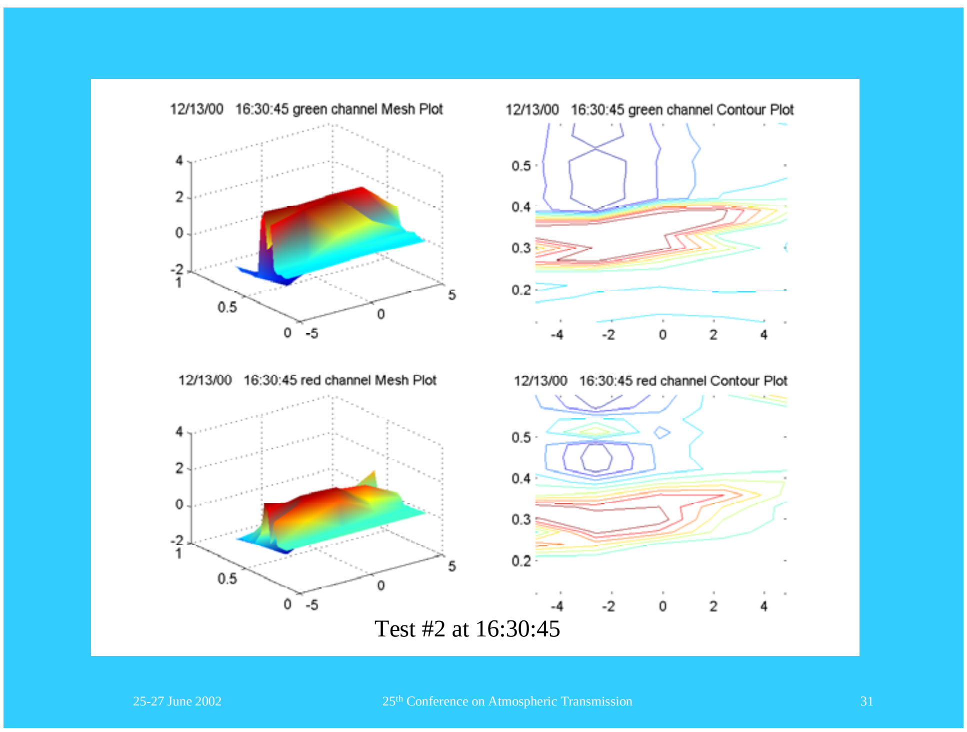
12/13/00 16:30:45 green channel Mesh Plot
12/13/00 16:30:45 green channel Contour Plot
12/13/00 16:30:45 red channel Mesh Plot
12/13/00 16:30:45 red channel Contour Plot
Test #2 at 16:30:45
25-27 June 2002
25th Conference on Atmospheric Transmission
31

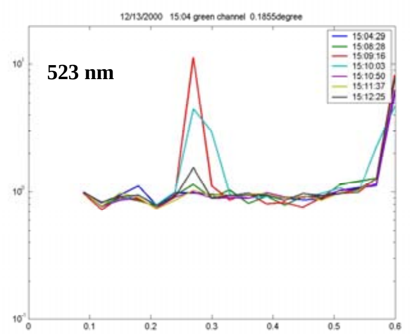

Small Puff Dust Cloud

Test #1 - 0.54 kg soil released in 5 sec, measured on fixed radial extracted from scan data for green and red wavelengths compared with calculation

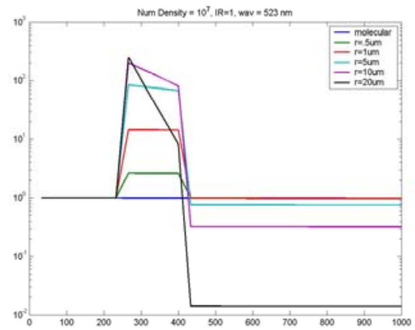

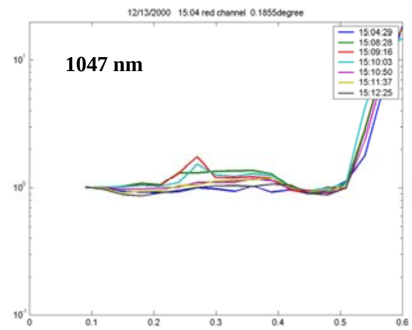

Vertical Extinction Profiles

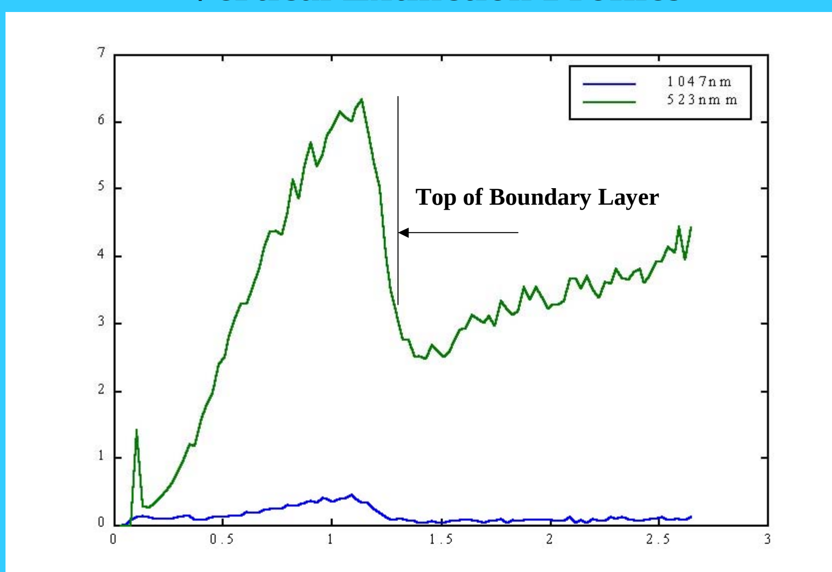

25-27 June 2002 25th Conference on Atmospheric Transmission 33

Vertical Profiles

Time sequence of vertical profile (75 degree elevation) during wind storm on 18 December 2000

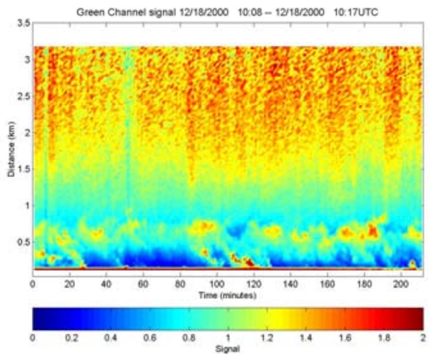

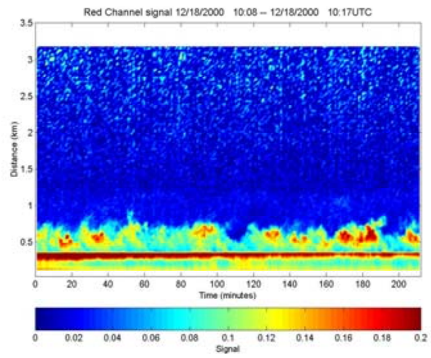

25-27 June 2002 25th Conference on Atmospheric Transmission 34

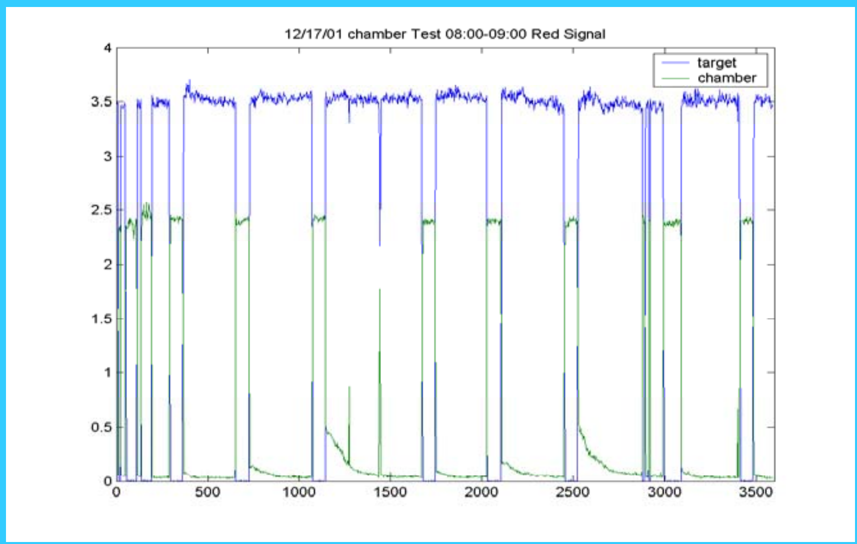

25-27 June 2002 25th Conference on Atmospheric Transmission 35

F-3. Manuscript Prepared for U.S. Environmental Protection Agency's 12th Annual Emission Inventory Conference: Emission Inventories-Applying New Technologies, San Diego, CA April 29-May 1, 2003.

Evaluation of Fugitive Dust Deposition Rates Using Lidar

Dennis Fitz and David Pankratz
College of Engineering-Center for Environmental Research and Technology
University of California, Riverside
1084 Columbia Avenue, Riverside CA 92507
dfitz@cert.ucr.edu

Russell Philbrick and Guangkun Li
Department of Electrical Engineering
The Pennsylvania State University
University Park, PA 16802
crp3@psu.edu

ABSTRACT

Ambient measurements suggest that source inventories of PM_{10} from geologic sources are overestimated by 50 percent or more. This discrepancy may be due to inaccurate emission calculations and/or due to the rapid deposition of PM_{10} after entrainment into the atmosphere. A two-wavelength scanning backscatter lidar was used to investigate PM_{10} deposition rates from artificially generated fugitive dust. Dust was generated by vehicles on unpaved roads, a tilling operation, and from a blower fan, that dispersed known amounts of finely ground calcium carbonate or native soils. The size and concentration of the resulting dust plumes were monitored for up to a half-hour and a distance of several kilometers. The changes in these dust plumes' characteristics with time are depicted using a lidar to measure the relationship between backscatter and extinction at two wavelengths. An outdoor test chamber was prepared and used to examine the particulate size distribution and optical scattering properties of several different natural dust types and different preparations of powdered $CaCO_3$ samples under controlled conditions. These same materials were used to generate plumes for open atmosphere tests. Backscatter and extinction values calculated from models, based upon Mie theory for spherical particles, are compared to actual signals. These models show the dependence of optical backscatter and extinction upon the size, number density and refractive index of the particles. Thus, simultaneous measurements of the backscatter and extinction at two different wavelengths permitted the examination of settling rates of dust particles as a function of size. The larger particles, which contain most of the PM mass, settle out of the air fairly quickly, however, the fine particles contribute primarily to the backscatter, and remain suspended much longer. The results suggest that rapid deposition of PM_{10} particles, and the relatively longer residence time of the optical plume associated with small particles (< 2:m), may have led to overestimates of airborne particle mass in plumes.

INTRODUCTION

Geologic material is a major component of the airborne particulate matter in the western United States. Airborne particulate matter is an air quality concern because:

- Recent studies have associated increases in airborne particulate matter with increased morbidity and mortality, particularly in elderly and respiratory impaired individuals[2, 3, 4].
- Reduced visibility due to airborne particulate matter has both degraded the aesthetic beauty of natural views and affects activities such as the scheduled operation of air traffic.
- The changes in suspended airborne particulate matter alter the optical properties of the atmosphere and may impact the radiative energy balance of the Earth's environment.

Source inventories for PM_{10} and $PM_{2.5}$ based on AP-42 algorithms show that geologic dust should contribute approximately 50% of the $PM_{2.5}$ in the western United States. Ambient measurements show that material of geologic origin typically contribute approximately 10% to the mass concentration[5]. There are several potential reasons for this discrepancy, the primary ones being inaccurate algorithms and data to calculate emission inventories and uncertainties of the lifetime of PM in the atmosphere.

Our overall objective of the project was to characterize the fate (deposition and transport) of PM emissions originating from mechanical disturbance of the soil (see Watson and Chow[5]). The results from the measurements will be used to validate the accuracy of the algorithms used to determine emission inventories from such sources. The study focuses on PM from unpaved roads and agricultural tilling. The tests also include artificially generated dust clouds of material of known size distribution to provide a validation of the analysis of the optical scattering properties and the algorithms for deposition of airborne particulate matter. The results allow a more accurate assessment of such fugitive dust sources to the regional PM concentrations. These assessments should then aid the formulation of cost-effective PM control strategies.

A specific objective of this project was to understand and define the differences between the measured and modeled concentrations of airborne dust carried in plumes from various sources. The results from the two measurement campaigns accomplished under this program during December 2000 and December 2001 have been analyzed and continue to hold our interest for investigations of the dynamical processes occurring in the planetary boundary layer. The preliminary results from the experiments conducted in December 2000 were presented during the last year.[1, 6, 7]

The interpretations and conclusions gained from the analysis of the results are discussed and example results that support the interpretations and conclusions are presented. The basic finding is that by combining measurements of the backscatter and extinction from the lidar with simple models demonstrates that the mass, represented primarily by the larger particles, settles out of a dust plume rapidly and results in a rapid decrease in optical extinction. The small particle fraction provides most of the optical backscatter and thus a plume carrying a relatively small amount of mass is still observed in backscatter for an extended period of time. This factor can be misleading and leads to an incorrect conclusion that the particle mass remains suspended for longer and is transported further than is actually the case. The simultaneous measurements of backscatter and extinction provide the clue that the model calculations of settling times must be reconsidered. The particle settling velocities in standard texts indicate longer residence times than those found in these experiments, and the results raise questions about what factors may contribute to a faster settling rate for the larger particles. The Stokes velocity enhanced by turbulent velocities change the migration velocity for particles in a range of aerodynamic sizes. Motion of heavy particles is dominated by gravitational effects and very light particles will be controlled by diffusion. In the normal surface layer, turbulence cells are present from generation by wind shears and by turbulent convection from surface heating and these must be considered.

The work was done in a test area where the generation conditions were controlled and where backscatter lidar could be safely used in the scanning mode to characterize the distribution of particulate matter. Tests were conducted by generating PM emissions to simulate emissions from vehicular travel on dirt roads and soil tilling operations. A series of individual test runs was conducted with data collected from real-time measurement methods.

RESEARCH APPROACH

The study was conducted at the University of California, Riverside, Agricultural Field Station in Moreno Valley, CA. The 720 acre facility is relatively level, except for some raised (~10 feet) dirt roads that run between some of the fields. There were no significant sources of PM around the facility. The project team coordinated with the UCR field site staff regarding any planned field plowing to avoid that activity during periods that tests were performed. The prevailing daytime winds were expected to be from the west during December.

A background meteorological station measuring wind speed (WS), wind direction (WD), temperature (T) and dew point (DP) was also located at this site. The meteorological tower provided wind speed and direction at 2, 5, and 10 meters, temperature measurements at 2 and 10 meters, and net radiation measurements at 1.5 meters. The signals from the meteorological sensors were scanned once per second by a Campbell CR10X data logger and processed into ten-second averages.

The SESI scanning micro-pulse lidar (MPL) was located 500 to 800 meters away from the plume generation region during the December 2001 measurement program. The lidar provided the backscatter signal profiles at two wavelengths (523 and 1047 nm) and has several features that make it the ideal instrument for mapping the dust clouds to be generated in this program. The instrument has a scanning platform, which can be used to provide a mapping of the airborne particulate matter. The instrument is eye-safe but maintains high sensitivity by using high average power, obtained from operating at a high pulse repetition frequency (prf), and expansion of the beam to produce lower energy flux per unit area. The MPL measures the backscatter signal profiles at 1047 nm in the near infrared (NIR) and 523 nm in the mid-visible spectrum. These wavelengths are most sensitive to scattering from particle sizes in the size range near 1 :m, and they are separated sufficiently to provide some sensitivity to changes in fine particle size distributions. The lidar results were obtained by simultaneously integrating the signal returns for 2 seconds in range bins that are 33 meters in length for each of the wavelengths.

During the open atmosphere testing, a high-resolution digital video camera (Sony Digital DCR-VX700) was mechanically coupled to the lidar to document the distribution of the dust generated and to verify the lidar pointing direction. Images were taken at each scanning position by the camera mounted on the top of the lidar to follow the path of the laser beam and provide a clear picture of the area being scanned. The scanning lidar with the camera was located upwind of the generation point. The scan covered the region about 10-20☜ on either side of the centerline between the location of the lidar and the generation point. An inclinometer was mounted on the lidar to measure the elevation angle.

Open atmosphere measurements were obtained during both measurement programs using a blower to generate plume puffs from soil and from calcium carbonate dust, and by using a vehicle (truck or tractor) to generate off-road dust as shown in Figure 1. The blower device for generating dust puffs used a 5 horsepower centrifugal blower. During the pilot study in December 2000, limited testing was carried out using calcium carbonate (~10 :m size) and a fogger (propylene glycol) of the type used to provide special effects for the film industry. The December 2001 tests used many different sizes of $CaCO_3$ dust and sifted soil types from several locations; including the local field, soil from California locations of Shafter, Westside and Kearney. During the 2001 campaign, an additional type of measurement was undertaken using a test volume where particle concentrations could be measured using a controlled 10-meter chamber, as shown in Figure 2. The 10-meter chamber was setup about 630 meters from the lidar instrument and aligned so that the beam could pass through the chamber. A target board was setup beyond the chamber at a range of 700 meters. The beam is about 25 cm in diameter and could pass though the chamber without any scattering from the chamber walls. PM_{10} concentrations were continuously monitored (TSI model 8520 DustTrak^{TM} with 10:m size selective inlets) at the front, middle and back end of the chamber with a two second resolution. An optical particle counter (Climet Model Spectro 0.3) was used to determine the particle size distribution in sixteen channels from 0.3 to 20:m at the middle of the chamber, near the location where the sample was blown into the chamber.

The Scanning Micro-Pulse Lidar (MPL) used for these investigations was leased from Science and Engineering Services Inc. (SESI) and operated by the Penn State University graduate students. The instrument provides a backscatter signal at 2 wavelengths and has several features that make it the ideal selection for mapping the dust clouds to be generated in this experiment. The instrument has a scanning platform which can be used to provide a mapping of the airborne particulate matter. The instrument is eye-safe but maintains high sensitivity from using a high average power, obtained because of high operating prf (several kHz), and by expanding the beam to produce lower energy flux per unit area. Two Nd:YLF lasers are used at their fundamental and frequency doubled wavelengths of 1047 and 523.5 nm with energy outputs of approximately 10 and 5 :J, respectively. The beams are expanded and transmitted through a 20 cm diameter telescope, which is also used to receive the backscattered signal. An avalanche photo-diode detector is used in a pulse counting mode to measure the returned signal at each of the two wavelengths. The instrument has several operating modes, however we selected the highest range resolution (33 meter data bins) and used a two-second integration of the signals for each profile. The most useful results are obtained by averaging the returns backscattered from the clear atmospheric path before generating a dust plume on the path. The results obtained by forming a ratio of the measured dust profile to that of the clear path then provides a measure of the optical backscatter and extinction signals associated with the generated dust plume.

The procedure for measurements in the chamber was to close the ends of the chamber, turn on the three fans located inside and then inject the dust. After one minute, the ends of the chamber were opened, fans turned off, and the laser beam measurements commenced. The lower panel in Figure 3 shows a sequence of three tests using the chamber. The sequence of events, which included closing of the chamber, injection of the dust puff and subsequent opening of the chamber, is clearly shown. The upper panel in Figure 3 displays the raw signal from the lidar during these same tests. The chamber and target board data are taken from the 19^{th} and 21^{st} range bins of the lidar corresponding to ranges of about 630 and 700 meters, respectively.

RESULTS

Only a small sample of the results obtained can be included in this paper. We have chosen to use a set of chamber tests and open air tests performed on one test day during the primary testing program in December 2001 as an example of the type on measurements obtained. The measurement record for chamber tests on19 December 2001 is summarized in Table 1. Figure 3 shows the raw lidar returns from the chamber and the target board and the signals from the DustTrak for the 0.7:m $CaCO_3$ tests #10 (50 mg), #11 (200 mg) and #12 (800 mg) on 19 December 2001. The measurements in Figure 3 from the Lidar and DustTrak show the signals change as the amount of material in the sample increases, 50, 200 and 800 mg, however the 50 mg signal is so small that those results are not very useful.

The upper panel of Figure 3 shows the signal return from the closed end on the chamber near 05:44, 05:50 and 05:55. When the chamber is opened, the lidar return from the dust in the chamber and the target board are observed. Since the chamber is only 10 meters in length (corresponding to only 1/3 of one range bin), the extinction signal is relatively weak and the hard target return is the only practical way to observe any extinction signal. Examination of the signals of the target board return shows that the extinction corresponding to the dust path can be detected. For example, the upper panel of Figure 3 at about 05:51 (test #11) shows the extinction signal at the same time as the larger return from the backscatter signal. When the backscatter signal is highest, the return from the target board is reduced, however the S/N is not sufficient to permit a quantitative measure of the extinction value from the target board returns. The lower panel of Figure 3 shows the three DustTrak measurements (front, middle and back of chamber) together with the lidar signal return, which has been normalized to “1” by using measurements of the clear atmospheric path before the test. The lidar signal in the chamber is high before opening due to the back scatter from a white card placed on the front of the chamber. The backscatter from the dust is observed in the lidar return when the path is open but the concentration within the chamber volume is not sufficient to observe any path extinction on the atmospheric path. A comparison of these three tests (#10 - #12) shows some difference in the settling rate of the dust that is probably due to the fans not being turned off exactly at the same time in this case. The increase in signals with increasing sample size is easily observed. During a measurement period when the Climet spectrum was obtained (1 minute), the DustTrak data (two second step) was averaged and compared with the integrated value of particles less than 10 :m reported by the Climet instrument, and the comparison was quite good. The range of these instruments includes most of the particles contributing to the optical properties, since heavier particles settle quickly. The instruments are capable of measuring particles less than 20 :m (Climet) and 10 :m (DustTrak) respectively, and so the concentrations of larger particles are not characterized.

The particle size spectrum from the Climet instrument of the 0.7 :m $CaCO_3$ sample is shown in Figure 4. A two component log-normal distribution has been fit to the measured spectrum. The particle size spectra of the various $CaCO_3$ crush samples measured on 19 December 2001 are shown in Figure 5 from the tests using the 200 mg samples. The variations between these curves are small on a log scale, however, the observed variation agrees with expected changes. It is apparent that the 0.7 :m sample is anomalously low compared with the other samples. The lower particle concentration observed in the 0.7 :m tests may be due to poor disbursal during injection, or may be lost because of the particles adhering to the plywood sides of the chamber. Examination of Figure 5 shows that the relative signals change as expected for the other size distributions measured. The Climet instrument measurements of the 0.7 :m sample, that are shown in Figure 5, are presented as mass density and number density in Figure 6. We use the particle spectrum shown in Figure 6 to calculate the expected optical signal expected for the lidar and examine the expected variations when the larger particle sizes are removed from the distribution, this analysis is described at the end of this report.

The results shown in Figure 7 provide the Climet particle spectra for the several types of soils measured during the chamber tests. Soil samples included local sifted field soil and soil samples from several California sites, including Shafter, Westside and Kearney locations. In addition, the results from 2 and 10 :m samples of $CaCO_3$ and a standard of Arizona Road Dust were measured, and the results are shown in Figure 7. It is obvious that the $CaCO_3$ samples contain a larger relative concentration of the smaller particles than do the soil samples. Also the Arizona Road Dust contains a larger fraction of small particles than any of the other soil samples.
The open field tests of these samples were conducted by generating sample puffs using the blower generator. In Figure 8, the time sequences of the lidar measured backscatter peak values and the integrated extinction through the cloud are shown for Test #44, which is a 600 g sample of 0.7 :m $CaCO_3$. This plot shows the ratio of the signals relative to the background atmospheric path prior to the test. The interesting thing to note is that the backscatter signal remains high for quite a long time after the extinction signal has returned to pretest levels. The fact that there is such a large difference in the residence time for particles in the size range between 1 and 10 :m is recognized from the expected settling velocity shown in Figure 9.[8]

Figure 10 shows a typical experiment depicting the generation of a dust cloud generated with the blower unit as observed by the digital video camera mounted on top of the lidar instrument. The dust generation equipment was located at ranges from 150 to 800 meters in various test scenarios. The lidar was used to either point at the center of the plume, as in the results of Figure 8, or was scanned automatically to make a horizontal cut through the test volume, and the elevation angle could be adjusted manually. Using the scanning lidar, the plumes were generally tracked out to 1.5 km along the path and on radials, which were set to sweep up to $\pm 30^o$ horizontally. The plumes probably could have been tracked much longer, at least along some radials (up to the lidar's maximum range of 20-30 km). Because it was more desirable to obtain data over shorter ranges, plume tracking generally stoped when the plume drifted to ranges greater than about 1.5 km.

A simple model calculation based upon the scattering theory for spherical particles by Gustov Mie has been used to simulate first order effects observed. Mie theory calculations provide the scattering angle dependence for spherical particles with various indices of refraction.[6, 7] While the dust scattering studied in these experiments cannot be described as associated with spherical particles, it still provides a useful comparison of the scattering properties. In particular, the Mie theory results should provide accurate results for the smaller particles, where shape is less important, and the relationship between the forward and backward scatter intensities (extinction and backscatter) should provide useful insight for this investigation. The theory also provides information on the variations in the absorption of the particles due to their complex index of refraction. The Mie scattering theory used for this investigation is a straightforward application of the scattering intensity in the two polarization planes that comes directly from electromagnetic theory, and all of the applications here use only the 0^o and 180^o scattering intensity. Figure 11 shows model calculations of visible and NIR backscatter and extinction for several mono-disbursed particle diameters and for a range of particle concentrations. The calculation simulates a 200-meter-thick uniform dust cloud and calculates values at 30-meter intervals (same as the bin size of the lidar result). The figure shows the differences in backscatter and extinction signals as the density and size of particles is changed. It is important to notice that the extinction only depends on the concentration and size of particles and weakly on the wavelength of absorption. However, the backscatter does depend strongly on the wavelength. The calculations shown in Figure 11 demonstrate that the backscatter intensity and the extinction depend on the particle size. The relatively larger backscatter for the NIR wavelength is expected based upon the fact that the longer wavelength allows the particles to remain longer in the Rayleigh scattering range, where the cross-section dependence ($r^6 \sim 2^6 = 64$) results in increased scattering. Increasing the particle size increases the backscatter up to the point where the scattering loss results in an optical thickness that reduces the backscatter signal. The value of using the results from the mono-disbursed distribution of particles depicted in Figure 11 is limited because real particle distributions always contain a significant range of particle sizes. However the same calculations can be carried out for a range of particles sizes, as shown in the following example.

The lidar backscatter signal and strength of attenuation from passing through the dust cloud generated by the blower unit is shown in Figure 12. These curves are obtained by comparing with the backscatter signal before the dust was generated, the signal strength starts increasing at the front edge of dust plume and forms a peak in the center of cloud. The backscatter coefficient can be estimated from the signal magnitude. After the laser beam passes through the cloud, there is a sudden drop of backscatter signal due to the attenuation of the laser beam. The extinction coefficient can be estimated by the attenuation amount, which is the signal drop after the laser signal passing through the dust plume. If we assume the dust particles inside the cloud are uniform and spherical, a certain relationship should exist between the values of backscatter and extinction coefficients that correspond to a dust plume with given set of particle sizes. This will allow us to simulate the laser backscatter profile passing through the cloud and specify the dust particle size and density from the analysis of the simulation.

Figure 12 shows one example from the 19 December 2001 test (#44) for the case of 0.7 :m calcium carbonate cloud containing 600 grams of material. Notice that the magnitude of the backscatter and extinction are similar to the values that would be expected from the simulation shown in Figure 11(a). After release, the backscatter signal does not change very much during the next two minutes (4 profiles) while the extinction is observed to recover. This point is even better observed in the presentation of the same results in Figure 8. The small particles in the sample material are sufficiently small that the settling time is slow, however the rapid recovery of the extinction is observed as the larger dust particles settle out of the sample.

The model calculations, shown in Figure 13, depict the backscatter and extinction which would be expected for the sample of 0.7 :m $CaCO_3$ particles represented in Figure 6, which shows the particle size spectrum for this material. The calculations shown in Figure 13 represent the changes which are expected to occur as the particles larger than a certain size are removed. The particle distribution shown in Figure 6 is truncated for particles greater than selected sizes to calculate the optical properties. The calculation is intended to represent the changes that would be expected for the case of larger particles settling from the distribution. It is interesting to see that this simple calculation does have many similarities to the results shown in Figure 12. The magnitude of the backscatter and extinction calculated from the particle size spectrum does agree well with the measured lidar profiles. The changes in the backscatter and extinction calculated from truncating the particle spectrum agree quite well with the time sequence of measured profiles. These comparisons show that the relative changes in the backscatter and extinction profiles are representative of the settling of larger particles from the airborne sample.

The experimental backscatter and extinction measurements can now be examined in the context of the simulation calculations. Progress has been made on the more difficult task of using the field measurements to solve the inverse problem and describe the particulate matter properties from the scattering profiles. Our goal is to describe size and distribution of the airborne PM and to show the variation in the settling rate of the particulate matter from various sources. The analysis is aimed at developing the inversion algorithm for fully describing the changes in particle size within the generated dust clouds.

CONCLUSIONS

Optical scattering measurements using lidar have been examined for each of the several tests using native soils and sized calcium carbonate samples to generate dust plumes, and some examples of these results are presented here. A set of measurements has been obtained using a 10-meter chamber to simultaneously measure the optical scattering properties with a lidar and with measurements of the particle density and size distribution. The model calculations show that extinction is more dependent on larger particle sizes. Based on the analysis of results obtained, the settling rates of the larger particle component result in reduction in the optical extinction prior to the decrease in backscatter signals, which are dependant on the scattering from a larger number of smaller particles. The analysis and interpretation from the data collected on fugitive dust of various types will be carried out using the lidar data obtained. The preliminary conclusion is that the rapid settling rate of the larger particles results in the lower quantity of fugitive dust as a fraction of emission inventory. The backscatter signals from small particles, which have a longer residence time, result in a much longer apparent residence time of airborne fugitive dust, however, the observed plume may not carry a significant fraction of particle mass. The data will be used to critically examine the settling rates for the various particle sizes. Even though the aerodynamic settling velocity of the airborne particles through the atmosphere has been studied for many years, the additional effects from turbulence generated by surface wind shear and by convection may also change the residence times expected for various particle sizes.

REFERENCE

1. Fitz, D., D. Pankratz, R. Philbrick, and G. Li: "Evaluation of the Transport and Deposition of Fugitive Dust Using Lidar," Proc. Environmental Protection Agency's 11th Annual Emission Inventory Conference: Emission Inventories-Partnering for the Future, Atlanta GA (2002)
2. Magari, S.R., R. Hauser, J. Schwartz, P.L. Williams, T.J. Smith, and D.C. Christiani: "Association of Heart Rate Variability with Occupational and Environmental Exposure to Particulate Air Pollution," *Circulation* 104, 986-991, 2001.
3. Peters, A., D.W. Dockery, J.E. Muller, and M.A. Mittleman: "Increased Particulate Air Pollution and the Triggering of Myocardial Infarction," *Circulation* 103, 2810-2815, 2001.
4. Mauderly, J., L. Neas, and R. Schlesinger: "PM Monitoring Needs Related to Health Effects," *Proc. PM Measurements Workshop*, EPA Report No. 2, Chapel Hill, NC, pp 9-14, July 1998.
5. Watson, J.G., J.C. and Chow: "Reconciling Urban Fugitive Dust Emissions Inventory and Ambient Source Contribution Estimates: Summary of Current Knowledge and Needed Research," Document No. 61110.4D2, Desert Research Institute, Reno NV, September 3, 1999.
6. Li, G., S.N. Kizhakkemadam, and C.R. Philbrick: "Optical Scattering by Airborne Dust Particles," Proc. Air Force Optical Transmission Meeting, Hanscom AFB, MA, June 2001.
7. Li, Guangkun, Sachin J. Verghese, C. Russell Philbrick, Dennis Fitz and David Pankratz: "Airborne Dust and Aerosols Description Using Lidar Backscatter," 25th Annual Conference on Atmospheric Transmission and Radiance Models, Lexington, MA, June 2002.
8. Seinfeld, J.H and S.N, Pandis: *Atmospheric Chemistry and Physics: From Air Pollution to Climate Change*, Wiley-Interscience, 1998.

ACKNOWLEDGEMENTS
We wish to thank Patrick Gaffney and the California Air Resources Board for funding this research. We appreciate Tony Taliaferro's assistance in setting up the equipment used in this study. The efforts of Sriram Kizhakkemadam and Gregg O'Marr significantly contributed to the lidar results and were important for the successful data collection.

DISCLAIMER
The statements and conclusions in this report are those of the researchers and universities and not necessarily those of the California Air Resources Board. The mention of commercial products, their source, or their use in connection with material reported herein is not to be construed as actual or implied endorsement of such products.

Table 1. Tests, which were conducted 19 December 2003 using a test chamber (#1 - #37) and open atmosphere puffs (#38 - #55), were followed by several tests on dust generated by a plowing tractor.

Test	Material	Amount	Size
#1	CaCO3	50 mg	0.7 µm
#2	CaCO3	200 mg	0.7 µm
#3	CaCO3	800 mg	0.7 µm
#4	CaCO3	50 mg	2 µm
#5	CaCO3	200 mg	2 µm
#6	CaCO3	800 mg	2 µm
#7	CaCO3	50 mg	4 µm
#8	CaCO3	200 mg	4 µm
#9	CaCO3	800 mg	4 µm
#10	CaCO3	50 mg	10 µm
#11	CaCO3	200 mg	10 µm
#12	CaCO3	800 mg	10 µm
#13	CaCO3	50 mg	15 µm
#14	CaCO3	200 mg	15 µm
#15	CaCO3	800 mg	15 µm
#16	Az Road dust	50 mg	
#17	Az Road dust	200 mg	
#18	Az Road dust	800 mg	
#19	UCR dust	50 mg	< 425 µm
#20	UCR dust	200 mg	< 425 µm
#21	UCR dust	800 mg	< 425 µm
#22	Kearney	50 mg	
#23	Kearney	200 mg	
#24	Kearney	800 mg	
#25	Kearney	3.2 g	
#26	Westside	50 mg	
#27	Westside	200 mg	

#28	Westside	800 mg	
#29	Westside	3.2 g	
#30	Shafter	200 mg	
#31	Shafter	800 mg	
#32	Shafter	3.2 g	
#33	CaCO3	50 mg	0.7 µm
#34	CaCO3	200 mg	0.7 µm
#35	CaCO3	800 mg	0.7 µm
#36	CaCO3	50 mg	2 µm
#37	CaCO3	200 mg	2 µm
#38	CaCO3	300 g	4 µm
#39	CaCO3	300 g	75 µm
#40	Kearney	300 g	< 425 µm
#41	Kearney	1.5kg	< 425 µm
#42	CaCO3	600 g	0.7 µm
#43	CaCO3	600 g	10 µm
#44	CaCO3	600 g	0.7 µm
#45	CaCO3	600 g	4 µm
#46	CaCO3 mix	600 g	300g@4µm 300g@15 µm
#47	CaCO3	600 g	15 µm
#48	Shafter	600 g	< 70 µm
#49	CaCO3	600 g	15 µm
#50	CaCO3	600 g	100 µm
#51	CaCO3	600 g	200 µm
#52	CaCO3	600 g	100 µm
#53	CaCO3	600 g	4 µm
#54	Westside	900 g	< 425 µm
#55	Westside	900 g	< 425 µm

(a)

(b)

(c)

Figure 1. Open air generation of dust plumes: (a) blower used to generate plume of dust from sifted soil, (b) blower generated plume of $CaCO_3$, (c) dust plume from a tractor plowing.

Figure 2. Chamber was used to generate and measure a controlled sample (clockwise views): (a) Front (west) and north sides of test chamber where samples are injected and measurements made, the chamber is shown with instrumented meteorological tower, (b) DustTrak optical scatter instruments (10 :m size orifice) and Climet particle spectrometer (16 channels - 0.5 to 10 :m), (c) View of lidar from back of chamber at range of 450 meters thru the chamber (notice fans used to circulate the sample), (d) View of the east side of 10-meter chamber.

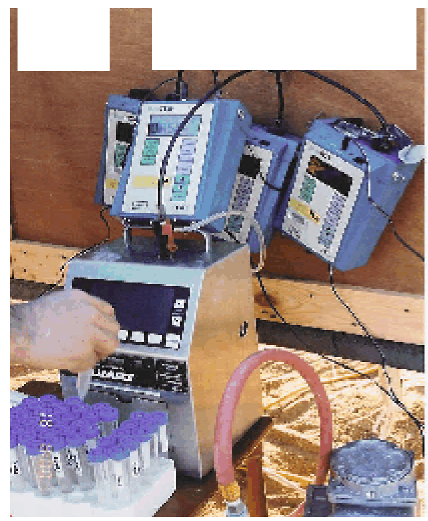

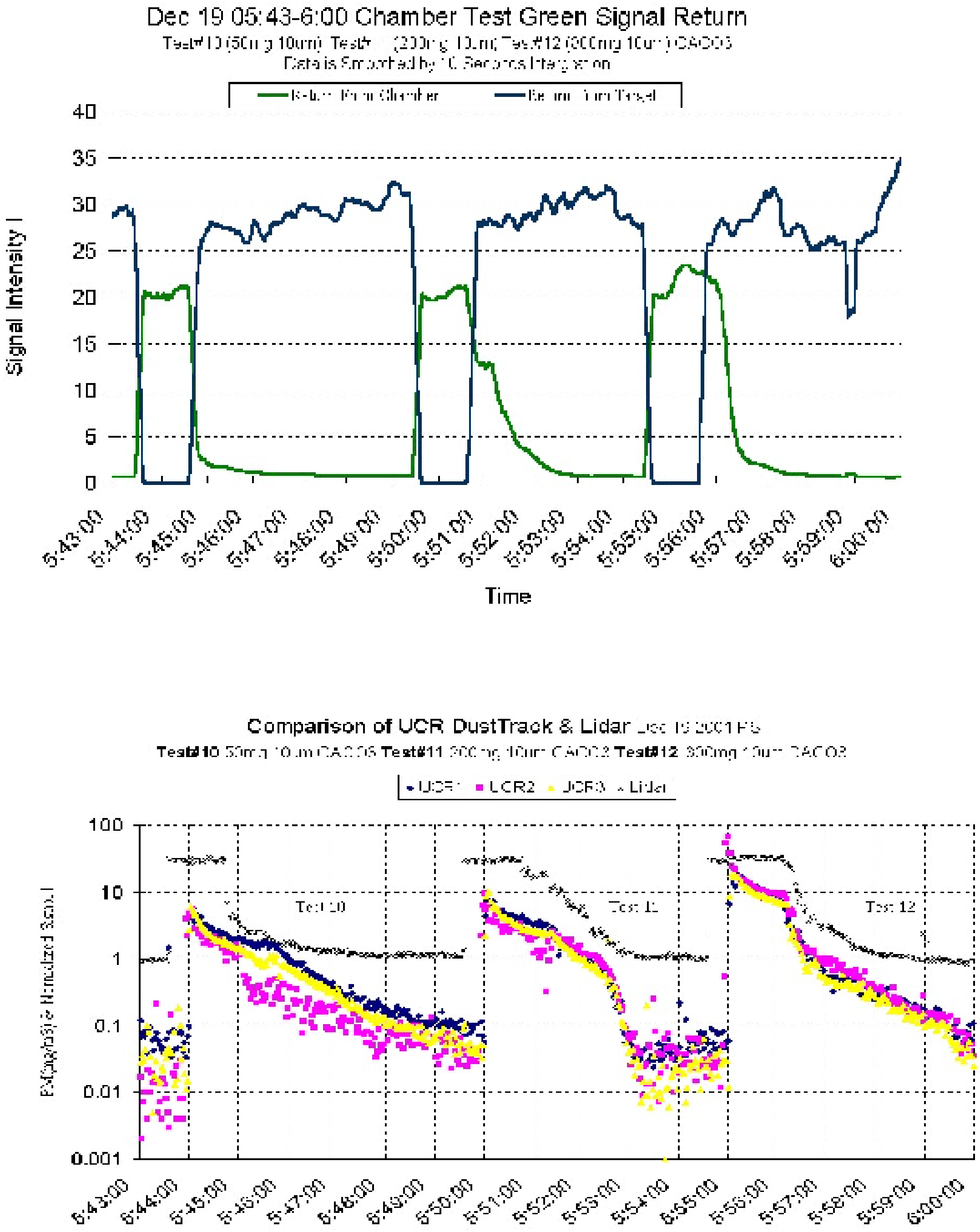

Figure 3. The chamber test measurements from Tests #10, #11 and #12 are shown. Upper panel shows the raw signal returns from the lidar at the range intervals corresponding to the chamber and the target board. The lower panel shows the signal from the DustTrak instruments and the normalized lidar return.

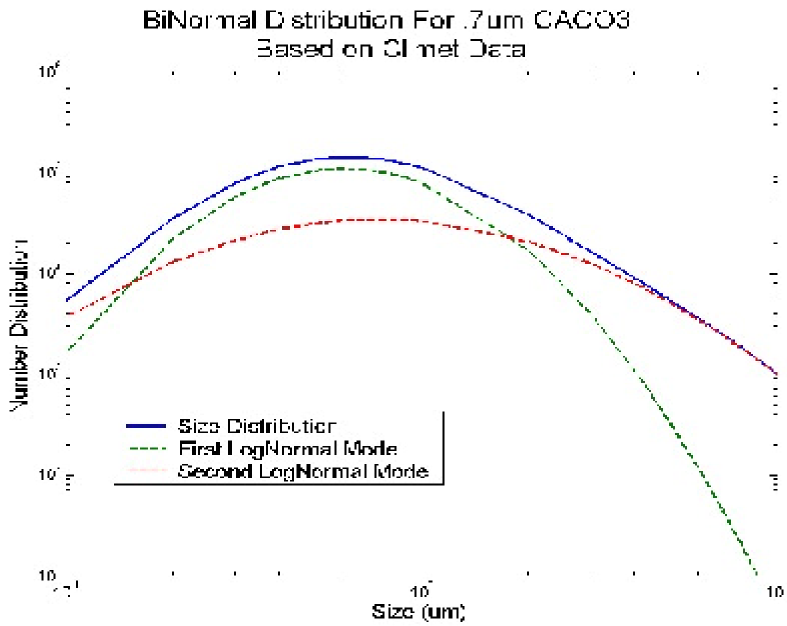

Figure 4. The log-normal distributions for a two components are fit to the Climet instrument measured curve for the 0.7 :m sample of $CaCO_3$.

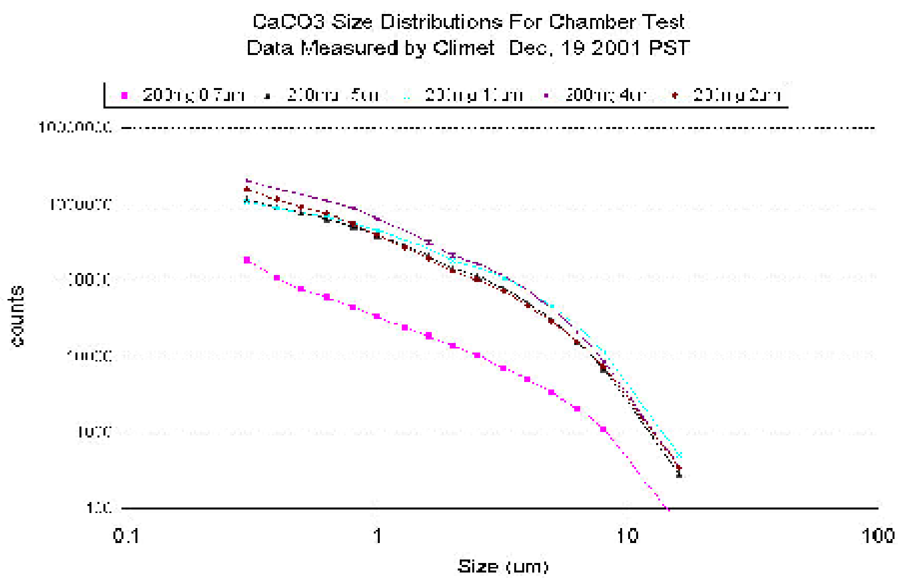

Figure 5. The Climet spectrum of the particle counts versus particle size for the several samples of $CaCO_3$ power that were used during the testing. Notice that the 0.7 :m case is an anomaly (see text) and the other samples do show a change that agrees with the increasing size of the samples.

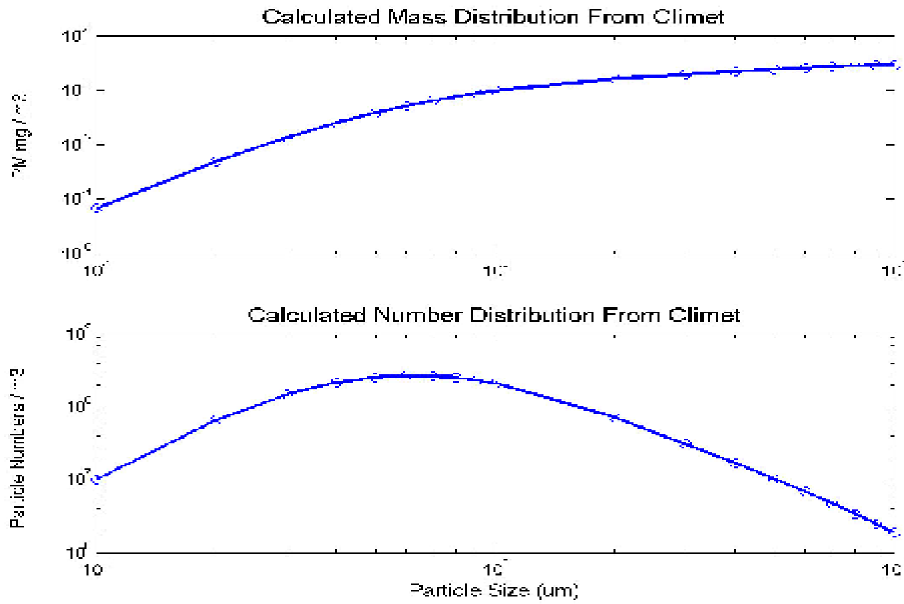

Figure 6. The Climet spectrum for the 0.7 :m sample of the $CaCO_3$ dust is shown for the measurements in Figure 5 converted to number density and to mass density.

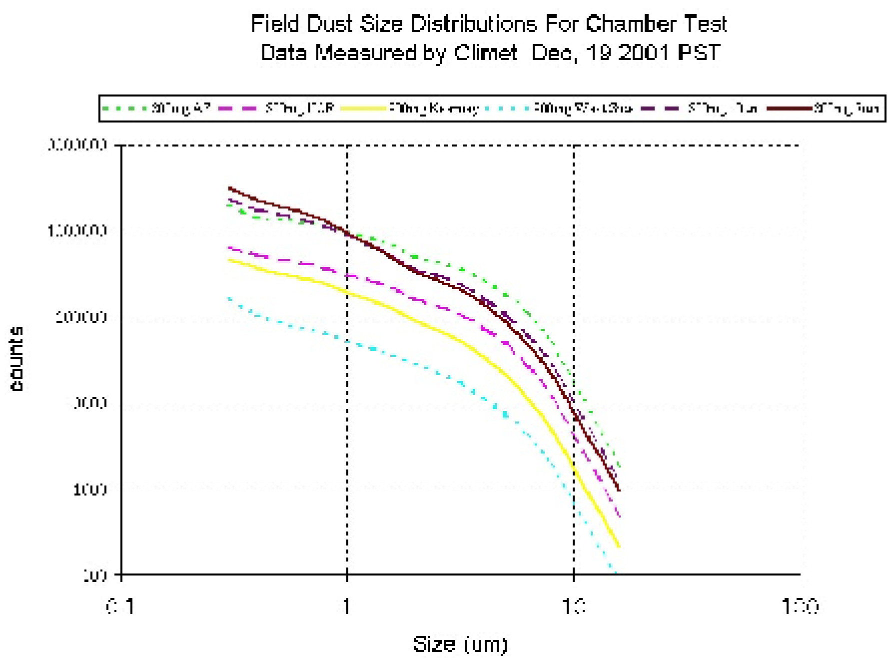

Figure 7. The Climet particle size spectra for the several different types of soil and powder used during the test are compared.

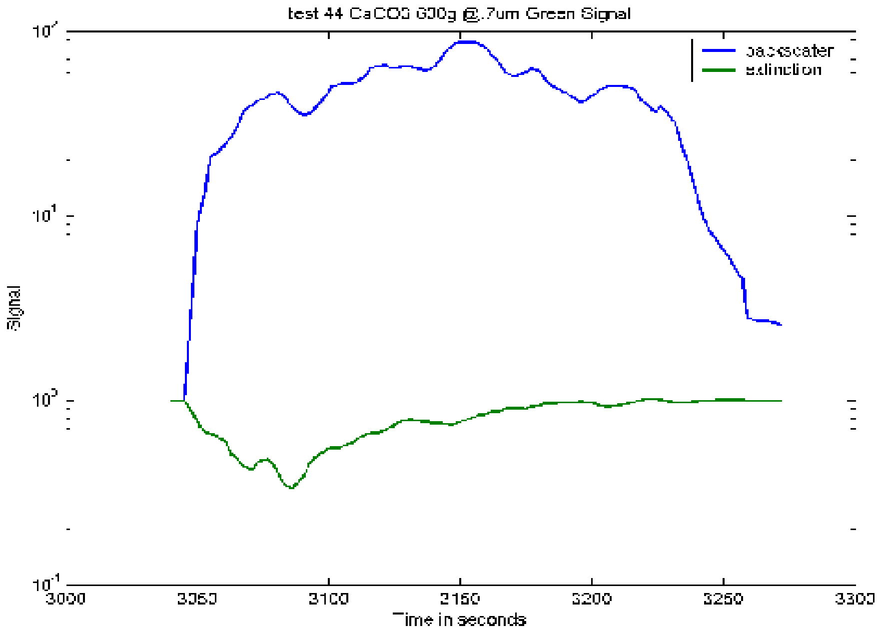

Figure 8. The open air time sequence of the lidar backscatter peak values and extinction values are shown for profiles of Test #44 on 19 December 2001 for the 0.7 :m $CaCO_3$ 600 g sample.

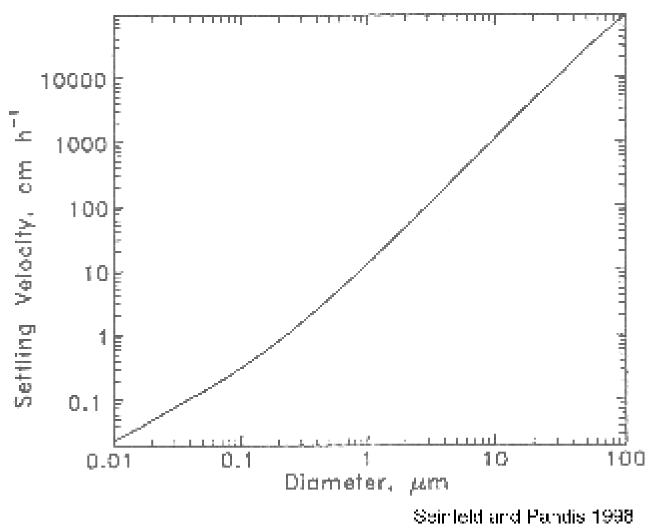

Figure 9. The expected settling velocity versus particle diameter from standard text (Seinfeld and Pandis[8]).

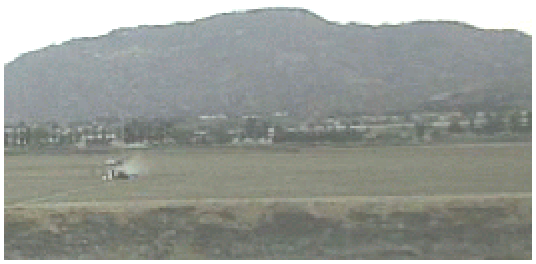

T+1 sec

T+30 sec

T+60 sec

T+90 sec

Figure 10. Example of a puff plume of local soil that is tracked by scanning lidar.

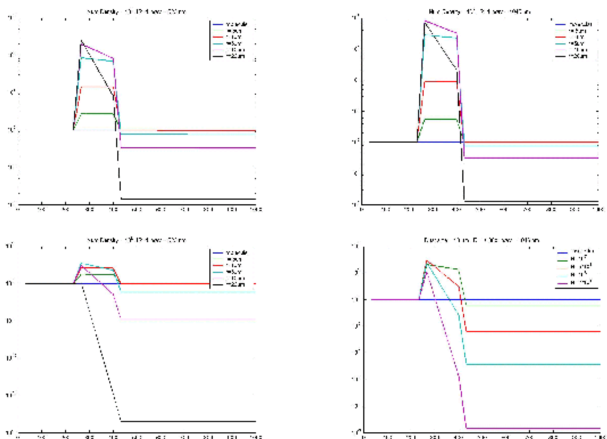

Figure 11. The calculations of the optical scattering properties expected for different size and density of particles are shown for the two wavelengths.

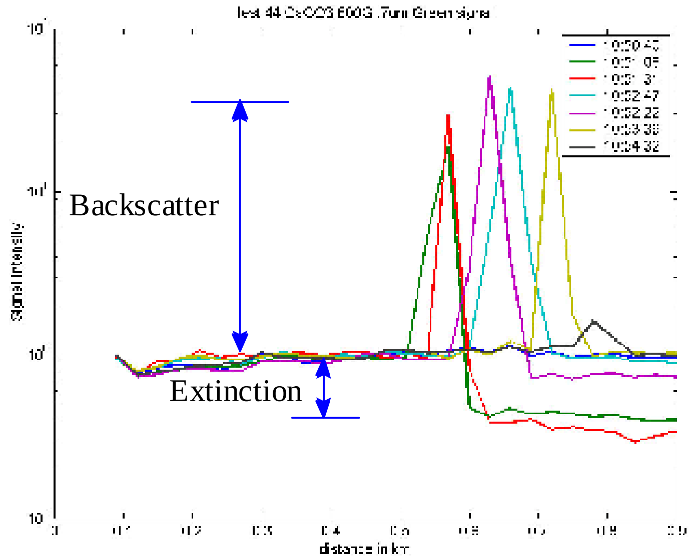

Figure 12. The results from Test #44 on 19 December 2001 show several of the lidar profiles that show the time variation in the backscatter and the extinction measured by the lidar. These range profiles are from the same data set that is shown in Figure 8.

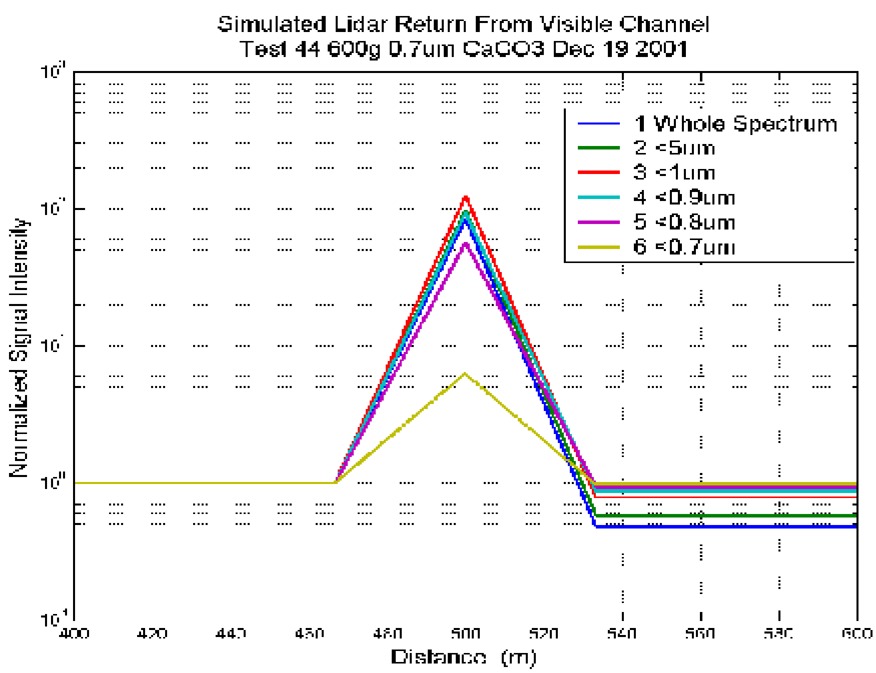

Figure 13. The results from a calculation of the backscatter and extinction expected when one sequentially removes the larger end of the spectrum of the scattering particles. The calculation is performed for the spectrum shown in Figure 6 and corresponds to the measurements shown in Figure 12.

Manuscript F-4. 24th Annual Conference on Atmospheric and Radiance Models, Hanscom AFB, MA June 6-8, 2001.

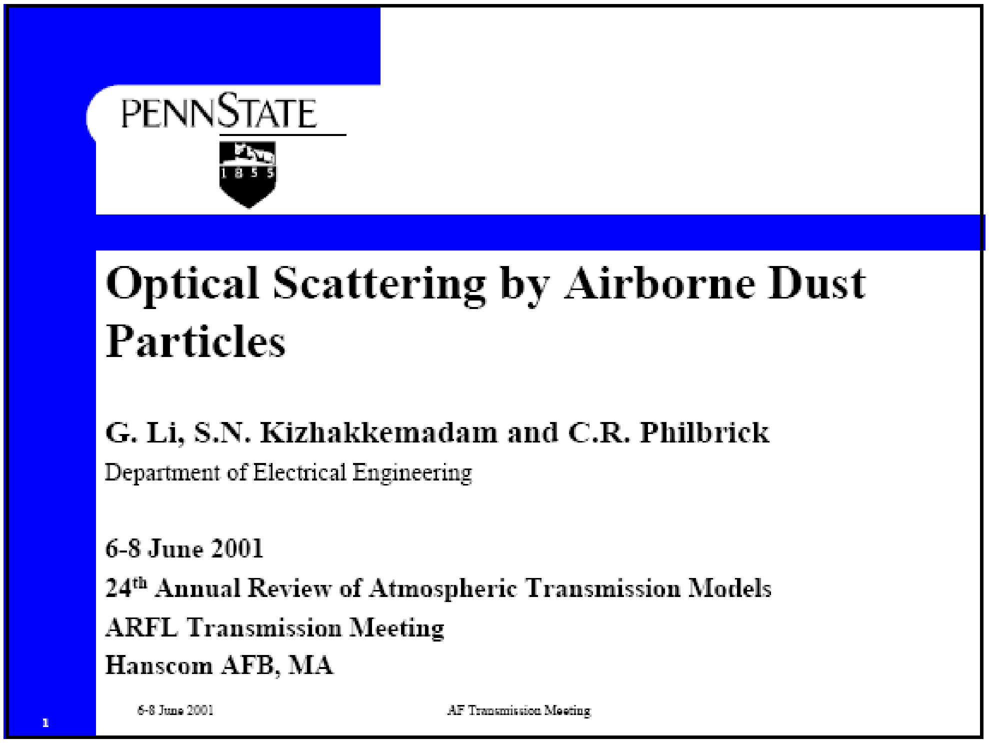

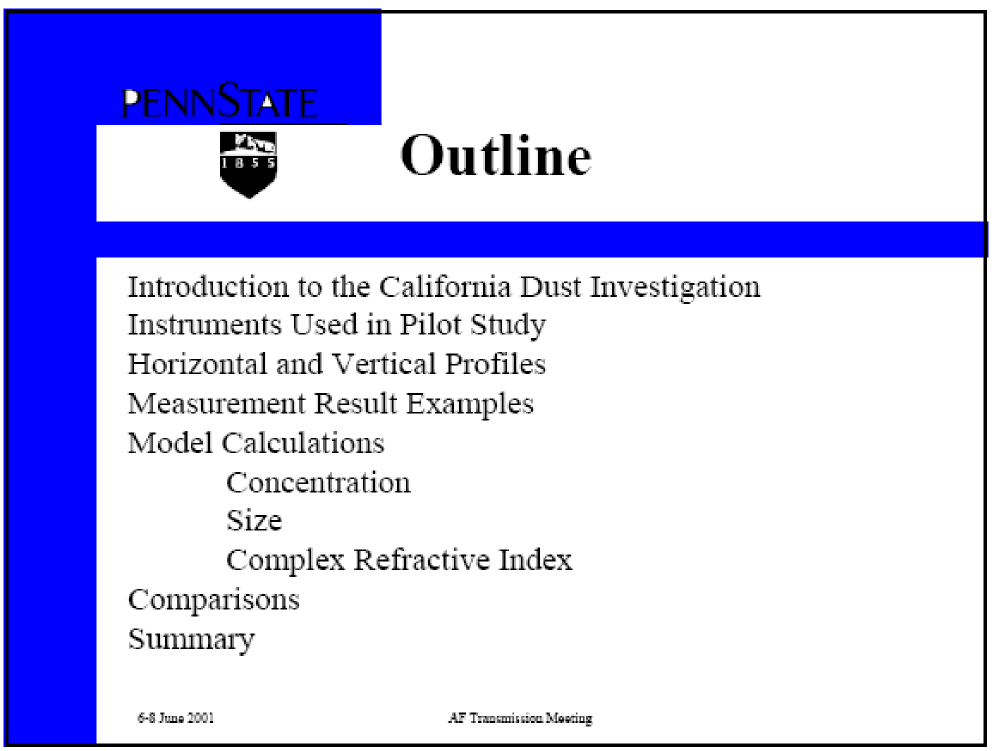

Introduction

Research Project: Evaluation of Geologic Dust Entrainment, Removal and Transport Mechanisms

Objective: Investigate the discrepancies between ambient geologic dust measurements and the contributions to source inventories for PM10 and PM2.5.

University of California Dr. Dennis Fitz
College of Engineering
Center for Environmental Research and Technology (CECERT)
Riverside, CA

Penn State University Dr. Russell Philbrick
Electrical Engineering Department
University Park, PA

Pilot Study – Conducted 12-18 December 2000
Main Investigation – Planned 29 July – 17 August 2001

6-8 June 2001 AF Transmission Meeting

Field Site

Field site located 5 miles east of Riverside CA – university farm station

Instrumented Tower

Meteorology properties and particle density and size Measured at several locations

LIDAR

Scanning Lidar measures particle distributions

Nd:YLF 1047 nm – 523 nm

5-10 μj pulses 1-10 kHz

30 meter range resolution

6-8 June 2001 AF Transmission Meeting

Portable Digital Lidar *(Dual Wavelength with Scanner)*

System Specifications

Operating Environment Controlled Indoor

Detection Range 30 - 60 km

Laser (dual wavelength) DPSS:Nd:YLF (523.5 nm/1047 nm)

Laser Control Remote Set or RS232

Average Energy VIS: >5 :J/pulse NIR: >10 :J/pulse

Pulse Repetition Rate (pulse duration) 1 - 10 kHz (10 ns)

Cassegrain Telescope Diameter (F.O.V.) 0.2 m (- 100 :rad)

Detector APD Photon Counting Module

Scanning Mode Sweep or Stay and Stare

Horizontal Scanning (vertical swiveling) ± 90/ (0/ - 90/)

Scanning Speed per sec Variable from 0.1/ to 30/

Optical Transceiver Dimensions (weight) 33" x 14" x 12" (40 lbs)

Computer Desktop or Laptop PC

Software Windows 95/98 based software

Dual Multichannel Scaler (dimensions) Rack-mountable (19" x 14" x 7")

Data Averaging Time Adjustable from 1 sec to 1 hour

Range Resolution 30 m, 75 m, 150 m, 300 m

6-8 June 2001 AF Transmission Meeting

Evaluation of Geologic Dust – California – Dec 2000

Scanning Micro-pulse Lidar

6-8 June 2001 AF Transmission Meeting

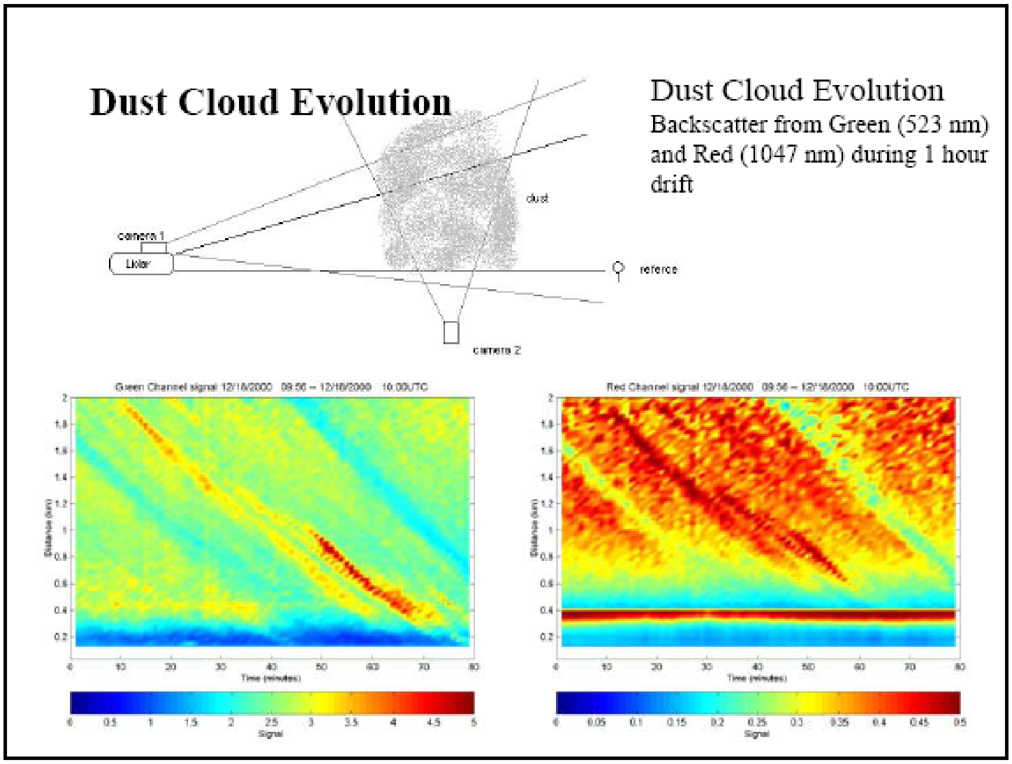
Dust Cloud Evolution
Dust Cloud Evolution
Backscatter from Green (523 nm) and Red (1047 nm) during 1 hour drift
dust
camera 1
Lidar
camera 2
Time (minutes)
Signal
Time (minutes)
Signal

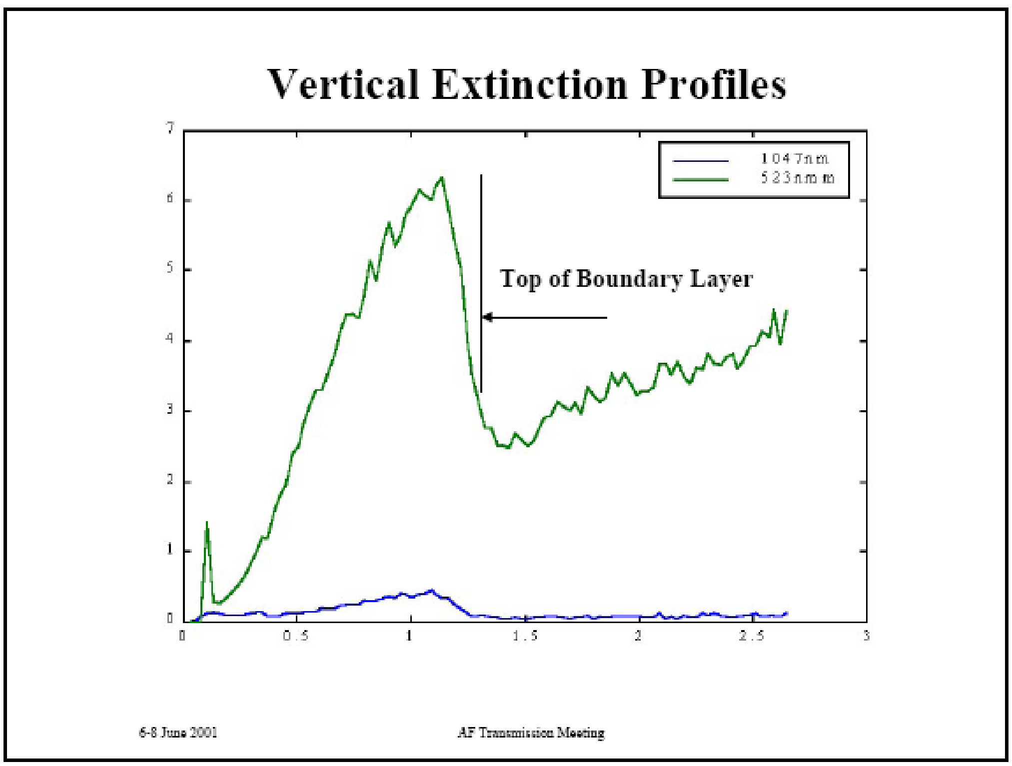
Vertical Extinction Profiles
1047nm
523nm
Top of Boundary Layer
6-8 June 2001
AF Transmission Meeting

Vertical Profiles

Time sequence of vertical profile (75 degree elevation) during wind storm on 18 December 2000

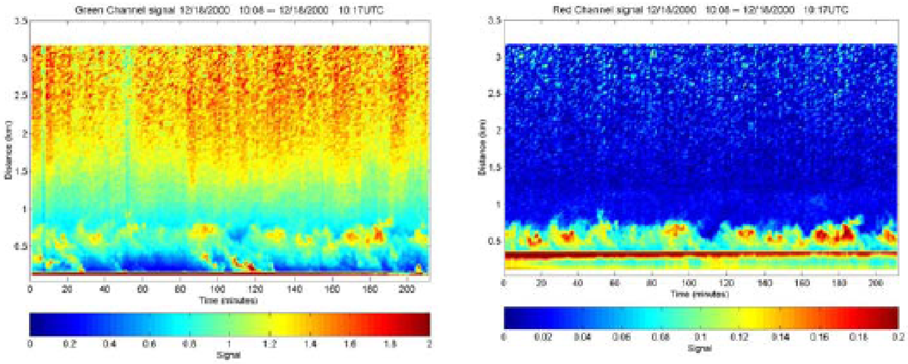

6-8 June 2001 AF Transmission Meeting

T = 1 sec

T = 30 sec

California Dust Generation Experiment – Dec 2000
Dust Generation Test #2 – 5.5 kg soil

T = 60 sec

T = 90 sec

6-8 June 2001 AF Transmission Meeting

Small Puff Dust Cloud

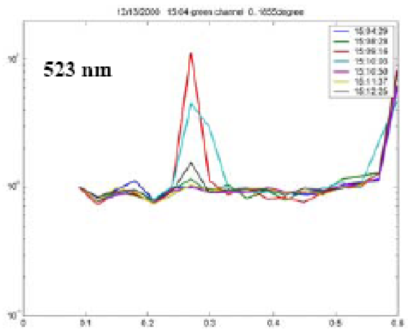

Test #1 - 0.54 kg soil released in 5 sec, measured on fixed radial extracted from scan data for green and red wavelengths compared with calculation

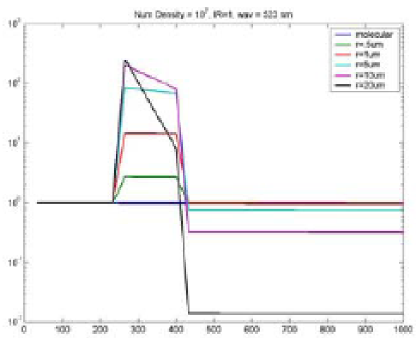

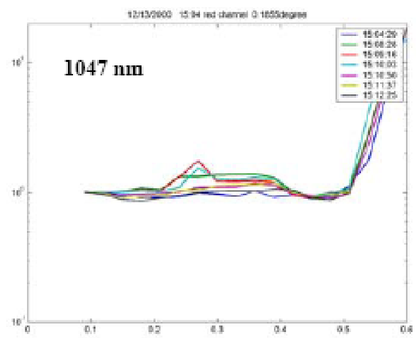

Test #2- 5.5 kg of soil in 50 sec

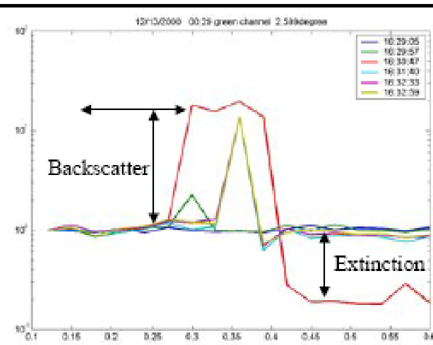

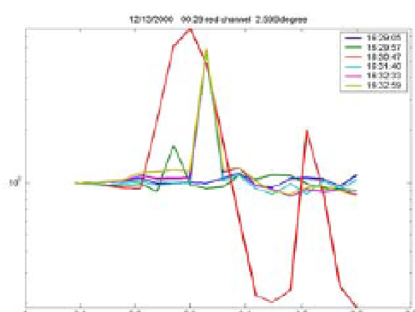

6-8 June 2001

AF Transmission Meeting

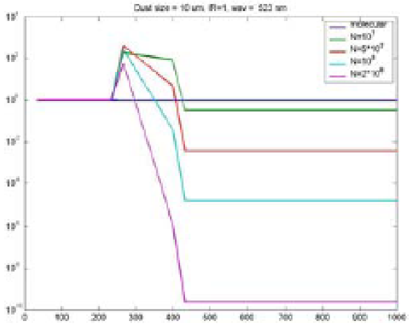

Model Calculation for Dust Cloud

Compare Changing Particle Densities for Different Complex Refractive Index at 523 nm

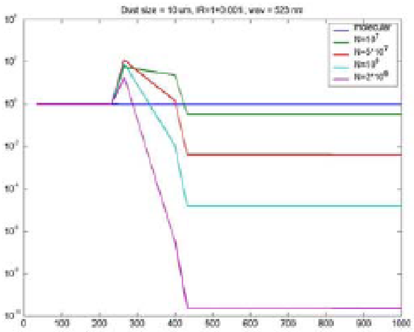

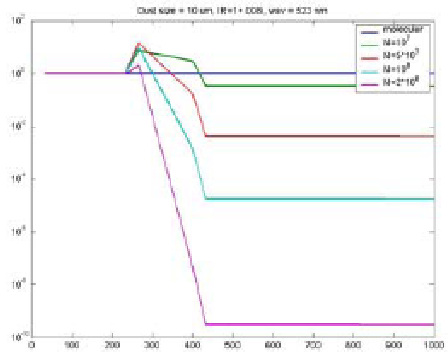

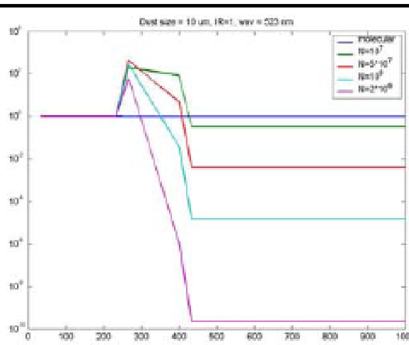

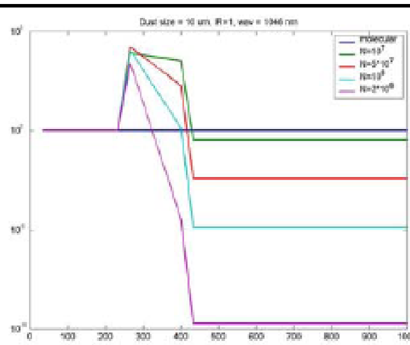

Particle Density

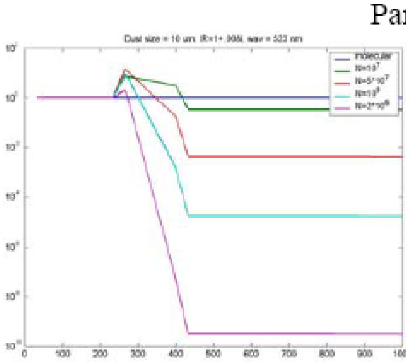

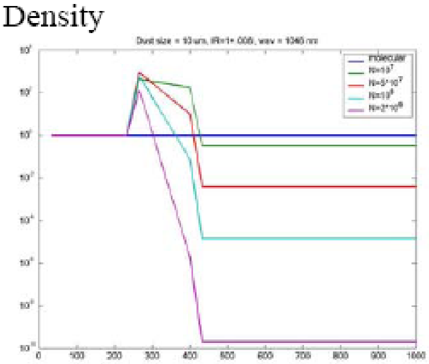

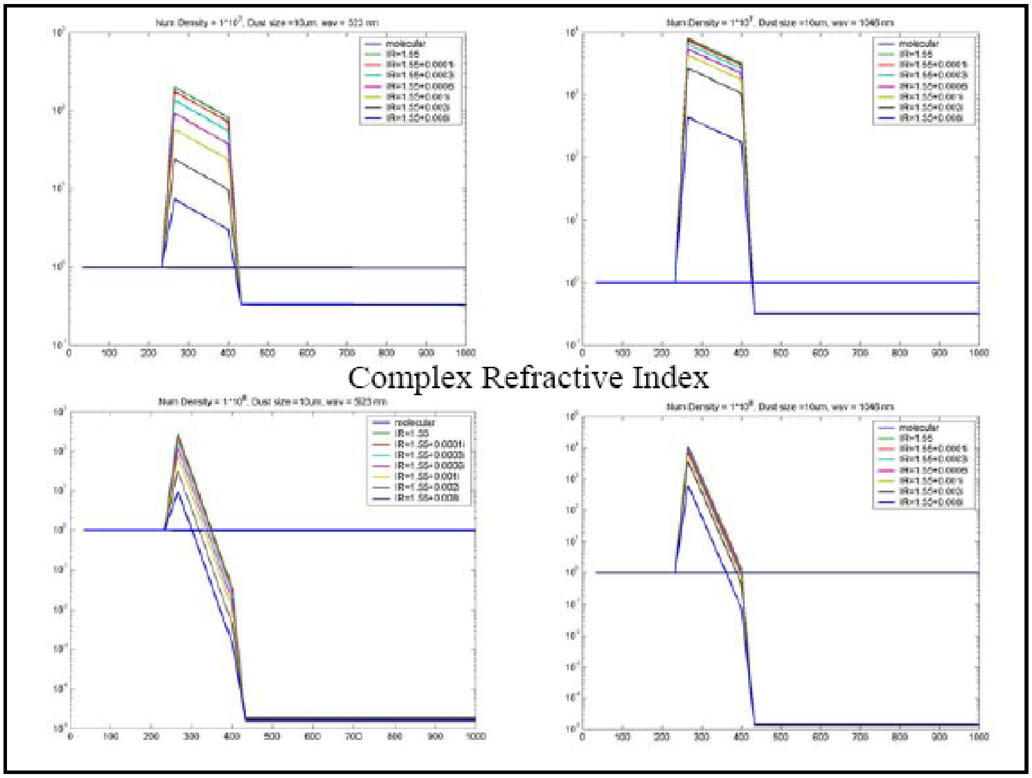

Complex Refractive Index

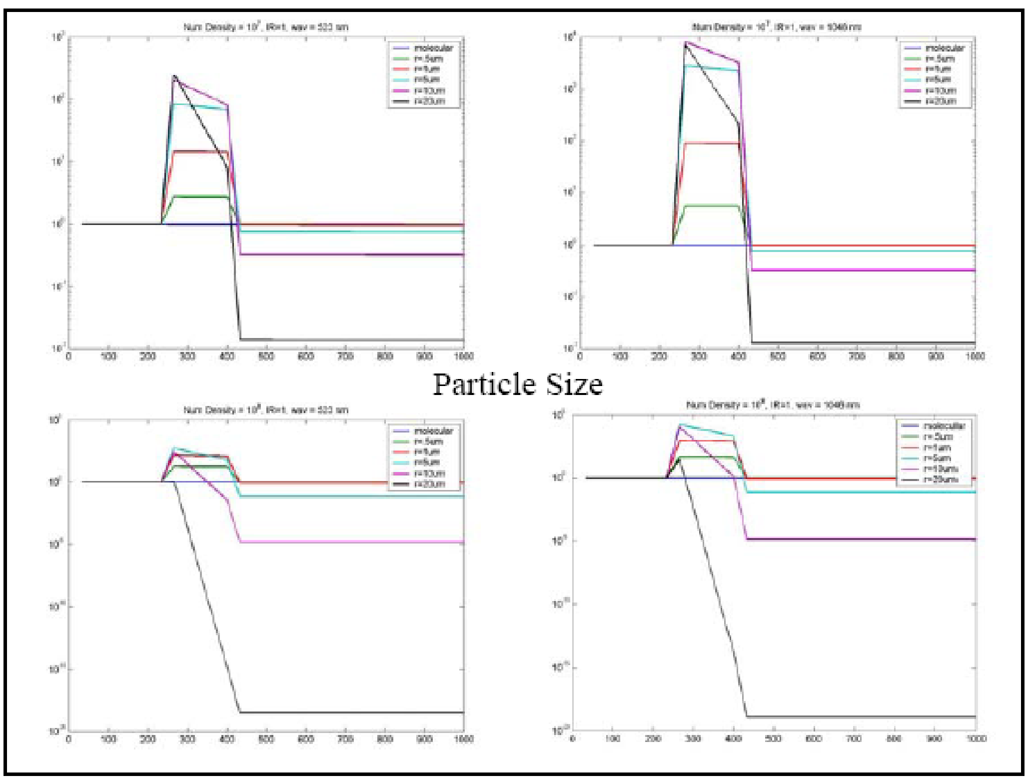

Particle Size

Extinction Efficiency Ratio

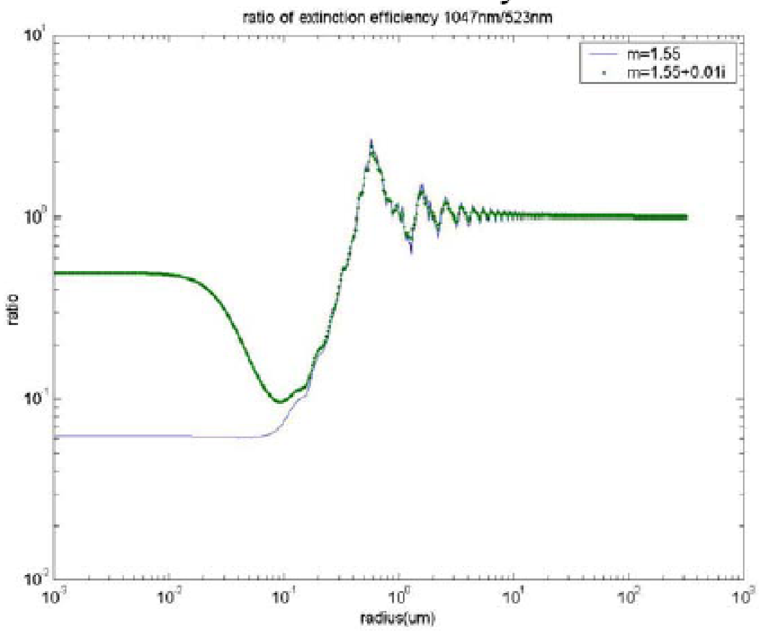

6-8 June 2001 AF Transmission Meeting

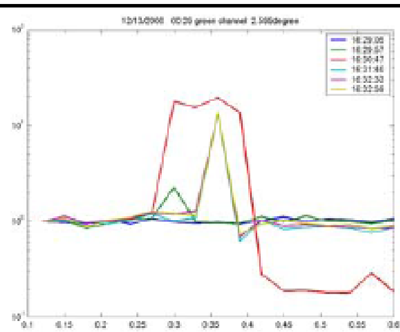

Test #2

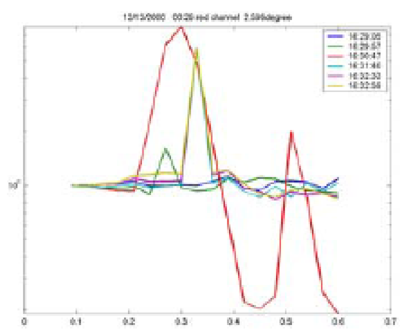

2-λ Backscatter and Extinction

Compare model dust-cloud backscatter and extinction with measured lidar values at 1047 and 523 nm for Test#2 5.0 kg soil

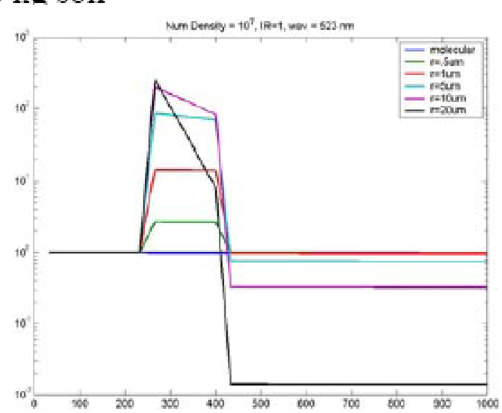

6-8 June 2001 AF Transmission Meeting

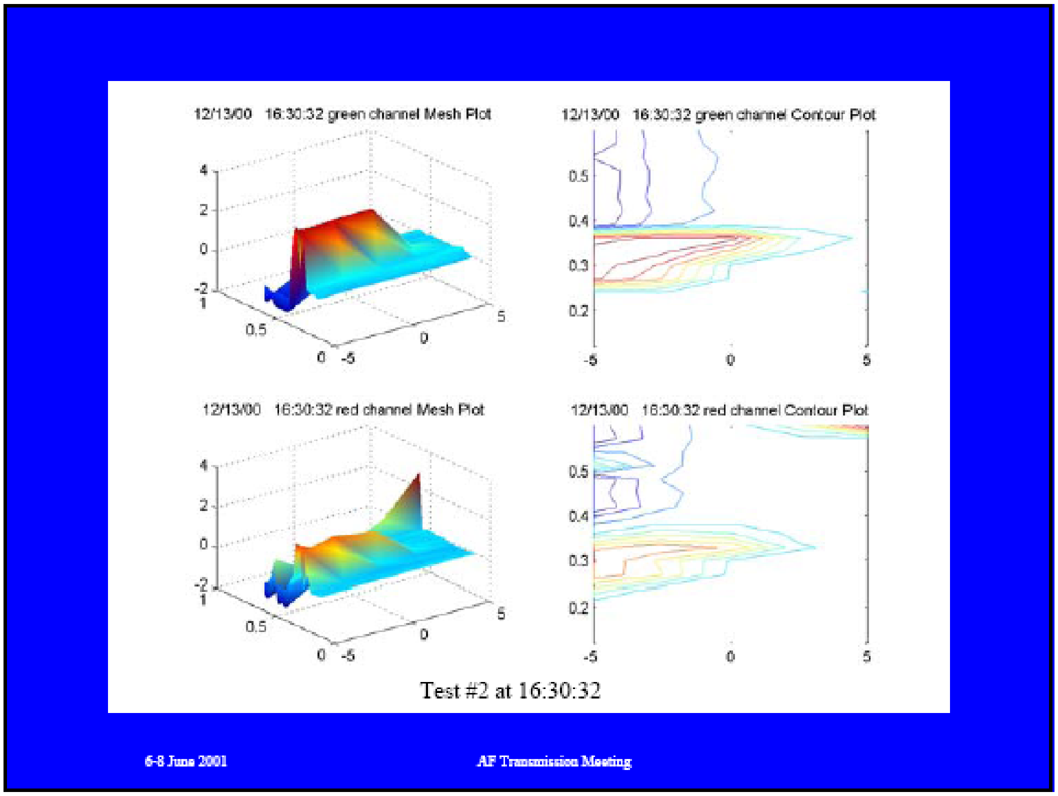
12/13/00 16:30:32 green channel Mesh Plot
12/13/00 16:30:32 green channel Contour Plot
12/13/00 16:30:32 red channel Mesh Plot
12/13/00 16:30:32 red channel Contour Plot
Test #2 at 16:30:32
6-8 June 2001
AF Transmission Meeting

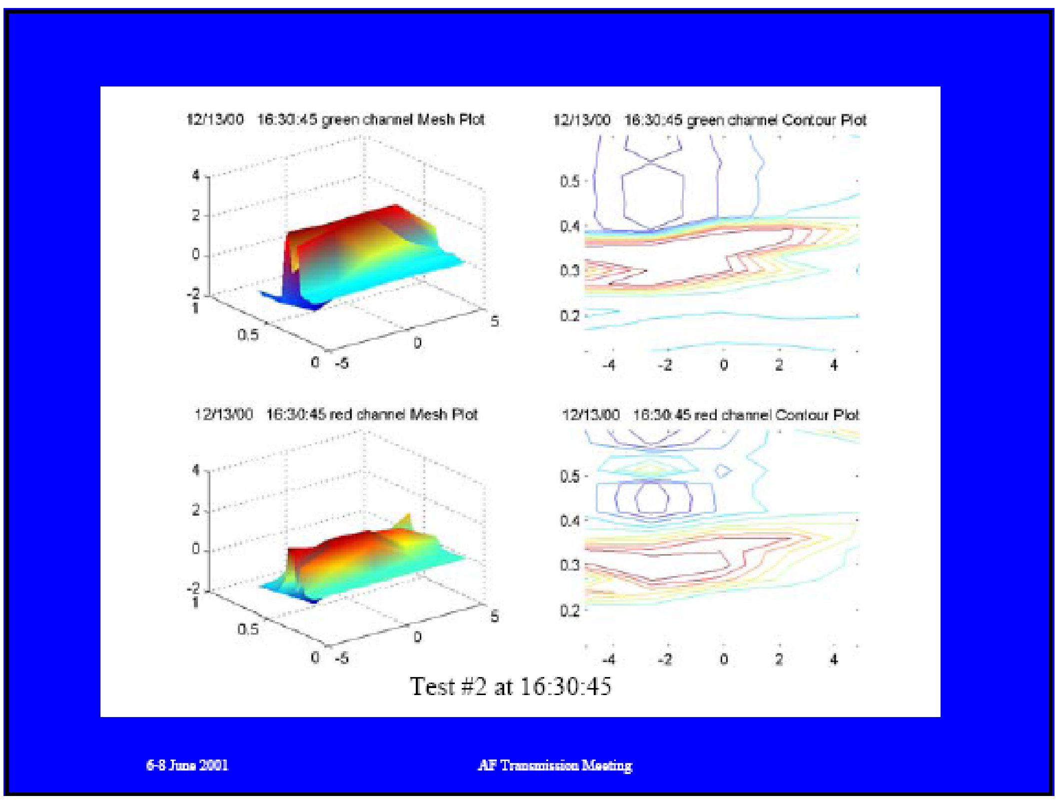
12/13/00 16:30:45 green channel Mesh Plot
12/13/00 16:30:45 green channel Contour Plot
12/13/00 16:30:45 red channel Mesh Plot
12/13/00 16:30:45 red channel Contour Plot
Test #2 at 16:30:45
6-8 June 2001
AF Transmission Meeting

2-λ Backscatter and Extinction

Test #8 Calcium carbonate
10 micron particles – 4.66 kg in 3.2 min

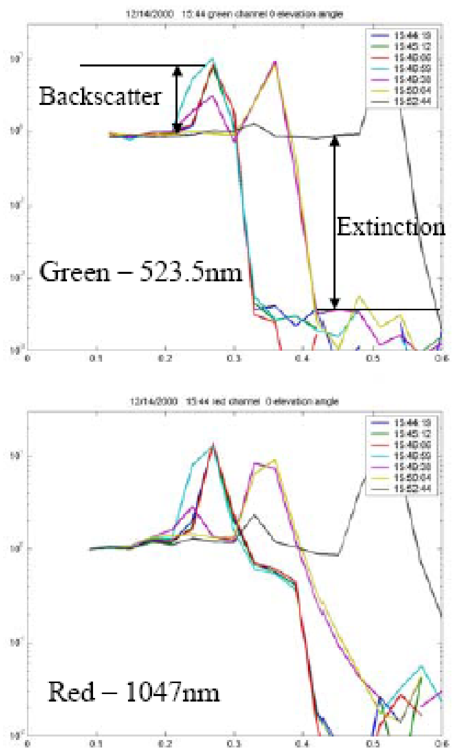

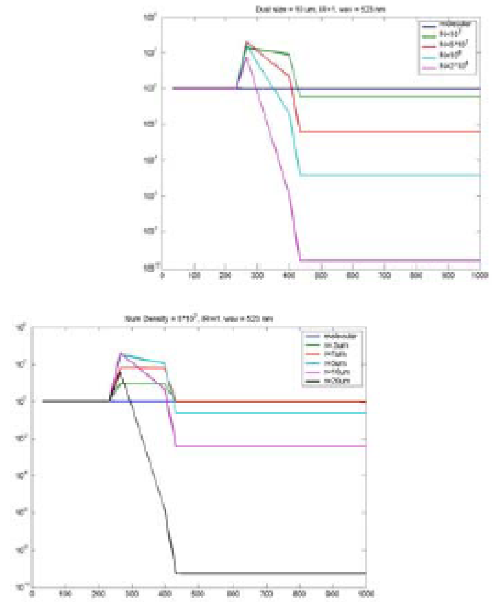

Summary

- Simple model for optical scattering compares favorably
- Extinction can be measured beyond the generated cloud
- Backscatter/Extinction sensitive to size in 0.1-1.0 μ
- August 2001 tests are planned to confirm optical scattering analysis and describe dust cloud evolution
- Investigations continue on the calculations needed to describe the scattering of dust with T-matrix and other approaches

22 6-8 June 2001 AF Transmission Meeting